POLITECNICO DI MILANO

School of Industrial and Information Engineering

Master of Science in
Energy Engineering

OPTIMIZATION OF A SYSTEM BASED ON SECTOR COUPLING FOR HOUSEHOLD ENERGY NEEDS FULFILMENT THROUGH THE MINIMIZATION OF NON-RENEWABLE ENERGY CONSUMPTION

Supervisor: Prof. Giampaolo MANZOLINI

Co-Supervisor: Mr. Hendrik TÖDTER

Student:

Alessia PICCIANI ID 874417

Academic Year 2017 - 2018

Alessia Picciani: *Sector Coupling* | Master Degree Thesis in Energy Engineering, Politecnico di Milano.
© Copyright April 2019.

Politecnico di Milano:
www.polimi.it

School of Industrial and Information Engineering:
www.ingindinf.polimi.it

Aknowledgements

I would like to thank firstly Mr. Hendrik Tödter from Technische Universität of Hamburg for having given me the opportunity to develop the present Thesis at TUHH under his supervision with care and kindness. I also thank Prof. Giampaolo Manzolini for having allowed me to experience this opportunity and for having followed my work as well.

Special thanks, finally, to all the people that I have met in these years at Politecnico di Milano, for making this journey better.
Thanks to all those who supported me in this path, including my parents and all my close friends.

Milano, April 2019 A. P.

Contents

Introduction **1**

1 Sector Coupling Challenge **3**
1.1 What is sector coupling . . . 3
1.1.1 Challenges . . . 3
1.1.2 Benefits . . . 4
1.2 Germany's potential . . . 5
1.2.1 Regulation framework: Energiewende . . . 5
1.2.2 Energy outlook . . . 6
1.3 Conclusions . . . 7

2 Load Profile Identification **9**
2.1 Electric appliances . . . 9
2.2 Heating . . . 10
2.2.1 Space heating . . . 12
2.2.2 Domestic Hot Water . . . 13
2.2.3 Heat pump operation . . . 13
2.3 Electric Vehicles . . . 16

3 Generation Profile Identification **21**
3.1 Solar energy . . . 21
3.1.1 Resource assessment and technology overview . . . 21
3.1.2 Mathematical model description . . . 22
3.2 Wind energy . . . 23
3.2.1 Resource assessment and technology overview . . . 23
3.2.2 Mathematical model description . . . 23
3.2.3 Battery storage . . . 24

4 Case Study Definition **27**
4.1 Load demand . . . 27
4.1.1 Electric appliances . . . 27
4.1.2 Space heating . . . 28
4.1.3 Domestic Hot Water . . . 28
4.1.4 Electric vehicles . . . 29
4.2 Generation Profile . . . 30
4.2.1 Solar energy . . . 30
4.2.2 Wind energy . . . 30

4.3 Analysis methodology 31

5 Control Logic **35**
5.1 Electric appliances 36
5.2 Heat pump 36
5.3 Storage battery and electric vehicles recharge 42

6 Simulation and Results **45**
6.1 Heat pump operation 45
6.2 Electric vehicles and battery charge 49
6.2.1 Strategy 1 49
6.2.2 Strategy 2 50
6.2.3 Strategy 3 50
6.2.4 Strategy 4 51
6.3 Energy balances 53

7 System Optimization **55**
7.1 Battery storage and EV recharge strategy 56
7.2 Heat storage 57
7.3 Economic and CO_2 emissions evaluation 60

8 Sensitivity Analysis **65**
8.0.1 Energy balances 67
8.1 Optimization for South locality 67

Conclusions **68**

A Complete Electric Appliances' Demand Description **75**

B Complete Design Heat Load's Description **81**
B.0.1 Procedure for Design Heat Load determination 82

C Determination of total irradiance on solar panel **87**

Acronims **89**

List of Figures

1.1 Graphical representation of the total energy demand trend from 2015 to 2050 [14] . . . 4
1.2 Four strategies to cut power sector emissions by half by 2030 [18] . 5
1.3 Germany's electricity generation by source . . . 6
1.4 Germany's heat generation by source . . . 6
1.5 Share of Total Final Consumption by source, for Residential (left) and Transport (right) . . . 7

2.1 System describing a heat pump cycle exchanging heat between two reservoirs [29] . . . 10
2.2 Thermodynamic cycle of a heat pump system [29] . . . 11
2.3 Daily DHW volume flow rate profile per person . . . 13
2.4 Variation of compressor efficiency with level of partialization [25] . . 14
2.5 Hydraulic connections between heat pump, tanks, space heating and hot water circuit [23] . . . 15
2.6 Weekdays use of the two vehicles . . . 17
2.7 Car trip probability distribution by time of the day . . . 18
2.8 Choice of car trip interval of time . . . 18

4.1 Electric appliances' weekly load demand split by component . . . 27
4.2 Overall electric appliances' weekly load demand . . . 28
4.3 Yearly variation of external temperature for North locality . . . 28
4.4 Yearly space heating load curve for North locality . . . 29
4.5 Daily Domestic Hot Water load curve . . . 29
4.6 Consumption pattern for the two electric vehicles for one week of the year . . . 29
4.7 Yearly profile of global irradiance on a 50°-tilted surface . . . 30
4.8 Electrical power output curve of the selected wind turbine . . . 31
4.9 Yearly actual power output of the selected wind turbine . . . 31

5.1 General control strategy . . . 35
5.2 Heat pump control strategy . . . 36
5.3 Heat pump control strategy: Case 1 . . . 39
5.4 Heat pump control strategy: Case 2 . . . 40
5.5 Heat pump control strategy: Case 3 . . . 41
5.6 Heat pump control strategy: Case 4 . . . 41
5.7 Main inputs for EV recharge strategy . . . 42

6.1 Definition of the operating condition of the heat pump 45
6.2 Variation of COP with external temperature, for different water delivery temperature 46
6.3 Buffer and DHW tank SoC variation and heat pump operation on 21st January 47
6.4 Buffer and DHW tank SoC variation and heat pump operation on 21st April 48
6.5 Buffer and DHW tank SoC variation and heat pump operation on 21st July 48
6.6 Weekly variation of battery charge and surplus for Strategy 1 for a typical day in January and July 50
6.7 Weekly variation of battery charge and surplus for Strategy 2 for a typical day in January and July 51
6.8 Weekly variation of battery charge and surplus for Strategy 3 for a typical day in January and July 52
6.9 Weekly variation of battery charge and surplus for Strategy 4 for a typical day in January and July 52
6.10 Loads and generation profiles for a typical week in Winter period . 53
6.11 Loads and generation profiles for a typical week in Summer period . 53
6.12 Variation of total grid energy value with different simulations 54

7.1 Yearly average grid energy consumption with variation of net battery capacity, for the four different recharging strategies 56
7.2 Yearly grid energy consumption with variation of buffer capacity and minimum winter buffer's State of Charge 58
7.3 Yearly grid energy consumption with variation of buffer capacity and DHW capacity 59
7.4 Yearly grid energy consumption with variation of battery capacity and buffer capacity (left) and DHW capacity (right) 59
7.5 Results for Economic and Emission analysis, Case 3 63
7.6 Results for Economic and Emission analysis, Case 4 63
7.7 Results for Economic and Emission analysis, Case 5 64

8.1 Yearly space heating load curve for South locality 65
8.2 Determination of the operating condition of the heat pump 66
8.3 Yearly profile of global irradiance on a 50°-tilted surface for South location 66
8.4 Yearly grid energy consumption for South locality with variation of buffer capacity and minimum winter buffer's State of Charge 68
8.5 Yearly grid energy consumption with variation of buffer capacity and DHW capacity 69

A.1 Electricity consumption of several appliances for a typical household and for a typical day of the week [20]. 75
A.2 Daily lighting consumption profile in winter (above) and summer (below) 76
A.3 Daily television consumption profile 76

A.4 Daily cooking stove consumption profile 77
A.5 Daily dishwasher consumption profile 77
A.6 Daily mobile phone consumption profile 78
A.7 Daily consumption profile of remaining appliances 79

B.1 House model 81

List of Tables

2.1 Daily energy demand of the two electric vehicles for a typical week of the year . . . 17
2.2 Distribution of car trips . . . 18

7.1 Optimization parameters . . . 55
7.2 Default parameters . . . 55
7.3 Discounted Cash Flow components for each system configuration . . 61
7.4 Results for Economic and Emission analysis, Case 1 . . . 61

A.1 Energy demand estimation of a group of appliances without specific consumption pattern . . . 79

B.1 Values of transmittance of several elements for the reference building [13] . . . 82
B.2 Values of transmission heat losses from the heated space to the exterior, for each floor . . . 83
B.3 Case specific parameters for the calculation of $U_{eq,k}$ . . . 84
B.4 Values for the calculation of $U_{eq,k}$ and $\Phi_{T,ig}$ . . . 84
B.5 Values for the calculation of $\Phi_{V,build}$ . . . 85

Sommario

Dopo la Conferenza delle Nazioni Unite sui Cambiamenti Climatici COP21 tenuta nel 2016, è stata chiara l'urgenza dell'intraprendere azioni specifiche per limitare il cambiamento climatico, arrivando così a stipulare un accordo volto a mantenere sotto i 2 °C l'aumento della temperatura terrestre rispetto ai valori del periodo pre-industriale. L'Unione Europea ha implementato una strategia energetica da attuare gradualmente entro il 2050 per tagliare le emissioni di gas serra dell'80-90% entro quell'anno [12].
Per raggiungere questo obiettivo, è necessario intraprendere misure che prevedono l'aumento della frazione di energia prodotta da fonti rinnovabili.

Lo scopo di questo lavoro è quello di analizzare il potenziale del *sector coupling* nell'ambito residenziale in modo da ridurre l'impatto ambientale rispetto a un sistema convenzionale. Esso consiste nell'uso di elettricità proveniente da fonti rinnovabili per il riscaldamento (*Power-to-Heat*) e il trasporto (*Power-to-Mobility*), settori che generalmente rappresentano importanti frazioni di emissioni di CO_2 in un Paese.

Per realizzare questo compito, la richiesta energetica di un'abitazione standard in Germania è stimata, in termini di domanda elettrica, riscaldamento degli ambienti e dell'acqua sanitaria e infine trasporto. Un sistema basato sull'uso di una pompa di calore e veicoli elettrici è implementato e una simulazione annuale, a intervalli orari, è sviluppata grazie all'uso del software *Matlab*. L'obiettivo è quello di rendere il sistema il più autosufficiente possibile, minimizzando l'elettricità proveniente dalla rete principale, utilizzando invece quella rinnovabile prodotta da pannelli fotovoltaici e una mictro turbina eolica montati sul tetto dell'abitazione. I principali parametri che influenzano la performance del sistema sono analizzati per ottenere la miglior configurazione capace di minimizzare le emissioni di CO_2. Infine, un'analisi economica è svolta per determinare la fattibilità del sistema da un punto di vista pratico.

Abstract

After the COP21 UN Climate Change Conference in 2016 it became clear that specific actions to limit climate change are necessary, thus leading to the stipulation of an agreement to keep below 2 °C the increase of global temperature, compared to values of pre-industrial period. European Union implemented an energy roadmap to 2050 to cut greenhouse gas emissions by 80-90% by that year [12].
In order to achieve this objective, necessary measures to undertake include the increase of renewable energy consumption share.

The aim of this work is to analyze the potential of sector coupling in the residential sector in order to get a reduced environmental impact with respect to a conventional system. It consists in the use of electricity from renewable sources for heating (Power-to-Heat) and transport (Power-to-Mobility), which represent important fractions of CO_2 emissions of a country.

To accomplish this task, the energy demand of a standard household in Germany is estimated, in terms of electrical appliances, heating, hot water and transport. A system based on a heat pump and electric vehicles is implemented and a yearly, one-hour time step simulation is developed thanks to the *Matlab* software. The objective is to make the system as self-sufficient as possible to minimize the electricity supplied by the grid, employing renewable electricity generated by solar panels mounted on the house roof and a micro wind turbine. The main parameters affecting the system performance are analyzed to obtain the best configuration able to minimize CO_2 emissions. Finally, an economic analysis is performed to determine the feasibility of the system from a practical point of view.

Introduction

In December 2015, at the COP21 UN Climate Change Conference in Paris, for the first time, 196 countries stipulated a deal to achieve a legally binding and universal agreement on climate. The aim is to keep below 2 °C the increase of global temperature, compared to the values of pre-industrial period.
Dangers of climate change are globally recognized, and therefore, specific actions have to be undertaken to protect human being and environment.

In this context, European Union implemented an energy roadmap to 2050, whose long-term goal is to cut greenhouse gas emission by 80-95% by that year, with respect to the values of 1990 [12].
EU countries also agreed on 2020 and 2030 intermediate targets and policy objectives, to help achieving a more competitive, secure and sustainable energy system.
Specifically, the targets for 2030 are:

- 40% cut in greenhouse gas emissions compared to 1990 levels;
- 27% share of renewable energy consumption, at least;
- 27% energy savings compared with the business-as-usual scenario, at least.

However, these goals have serious implications on the current energy system, that needs to be redesigned and improved to deal with such large changes.
Decarbonization, energy efficiency and market regulations are the key-words on which it's necessary to focus [12].

Despite the very specific targets, there is not a unique solution to achieve the goals, therefore, each country is managing the transition in a different way.
Germany, where the share of electricity production from renewables was 31% in 2016 [5], is one of the countries leading the energy transition; the Agora Energiewende's report proposes the specific steps in a ten-point agenda that the country should adopt for achieving the 2030 goals [18].
The challenges to face are many, and attention should be given in particular to the flexibility of the new energy system, through demand side management, enhancing energy storage and fostering a system based on sector coupling.
Sector coupling refers to integration of different energy consuming sectors, such as industrial, residential and transport with the power producing sector, aggregating them into a single energy system. The primary motivation for this new approach is to decarbonise the energy system in order to accomplish the climate goals.

The aim of this project work is to analyse the potential of sector coupling in the residential sector, as it represents an important fraction of energy demand and greenhouse-gas emissions.
Considering a standard family house model, its energy demand is estimated, in terms of electrical appliances, heating, hot water and transport.
The electricity-producing sector is linked to that of thermal energy and transport thanks to the adoption of electric heat pumps and electric vehicles, respectively.
Basing the electricity production only on sun and wind resources, a suitable configuration able to meet the demand must be identified, minimizing the energy withdrawn from the grid and ensuring high level of self-sufficiency.
Photovoltaic panels and a micro wind turbine are employed, together with a battery storage system and buffer tank storages, in order to ensure flexibility to the system.

A yearly, one-hour time step simulation of the system is implemented with the *Matlab* software, estimating the renewable energy generated and delivered to the users.
The same simulation is performed for two different locations of Germany, one in the North and one in the South, to highlight how resources availability and climate conditions affect the potential of sector coupling.
Different strategies for heat and electricity provision are investigated and the main parameters affecting the behaviour of the system are identified. The optimization of the system occurs through the minimization of total grid energy consumption.
Moreover, an economic analysis is also performed to determine the feasibility of the system from a different point of view: the analysis eventually determines at which expense the system is able to reduce CO_2 emissions of 1 kg over the plant lifetime.

Chapter 1

Sector Coupling Challenge

1.1 What is sector coupling

Sector coupling is the use of electricity from renewable sources in the heating sector (Power-to-Heat), the transport sector (Power-to-Mobility) and in industrial processes [14]. It aims at creating a single energy system in which all sectors are interconnected, through different energy vectors.
The Combined Heat and Power generation plants and rail transport are some of the already existing forms of sector coupling and the idea is to extend this approach. The development of sector coupling can occur in several ways, such as pushing the adoption of electric cars and battery storages or promoting power-to-heat plants such as heat pumps, electric boilers or devices for heat storage that exploit excess electricity.
Finally, fostering the adoption of Power-to-Gas plants would allow the production of fuels, such as hydrogen, that could be stocked and used when necessary.

1.1.1 Challenges

From a technological point of view, it is clear that the enhancing of sector coupling has consequences on the asset of the current energy system because of the rise of electricity demand. A further expansion of renewable technologies must be taken into account, in order to avoid the shift of emissions from end-use sector to the producing one, without a substantial reduction. Efforts need to be addressed also to the achievement of high levels of conversion efficiency of the processes in order to keep the growth of energy demand within a small range, despite sector coupling. Higher efficiency target concerns as well the improvement of buildings heat insulation.
Figure 1.1 shows graphically how electricity consumption keeps almost stable until year 2050: indeed, the increase energy efficiency balances the increase of electricity consumption due to sector coupling. On a global level, total energy demand decreases.

Finally, it is crucial the implementation of adequate control strategies to match demand and supply, smart technologies for the grid management and effective

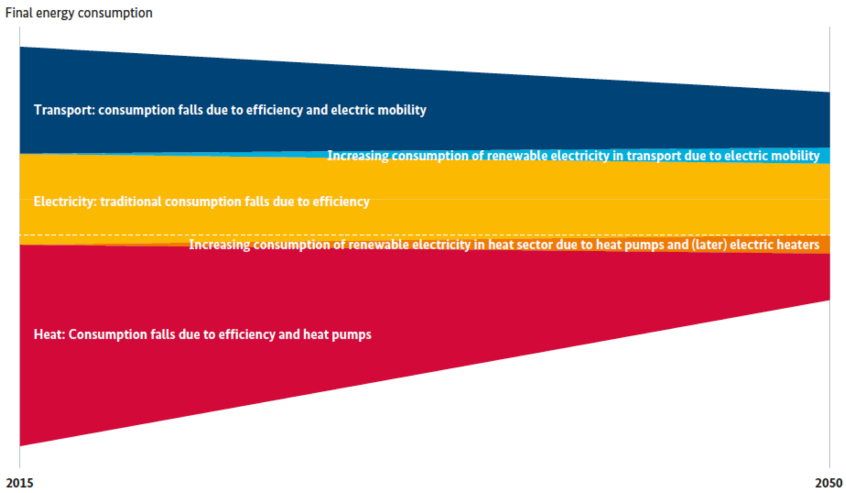

Figure 1.1: Graphical representation of the total energy demand trend from 2015 to 2050 [14]

energy storage systems, that are essential when unpredictable energy generation technologies are concerned.
From an economic point of view, adequate business models need to be adopted, in order to sustain financially the energy transition.

1.1.2 Benefits

Despite the great effort required by the energy transition, there are many reasons for the coupling of power, heat and transport sectors.
From an environmental point of view, the progressive shift towards renewables sources of energy will enable the reduction of emissions, not only on a global level, but also locally with the adoption of electric vehicles, bringing better livelihood in the urban areas.
Another notable aspect of the adoption of sector coupling is the increase of flexibility of the electric supply system, despite the adoption of renewable sources: indeed, they usually represents an obstacle to the match of energy supply and demand, however the interconnections of sectors could be very helpful, together with energy storage. For example, in domestic applications, batteries could be recharged when a large renewable generation is available; heat storages could be filled up (power-to-heat) tanks to excess power production, thus indirectly electrifying the heating sector. Moreover, surplus electricity could be also used to produce hydrogen or synthetic gas (power-to-gas), without having to curtail the renewable production during peak periods; in this way, the gas that stores the energy could either be used to fuel vehicles or could be transformed into electricity or heat in times of insufficient sun and wind production.
All these examples show how the flexibility of the system is strictly interconnected with load management.
Finally, the reduction of oil and gas import caused by the increased renewable share in the country's energy mix, has a clear benefit on country's self-reliance, security of energy supply and economic independence from exporting countries.

1.2 Germany's potential

Sector coupling is only one of the possibilities available to facilitate the achievement of the environmental targets; every country will adopt different strategies, according to its availability of resources and to the different distribution of energy demand between the different sectors.
The aim of this chapter is to demonstrate why sector coupling in German residential sector is a reasonable and feasible solution.

1.2.1 Regulation framework: Energiewende

Among EU countries, Germany was an early adopter and driver of what has now become a global trend towards energy transition.
Since year 2000, a comprehensive new strategy, the Energy Concept, was adopted by the federal government, for a long-term integrated energy pathway to 2050.
Following the Fukushima nuclear accident in 2011, Germany decided to accelerate the phase-out of nuclear power, starting with the immediate closure of the eight oldest plants.
This decision, together with the political target to progress towards a low-carbon energy sector, resulted in the adoption of a suite of new policy measures, needed to accelerate the energy transition. This new set of policies is known as *Energiewende* and aims at supporting renewable energy, grid expansion and promoting energy efficiency, maintaining a balance between sustainability, affordability and competitiveness.

The specific climate target is to cut by 55% of GHG emissions by 2030, compared to 1990 levels; in Fig.1.2 four strategies to reduce power sector emissions are showed: it is possible to see that the emissions targets can be met in particular thanks to the increase of the renewable contribution in the energy mix, and despite the adoption of sector coupling because of the stable energy demand.

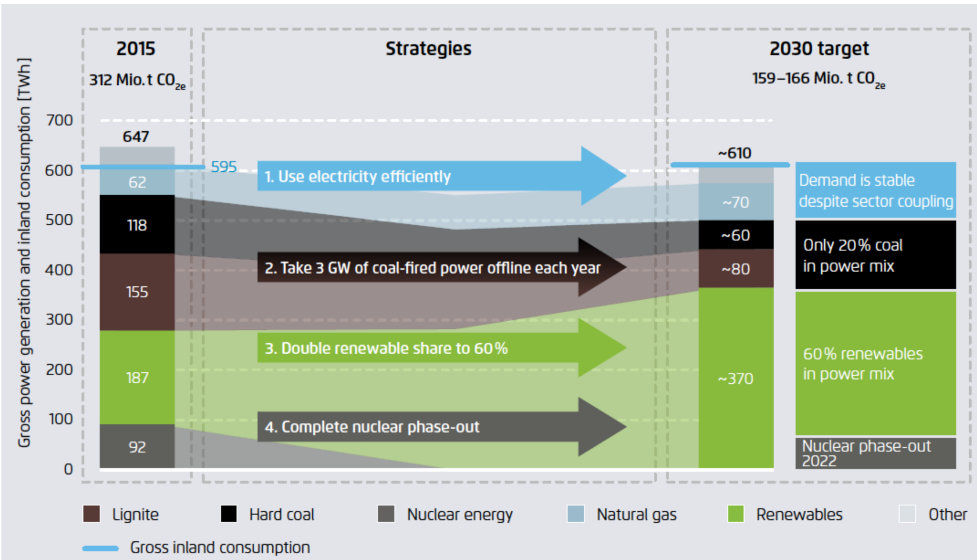

Figure 1.2: Four strategies to cut power sector emissions by half by 2030 [18]

1.2.2 Energy outlook

The International Energy Agency (IEA) provides a wide range of energy-related statistics and data for every country, that are useful to portray the global picture under different aspects.
Data available for the year 2016 show that Germany produced 642,9 TWh of electricity, with a share of renewables sources (wind, solar, hydro, biofuel, waste, geothermal) of 31%, as illustrated in Fig.1.3.
Despite hitting the target of at least 27% of renewable production by 2030, coal still plays an important role, accounting for about 43% of the total national electricity generation.
Comparing instead data with those of previous years, it is evident the progressive dismissing of nuclear power: in accordance with the government decisions, nuclear production decreased from 22,2 to 13% of the total national production from 2010 to 2016, being replaced by renewable sources.

However, the fraction of renewable generation, accounts for only the 22,4% when dealing with heat production (Fig.1.4) thus representing one of the biggest challenges to face.

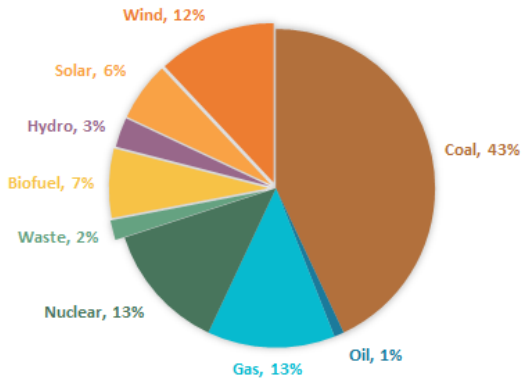

Figure 1.3: Germany's electricity generation by source

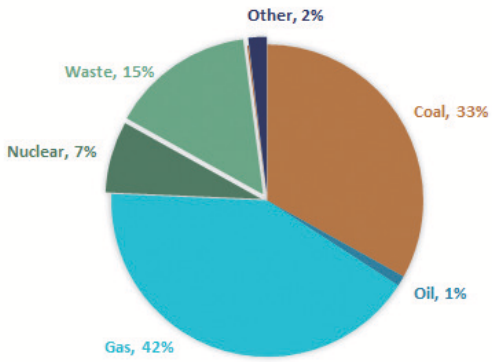

Figure 1.4: Germany's heat generation by source

It is also significant to analyze the share of Total Final Consumption of energy required by several sectors: Industry (25,1%), Transport (25,3%) and Residential (24,1%).
The three sectors are characterized by almost the same energy demand but very different share of energy sources, as shown in Fig.1.5 (only residential and transport sectors are presented, being more relevant to the topic of this project work).

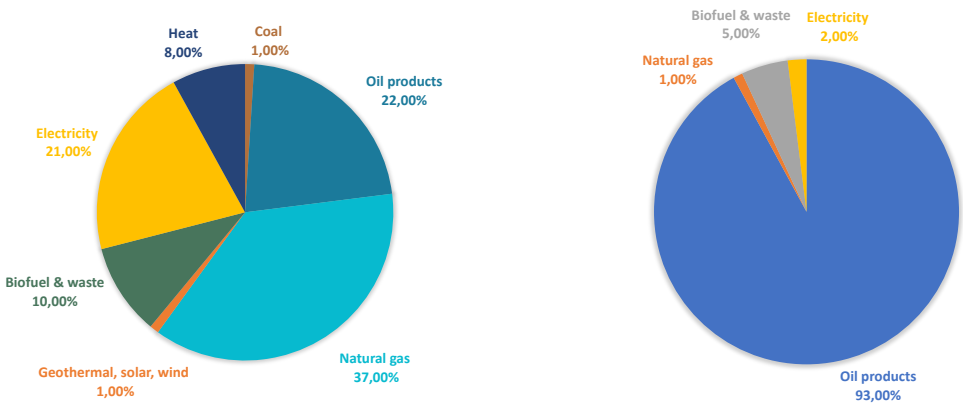

Figure 1.5: Share of Total Final Consumption by source, for Residential (left) and Transport (right)

Clearly, the country still strongly relies on fossil fuels in these sectors, in particular oil and natural gas: this is one of the main difficulties to overcome, in order to enable the desired energy transition because it implies a deep change of the current energy system.

1.3 Conclusions

To sum up, it is possible to say that Germany's energy transition has largely happened in the electricity sector, where the share of renewable electricity generation is above 30%.
However, other sectors different from the power-generation one, still heavily rely on fossil fuels as primary energy sources: for example, natural gas represents the primary source for heating, while oil derivatives are still the main fuels for internal combustion vehicles.
This current situation represents a huge opportunity for the adoption of sector coupling: the large share electricity production from renewable sources (which is already a matter of fact) can be able to gradually substitute the use of fossil fuels. In particular, decarbonization of transport and buildings sectors will be crucial in order to make the country's economy mostly carbon-neutral by 2050.

Finally, other available options such as the adoption of biofuels, to make transportation and heating powered by renewables, cannot represent the main solution to decarbonization. Indeed, biomass' main limit is represented by large-scale energy production: arising issues of the so called "food vs fuel" and "maizification" cannot be neglected [24].

Chapter 2

Load Profile Identification

In this chapter, the general load profile identification procedure is described. The load demand of two different German households is estimated: one located in the North and the other in the South of the country.
It is identified a standard model of a typical residential household, basing on several assumptions and on reference values that can be found from norms or specific studies on households behaviours, as described in the dedicated paragraphs.
Nevertheless, a precise estimation of the household's energy demand is necessary to obtain realistic results.

The aim of this analysis is to shape the load curve of the electricity consumption throughout a whole year, on an hourly basis. Following a bottom-up approach, the demand of each sector (electrical, heating, transport) is disaggregated in its different components.
First it is estimated the load required by electrical appliances, splitting up the demand of each specific appliance, according to its use.
Then the demand for space heating is assessed, excluding that for cooling because localities chosen for the analysis belong to climatic zones characterized by an average annual external temperature of about 10 °C [11].
Finally domestic hot water consumption and electric vehicles use are evaluated.
Chapter 4 presents the resulting load curve obtained for the specific case study.

2.1 Electric appliances

Electrical appliances' load curve is determined for a typical day of the year: first, all the possible appliances present are listed, then the nominal power consumed by each of them is determined, and finally the duration of each use throughout the day is estimated.
The consumption of each appliance, when possible, is evaluated from the values reported on energy labels established by the European Commission. Low energy-consuming models are chosen, in accordance with the aim of achieving high efficiency.

The consumption pattern for some appliances is reasonably repeating in the same way for all days of the year, such as for the cooking stove, assuming that

households' habits maintain constant; a possible and realistic load curve is built, basing on information present in studies investigating households consumption patterns. These reports are useful to compare and validate the shape of the curves obtained, while the values of power consumption are averages over the investigated population, that underestimate the actual peaks of consumption.
Other kinds of appliances, may have considerable variable consumption from day to day, as oven or washing machine; in these cases it is implemented a random function on *Matlab* that allows to generate a different profile for every day: while the energy consumption in the interval of use is known, the function determines in which day of the week and in which interval of time the appliance will be switched on.
Some other appliances may have random consumption, but occurring for a very small period of time if compared to the one-hour discretization adopted. In these cases, their contribution is summed up together, estimating the global energy consumed, and distributing it uniformly during the possible functioning time of the appliances.
Finally, it is necessary to distinguish between weekend days and working days, and between winter and summer period, that influence the use and consumption of several appliances.

In Appendix A the detailed procedure of evaluation of load demand is reported.

2.2 Heating

Heat demand is supplied by a heat pump, a cyclic machine that allows to extract heat from a low-temperature reservoir at T_C (the external environment) and transfer it to a higher-temperature reservoir at T_H (internal ambient), as shown in Fig.2.1.
Heat pumps are closed circuits in which a refrigerant fluid goes through several

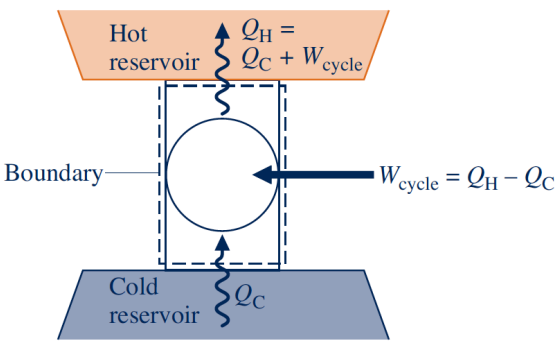

Figure 2.1: System describing a heat pump cycle exchanging heat between two reservoirs [29]

thermodynamic transformations: compression, condensation, expansion and evaporation, as illustrated in Fig.2.2.

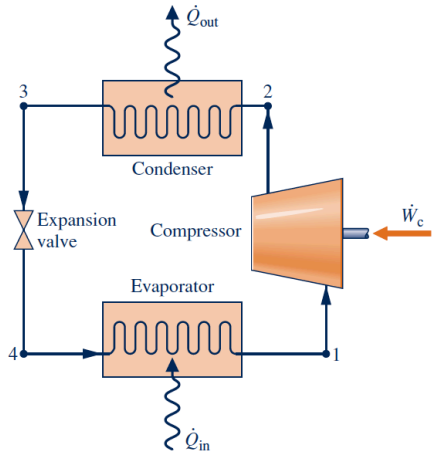

Figure 2.2: Thermodynamic cycle of a heat pump system [29]

They can be adopted to supply heat for both space heating and sanitary hot water, employing proper heat exchangers between the refrigerant fluid and water delivered to the users.

The performance of a heat pump is measured by the Coefficient Of Performance (COP), that corresponds to the ratio of the useful effect Q_{H} (heat delivered to the house) and input W_{cycle} (electricity input). It depends on the temperature of the two reservoirs and it can be demonstrated that Eq.2.1 corresponds to the ideal COP expression.

$$COP = \frac{Q_{\mathrm{H}}}{W_{\mathrm{cycle}}} = \frac{T_{\mathrm{H}}}{T_{\mathrm{H}} - T_{\mathrm{C}}} \tag{2.1}$$

The value of COP decreases when lowering the external ambient temperature $\mathrm{T_C}$ and increases when the temperature difference between the two sources decreases. For example, considering a hot water delivery temperature equal to 50 °C and external air temperature equal to 0 °C, the ideal COP is equal to 6,5, which means that for each electrical kilowatt absorbed by the heat pump, 6,5 thermal kilowatts are delivered to the internal environment. However, to account for irreversible losses occurring in the process, it is necessary to rely on COP values reported in manufacturers' data sheets.

Heat pumps can be differentiated according to the cold reservoir adopted, which can be air, water or ground. In this analysis, an air-source kind is employed because of unlimited availability of the source but mainly because of simplicity of realization that makes this technology easier to adopt.
However, unlike water and ground, air temperature goes through wide changes during a year, making the performances of air-source heat pumps very susceptible to weather conditions.
The other parameter influencing COP is the temperature required by the heat delivery system $\mathrm{T_H}$. Consequently, the choice of a low heat delivery temperature system results in higher efficiency: this can be achieved through the adoption of

radiant panels that require water temperature around 35 °C, against the 60 °C or more required by classic radiators.

Finally, Eq.2.2 shows that the electricity absorbed by the heat pump P_{el} is directly proportional to the heat demand $\mathrm{Q_H}$ and inversely proportional to the value of COP at given temperatures.

$$P_{\mathrm{el}} = W_{\mathrm{cycle}} = \frac{Q_{\mathrm{H}}}{COP} \tag{2.2}$$

Paragraphs 2.2.1 and 2.2.2 illustrate how the demand for space heating and Domestic Hot Water (DHW) is evaluated, in terms of thermal energy.
Afterwards, in paragraph 2.2.3 the behaviour and control logic of the heat pump is described in order to obtain the electric load of heat demand.

2.2.1 Space heating

European Standards provide methods to evaluate the energy needs for space heating.
Specifically, the EN 12831-1:2017 norm allows to accurately compute the thermal losses occurring through the building walls of the considered house, determining the design heat load of the building itself. The design heat load is referred to the condition of design external temperature (the lowest achievable air temperature), absence of irradiation and internal gains.
A standard model for the house is characterized: it is supposed to be a single family household, composed by 2 floors, of 75 m^2 each, with all external walls facing the outdoor ambient.
Up-to-date reference values for transmittance of the walls and surfaces are taken in order to achieve high heat insulation levels and can be found from available National Annex to the norm or specific study reports .
In the Appendix B the detailed procedure for the estimation of the design heat load can be found.

Once the design heat load is determined, the yearly energy need for the considered house must be evaluated. A simple method to do so is to consider a linear variation of the demand with the ambient temperature: heat demand reaches a maximum value in correspondence of the design external temperature and reduces linearly, until it becomes zero when the external temperature is $\mathrm{T_{SET}}$=16 °C. This value of $\mathrm{T_{SET}}$ is the one for which it is assumed that there is no need to switch on the heating system to achieve the design internal temperature of 20 °C: in warm days, characterized by temperature higher than 16 °C, the contribution of solar gain may be considerable.
Even though also summer period is characterized by days in which external temperature is below 16 °C, the heating system is usually kept switched off by the users. The no-heating period can be identified in an interval of time characterized by an average external temperature higher than 16 °C, that generally goes from middle of June to middle of September, according to the weather data of the considered year.

2.2.2 Domestic Hot Water

The energy demand for DHW load is evaluated starting from the identification of the daily water consumption and then by introducing a proper distribution pattern throughout the day.

Data on households' water consumption in Germany set a value of 44 litres/-day/person for bathing, showering hygiene [31]. This value can be rounded to 50 litres/day/person to account for other amounts of hot water that may be consumed besides that.
In order to determine the consumption distribution throughout the day, it was chosen to adopt a standardized profile, function of the fraction of the total amount of water consumed [22].
The pattern obtained is considered to be constant throughout the year and is shown in Fig.2.3.

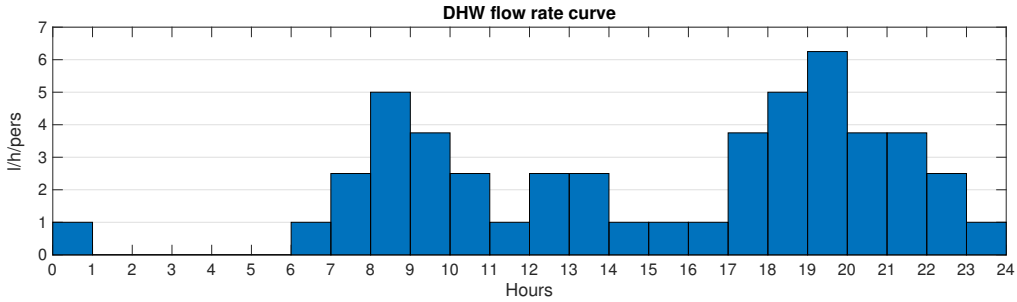

Figure 2.3: Daily DHW volume flow rate profile per person

The heating power required to increase water temperature from the mains to the supply temperature is described by Eq.2.3.

$$\dot{Q}_{\mathrm{DHW}} = \dot{V}_{\mathrm{DHW}} \cdot c_{\mathrm{P}} \cdot (T_{\mathrm{supply}} - T_{\mathrm{mains}}) \tag{2.3}$$

Where

- $\dot{Q}_{\mathrm{DHW}}$: power necessary to heat up water [W]
- $\dot{V}_{\mathrm{DHW}}$: volume flow rate of DHW for all households [l/h]
- c_{P}: specific heat of water, equal to 4186 J/kg/K
- T_{supply}: hot water temperature of supply, set to 55 °C
- T_{mains}: cold water temperature form the mains, equal to to 12 °C

2.2.3 Heat pump operation

Once the previous calculations are performed, it is possible to translate the thermal energy required by DHW and space heating into electrical power absorbed by the heat pump.

The first step is to determine the size of the heat pump, whose maximum power must be able to satisfy the overall demand at design external temperature.
Afterwards, it is necessary to describe the variation of the COP with external temperature, for the two heat delivery temperatures: when space heating only is required, the temperature can be set to 35 °C, while it is set at 55 °C when domestic hot water must be supplied.
Manufactures provide the real COP curves of the specific model with the variation of external temperature: they can be obtained plotting the curves point by point.

Another relevant aspect to take into consideration is that of partial load operation, when heat demand is lower that the nominal power of the machine. Modern heat pumps are endowed with inverter technology that modify the rotational frequency of the compressor with the variation of heat load.
This technology allows to avoid frequent on/off cycles in which the machine always operates at maximum power, causing, on the long run, a damage to the machine itself.
However, the operation at partial load is characterized by a decrease of the compressor efficiency when load reduction is required. A good compressor should be able to work efficiently also at off-design conditions: a desirably behaviour is represented in Fig.2.4, which is taken as reference in this analysis.
The level of partialization, which is the fraction of actual heat delivered over the nominal one, is limited to the 20% for practical reasons: below this value it is not possible to use the heat pump anymore. In this analysis it is chosen to limit the partialization to 25% of nominal power to reduce the on/off cyclic operation of the heat pump.

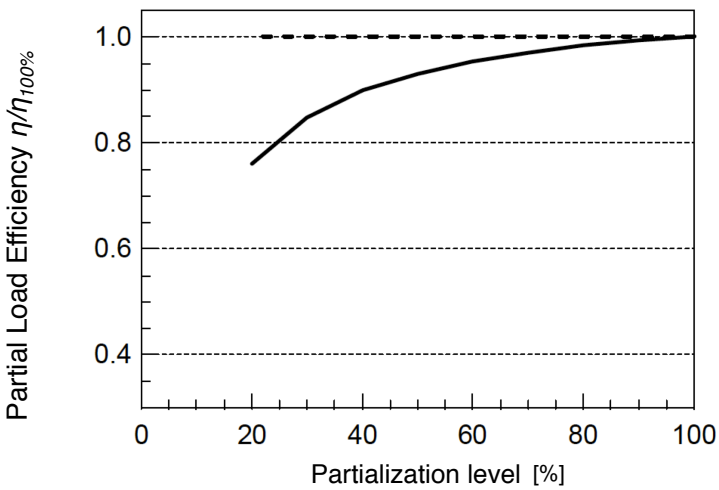

Figure 2.4: Variation of compressor efficiency with level of partialization [25]

In order to face conditions of very small or very high load demand and to increase the flexibility of the system, heat pumps are always coupled to water storage systems: water is the most common medium employed in domestic systems because of the good heat capacity, affordability and availability.

Two separate storage tanks are adopted, one for space heating, at lower temperature (35 °C), and the other for DHW, kept at 55 °C.
Figure 2.5 represents a simplified hydraulic connection of the heat pump (placed outside of the building) with the two distinct tanks, the hot water delivery system, space heating and radiators (although not considered in this analysis). It is possible to see that a serpentine heat exchanger, internal to the DHW tank, allows to directly heat up the water coming from the mains, which receives heat from the stored water. The water flowing in the space heating circuit and in the tanks belongs instead to a closed circuit.
Finally, a three-way valve is present to shift from the delivery of hot water to space heating and vice versa and a pump ensures the flowing of the fluids.

The use of buffer tank is not always required in heating systems, however it can be beneficial: it functions as a hydraulic separation between the heat pump and the rest of the heating system, being characterized by very different volume flow rates. Moreover it extends the useful life of the machine because of the reduced switching on times, especially during the transition periods in spring and autumn characterized by moderate heat demand.
The DHW tank is instead always necessary to supply directly hot water for sanitary use because its delivery must be immediate.

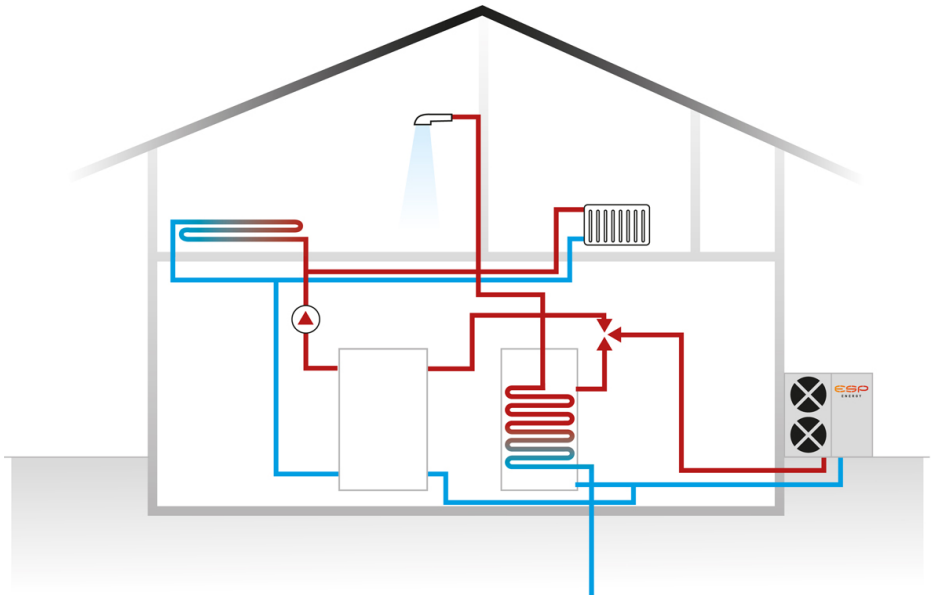

Figure 2.5: Hydraulic connections between heat pump, tanks, space heating and hot water circuit [23]

The sizing of the heat storages is a result of the optimization process, however it can be assumed in first approximation that DHW tank should be able to satisfy at least the daily water demand (200 litres), while the buffer tank should have a volume of at least 30 litres per kilowatt of the heat pump [19].
The stratification effect is neglected in both tanks: in the buffer tank because of

the low temperature that doesn't produce significant separation of the fluid while in the DHW one no stratification occurs because it is regularly discharged and charged during one day.
It is therefore assumed that the storages are kept at uniform temperature and thermal losses can be accounted for in a simple way. Thermal losses from the external surface depend on the size of the storage and on the temperature of the fluid: tanks catalogues provide information about the specific loss per unit of temperature difference between inside and outside, for each available size of the tank. Plotting point by point it possible to obtain the curve of the specific loss as function of the size of the tank. Generally, losses are in the range 1,65 W/K for the 150-litres type to 2,45 W/K for the 300-litres one.

The size of the storage is then translated in terms of energy, knowing the initial temperature of the stored fluid and the average return temperature of water from the circuits. Knowing the energy needs, the necessary volume in litres can be found from Eq.2.4:

$$Volume = \frac{Energy}{\rho \cdot c_{\mathrm{P}} \cdot (T_{\mathrm{storage}} - T_{\mathrm{return}})} \cdot 3600 \tag{2.4}$$

Where

- $Energy$ is the stored amount in Wh
- ρ is the density of water and is assumed to be 1 kg/l;
- c_{P} is the specific heat of water, equal to 4186 J/kg/K;
- T_{storage} is 55 °C for the DHW tank and 35 °C for the buffer tank;
- T_{return} is in both cases 25 °C.

The analysis is thus performed in terms of flows of energy (power) that is transferred from the tank to the users.

2.3 Electric Vehicles

The last load to determine is that for electric vehicle use: it is assumed to have two identical cars, characterized by 40 kWh of battery capacity and 300 km of autonomy: hence the specific energy consumption is 0,134 kWh/km.
The load required depends on the daily distance travelled and this value differs from weekdays to weekend days: from mobility surveys on driving patterns it is estimated that the daily travel distance in Germany is approximately 50 km for each car from Monday to Friday, while it increases slightly to 60 km on Saturday and Sunday [30].
The resulting assumed load demand for each vehicle is summarized in Tab.2.1:

		EV1	EV2
Mo-Fri	Daily travel distance [km/day]	60	40
	Energy consumed [kWh/day]	8	6
Sa-Sun	Daily travel distance [km/day]	60	30
	Energy consumed [kWh/day]	8	4

Table 2.1: Daily energy demand of the two electric vehicles for a typical week of the year

Weekdays load

During the weekdays, the load curve demand is estimated assuming a certain behaviour of consumption that it's suitable to people working during daytime, as shown in the table: when the row corresponding to each vehicle shows value 0 it means that it is not at home, while if the value is 1, the vehicle is at home and its battery can be recharged, if needed.
Fig.2.6 shows when the two vehicles are at home for each week day.

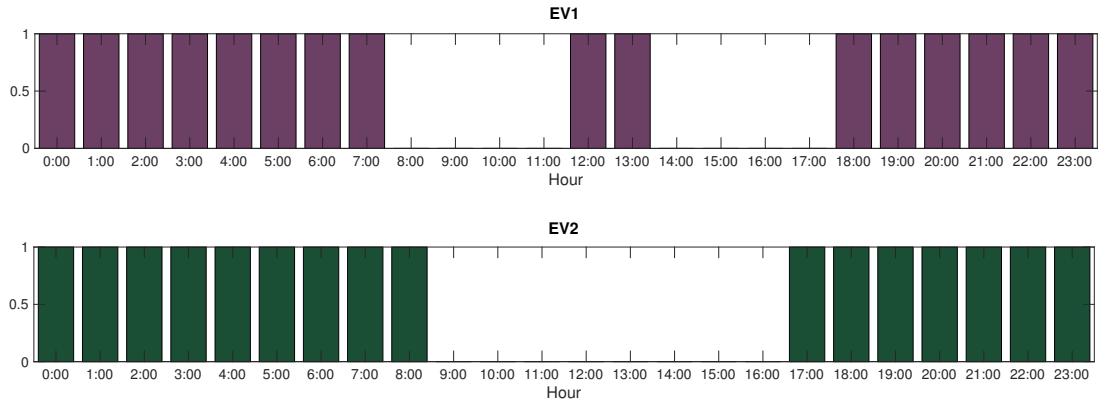

Figure 2.6: Weekdays use of the two vehicles

Weekend load

During weekend days, instead, the travel pattern cannot be considered constant, hence it is useful to rely on the mobility surveys [30] that presents data about the distribution of car trips by intervals of time during Saturday and Sunday, shown in Fig.2.7.
From the probability data it is possible to retrieve the total number of car trips occurring, for that specific interval of time and for the day considered, throughout the whole year: having 52 weeks in a year, the values are obtained as $probability * 52/100$, rounding to the closest integer. Moreover, it is assumed that no car trips occur from 1 to 6 of the morning. The results are summarized in Tab.2.2.
Figure 2.8 illustrates how to translate the probability into the Matlab code: it is first built a vector of 52 elements, having a certain number of identical values inside, as many as the number of trips occurring in that interval during the year, according to the day considered.
For each week of the year, the random function "randi(52)" selects a random value

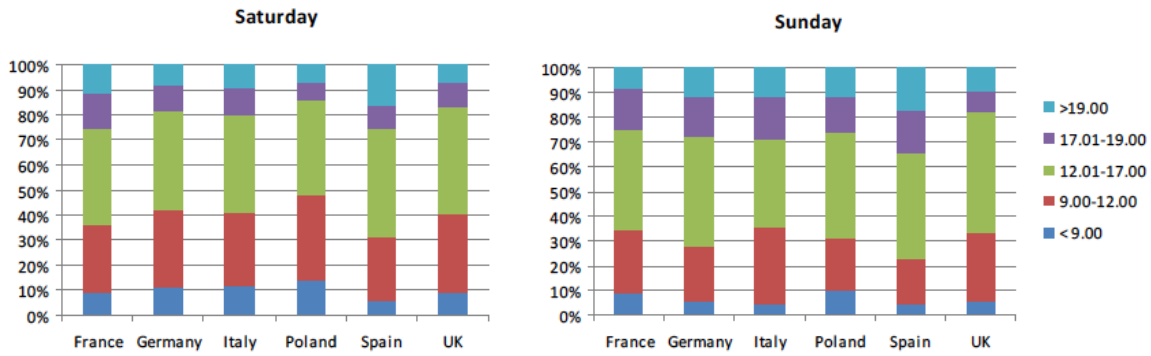

Figure 2.7: Car trip probability distribution by time of the day

		0:01-9	9:01-12	12:01-17	17:01-19	19:01-24
Saturday	Probability	10%	31%	40%	10%	9%
	Number of trips	5	16	21	5	5
Sunday	Probability	5%	23%	44%	16%	12%
	Number of trips	3	12	23	8	6

Table 2.2: Distribution of car trips

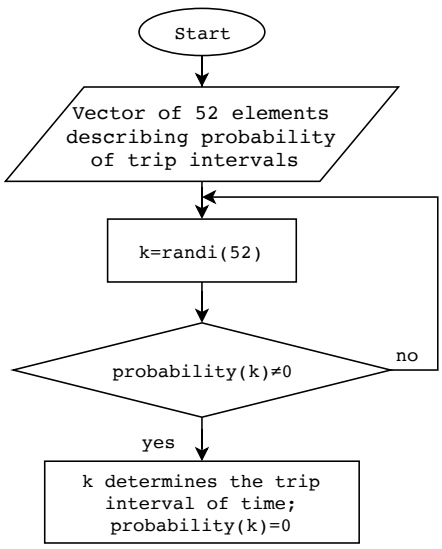

Figure 2.8: Choice of car trip interval of time

from 1 to 52: it is thus possible to pick inside of the predefined vector a value that corresponds to a specific interval. To make sure of obtaining the real probability of trip occurrence, at each iteration a value zero is substituted to the number picked by the random function: a new random value must be generated until it is picked up a number different from zero.
The procedure is the same for both vehicles: they have same probability but because of two different random functions, the selected values for trip occurrence will differ.

Once the intervals of time of car trip occurrence are obtained, the load curves of weekdays and weekend days are built, knowing the distance travelled, hence the power consumed. The vector describing the power consumption is always zero, except for the first instant of time after the end of the trip, for which it is assigned the total energy consumed during the trip. The resulting load curve of the two vehicles are shown in chapter 4.1.4.

Chapter 3

Generation Profile Identification

The purpose of this project work is to maximise the renewable fraction of electric energy consumption, specifically through the exploitation of solar and wind energy. At first, a feasibility study to estimate the potential producibility of the system must be undertaken: accordingly, it is necessary to collect data about available solar irradiation and windiness of the selected location.
Nowadays many reliable databases are available and in this case it is chosen to adopt values given by *Meteonorm*: the data are presented on hourly basis, referring to the year 2015, and include:

- Wind speed at several heights: 10, 22, 50 m;
- Temperature;
- Direct irradiation on horizontal surface [W/m^2];
- Diffuse irradiation on horizontal surface [W/m^2];

Afterwards, the technologies for power generation are chosen: in domestic applications, photovoltaic panels are commonly employed to exploit solar energy, while domestic wind energy production is still not as developed and widespread. However, it assumed that a micro wind turbine is adopted to support the solar energy production.
Finally, the yearly production is estimated on hourly basis combining weather data and a suitable mathematical model to describe the energy generation for the selected technology.

3.1 Solar energy

3.1.1 Resource assessment and technology overview

Solar energy is universally available at any location but with different intensity, according to the latitude of the location. At ground level, instead, solar radiation is affected by climatic conditions, that change greatly both throughout the day and different seasons of the year.

The exploitation of solar energy occurs through photovoltaic panels that are able to convert the solar radiation in direct current, thanks to the photoelectric effect. The incident radiation on the surface of a semiconductor material determines the generation of an electric field between the two layers of the panel, characterized by different charge. The electric potential inside the cell gives origin to a transfer of electrons that can be directed into an electrical circuit to produce current.

This technology is nowadays well established in the market, and although research led to the development of more advanced models, monocrystalline silicon panels are still the most adopted ones [28].

The evaluation of the energy produced is possible by first determining the total incident solar radiation on the panel, as shown in the next paragraph.

3.1.2 Mathematical model description

According to the isotropic sky model [22], the total irradiance on a tilted surface can be obtained from Eq.3.1, being the sum of the contributions of three different components: respectively, diffuse, reflected and direct (beam) irradiance.
Appendix C reports the complete procedure for its computation.

$$G_{\mathrm{T}} = G_{\mathrm{d}} \frac{1 + cos\beta}{2} + \rho_{\mathrm{g}} G \frac{1 - cos\beta}{2} + G_{\mathrm{b}} \frac{cos\vartheta}{cos\vartheta_{\mathrm{z}}} \tag{3.1}$$

Once the total irradiance is known, it is possible to obtain the value of the total irradiance on the solar panel, from Eq.3.1 and to compute the power produced by one panel according to Eq.3.2 [28].

$$P_{\mathrm{panel}} = P_{\mathrm{STC}} \cdot \frac{G_{\mathrm{T}}}{G_{\mathrm{STC}}} \left(1 + \gamma_{\mathrm{panel}} \cdot (T_{\mathrm{module}} - T_{\mathrm{STC}})\right) \tag{3.2}$$

Supplier's datasheets provide the specific characteristics of the panel that are necessary for the calculation of P_{panel}: γ_{panel} represents the temperature coefficient that determines the percentage variation of power output for each degree of difference between actual module temperature and standard one. T_{STC} and G_{STC} are the values of temperature and irradiance at Standard Test Conditions (G=1000 W/m^2, T=25 °C) that produce a power output equal to P_{STC}. Module's temperature can be determined in different ways, here it is chosen to adopt the Sandia's model that takes into account external air temperature, global irradiance and wind speed, v_{wind}, as shown in Eq.3.3.

$$T_{\mathrm{module}} = T_{\mathrm{external}} + G_{\mathrm{T}} \cdot \exp(a + b \cdot v_{\mathrm{wind}}) \tag{3.3}$$

The parameters a and b are experimental values and depend on the type of panel adopted: for a glass/cell/polymer sheet and close roof mount the values considered are a=-2,98 and b=-0,0471.

Thus, the total power produced by the photovoltaic system can be obtained multiplying P_{panel} times the number of panels adopted and by the average efficiency of

the inverter: solar panels produce direct current that generally cannot be exploited directly by domestic appliances and must be first converted in alternating current. It is reasonable to assume that inverter and overall system efficiency can be set to 90%, including all electrical losses.

3.2 Wind energy

3.2.1 Resource assessment and technology overview

Unlike solar energy, available at any location (although dependent on climatic condition), wind power is extremely site specific and varies significantly during the day and also from season to season.
Wind turbines are devices able to convert the kinetic energy of wind into mechanical energy, that is then transformed into electrical energy through a generator.
Power produced is proportional to the cube of wind speed at the turbine rotor, therefore it represents an important parameter that must be evaluated carefully when estimating the yearly energy generation: it is reasonable to choose a site characterized by an average wind speed higher than the cut-in one of the turbine, that is the value below which no energy can be produced.
Wind speed is certainly dependent on climatic conditions, but also depends on height: the greater the distance from the ground, the higher the wind speed, according to the boundary layer theory. Moreover, increasing height allows to reduce the interference of nearby buildings, trees and other elements that cause a reduction of wind speed. It is hence necessary to choose a suitable height of installation of the turbine's rotor.

Nowadays, wind turbines are mostly employed for large-scale power generation, however, it is possible to find also several domestic applications, that employ micro-turbines producing power in the range of few kilowatts.
In these cases, turbines are likely to be installed on the top of the roof of the building for simplicity of installation, since a supporting tower is not required, but also to avoid building interference with the wind trajectory. However, a two-floors single-family house, is unlikely to reach a sufficient roof height: therefore it is considered to install a stand-alone wind turbine with an own tower, in order to reach a height of 10 m, which is assumed to be the minimum height such that wind turbulence is avoided and a sufficient wind speed is reached.

3.2.2 Mathematical model description

The theoretical estimation of the power produced by a horizontal-axes wind turbine is possible thanks to the Betz theory that provides a simplified but useful model of the system. Starting from mass and momentum balances between two sections, one upstream and one downstream of the turbine, it is possible to obtain the maximum theoretical power production from Eq.3.4 [22].

$$P = \frac{1}{2} \cdot \rho \cdot A \cdot v_0^3 \cdot c_\mathrm{p} \tag{3.4}$$

Where

- ρ: density of air [kg/m^3];
- A: spanned area of the rotor [m^2];
- v_0: free stream wind speed (upstream the rotor) [m/s];
- c_p: ideal coefficient of performance, which is equal to 0,593. It represents the maximum fraction of available wind energy at turbine rotor that is actually exploitable.

In addition to that, an efficiency factor has to be considered to adjust the ideal formulation of the power produced.

The practical estimation of the power produced by the turbine depends substantially by the data provided by suppliers. Generally, it is presented a curve describing the electrical power output, function of wind speed, where three different critical values can be identified.
The first value is the already-mentioned cut-in speed, that sets the minimum wind speed for power production; the nominal speed, instead, is the one for which it is possible to achieve the nominal power output. The power produced between cut-in and nominal speed, as described in Eq.3.4, is proportional to the cube of wind speed, but in practice, values reported by the suppliers differ from this curve: it is then necessary to plot the curve point by point to obtain the intermediate values and have a more precise estimation of power produced.
Finally, the third critical wind speed value is the cut-off speed, above which no more energy is produced to prevent the turbine to be damaged. The power trend between nominal and cut-off speed is generally flat (increasing wind speed does not generate an increase of power output), or could also be decreasing. This differs from model to model, because of the different control strategies adopted for the regulation of power generation.

Finally, once the power curve is obtained, it is necessary to consider corrections due to external temperature variation, as shown in Eq.3.5, that affects air density: cold days are beneficial because of higher air density and thus greater power output.

$$P_{\text{wind,corr}} = P_{\text{wind}} \frac{T_{\text{STD}}}{T_{\text{external}}} \tag{3.5}$$

Where T_{STD}=288,15 K.

3.2.3 Battery storage

The importance of a battery storage system to couple to the renewable generation is nowadays out of the question, being vital to the compensation of the variable nature of these sources. Acting as a energy buffer tank, batteries allow to accumulate the excess energy produced during the day and to release it when the generation is not able to meet the demand.

A battery storage system is an electrochemical device that converts the stored chemical energy into electrical energy, operating also in the reverse way during the charging process. It is basically composed of two electrodes, one with positive and one with negative charge, which provide a certain electrochemical potential and which are immersed in an electrolyte, a substance able to transfer ions. Chemical reactions occur at both electrodes, which can absorb or release electrons: these are then collected to generate the energy flow.
The system is essentially dependent on the type of reactions that occur at the electrodes: a variety of different battery storage technologies are available, depending on the materials of the electrodes and electrolyte used. These differences have an influence on several parameters that have to be taken into account for the choice of the battery. In particular, specific energy (stored energy per kg of battery), lifetime and efficiency (ratio of the energy discharged divided by the energy charged within a certain period) are some of the most relevant.
Specifically, Lithium-ion technology presents outstanding performances from the point of view of the efficiency, close to 100%, and good values for energy density, in the range of 90–190 Wh/kg [32]. However, the downsides of this technology are its high cost and the lifetime reduction with deep discharge. Nonetheless, Li-ion batteries are gradually taking the place of the typical Lead-Acid batteries, which present many technical disadvantages but are less expensive.
Therefore, Li-ion batteries present the highest potential for future improvement and match well with the purpose of clean energy production [27].

The optimization process for the minimization of non-renewable energy consumption determines the size of the battery system, in terms of capacity: it refers to the net capacity, that represents the actual availability of storing energy. The necessary rated capacity is therefore derived from the value of net capacity obtained, according to the chosen battery model, which allows to obtain a value of net capacity as close as possible to the optimal one.

Chapter 4

Case Study Definition

In this chapter, the reference case study adopted for the analysis is presented to illustrate the results obtained for the load curves and generation profiles.
The typical household is assumed to be a family unit of four people, reasonably 2 working parents and 2 children, living in a single residential house.
It is assumed to adopt as reference case the North locality (latitude: 54,3734°, longitude: 9,3581°), which only determines a variation in the heating load curve.
Moreover, the methodology adopted for the analysis is presented.

4.1 Load demand

4.1.1 Electric appliances

Summing up the contributions of the different appliances considered in Appendix A, Fig.4.1 and Fig.4.2 illustrates the load curve for one typical week of the year. It is possible to observe how the demand is variable from day to day because of the random utilization of several appliances, and how it differs from week days to weekend days.

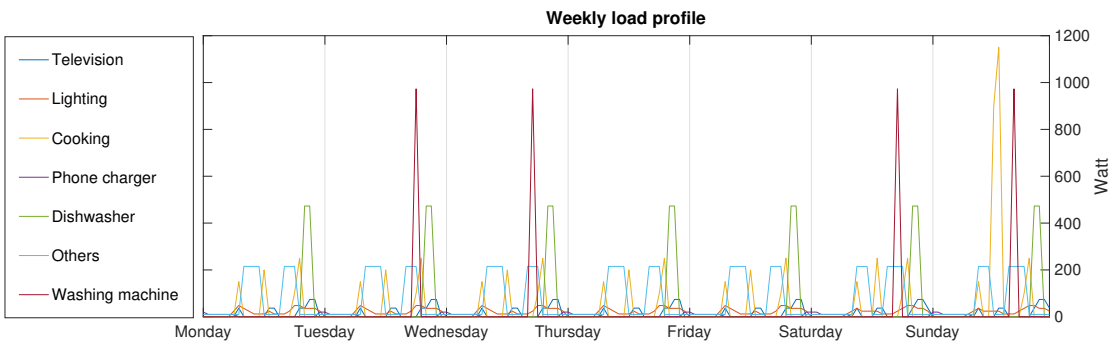

Figure 4.1: Electric appliances' weekly load demand split by component

Observing the week days profile, it is evident that evening generally presents higher peaks of demand; weekend days are instead characterized by higher overall energy consumption, assuming that the households have more time to spend at home.
The overall yearly energy consumption results to be 2171,1 kWh, which is well

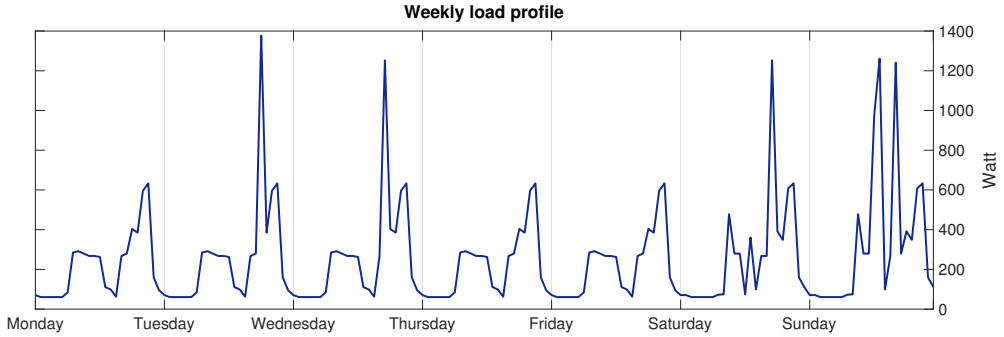

Figure 4.2: Overall electric appliances' weekly load demand

below the average of a German household (around 3000 kWh [21]): this is in line with the expectation, because of the choice of adopting low-energy-consuming and up-to-date models.

4.1.2 Space heating

The energy demand for space heating is essentially dependent on the external air temperature, whose trend is illustrated in Fig.4.3, and on the value of the design heat load, obtained following the procedures described in Appendix B.

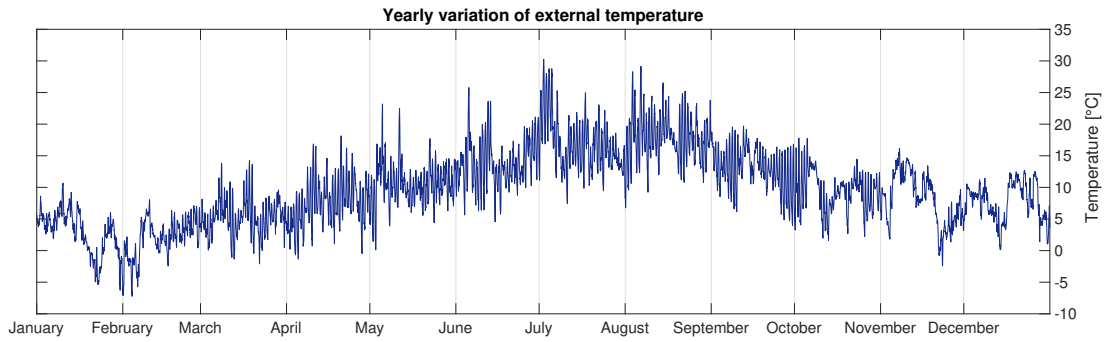

Figure 4.3: Yearly variation of external temperature for North locality

From the National Annex to the EN 12831 norm for the calculation of the design heat load, the design external temperature corresponds to $-10\,°C$ for the North location: the corresponding heat load is 4625 W.
Considering a linear variation of the heating demand with the external temperature, as described in 2.2.1, the final load profile is presented in Fig.4.4. The heating load is set to zero in the summer period, characterized by average external temperature higher than $16\,°C$. The total yearly heating demand results to be equal to 10,152 MWh_{th}.

4.1.3 Domestic Hot Water

The final load for domestic hot water, considering a four-people household, is presented in Fig.4.5, showing the daily profile. It keeps constant throughout the year and the total demand is equal to 3,866 MWh_{th}.

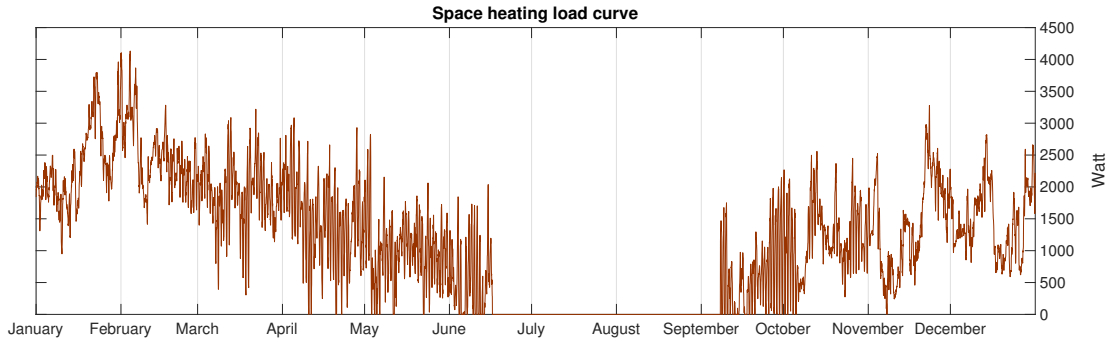

Figure 4.4: Yearly space heating load curve for North locality

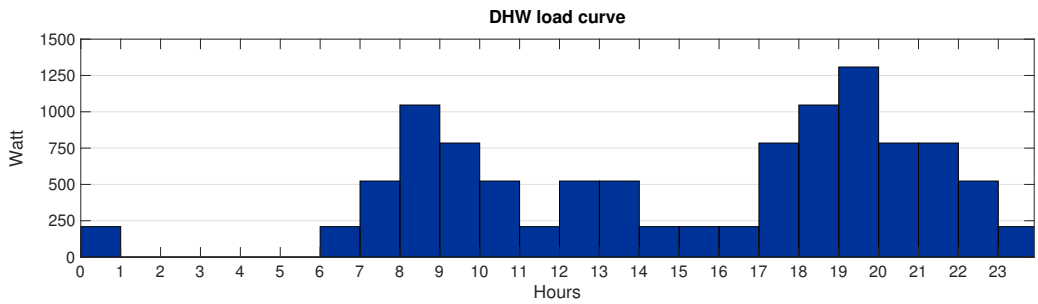

Figure 4.5: Daily Domestic Hot Water load curve

4.1.4 Electric vehicles

The consumption pattern of the two electric vehicles is shown in Fig.4.6, which represents the trend for one week of the year: while weekday load keeps constant, weekend load is subject to a random pattern, described in 2.3, which defines a different profile for each week of the year and for each vehicle. The total yearly energy demand results to be 4,888 MWh.

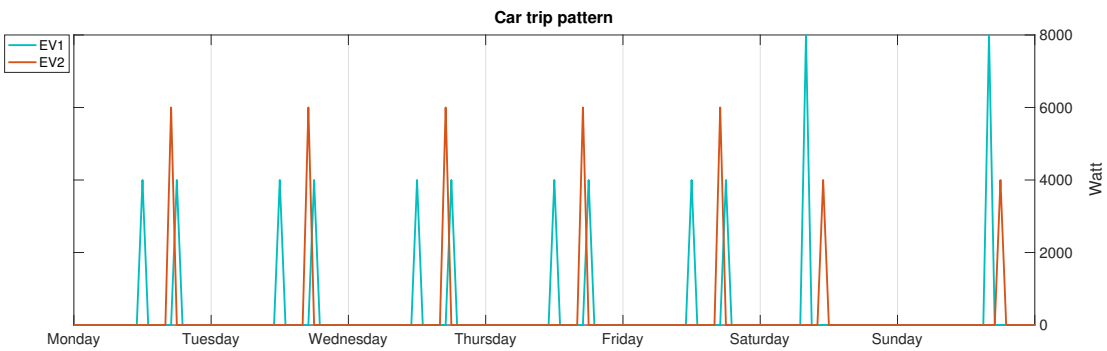

Figure 4.6: Consumption pattern for the two electric vehicles for one week of the year

4.2 Generation Profile

Starting from the information on irradiance and windiness of the selected locality, the yearly profiles of solar and wind production are illustrated.

4.2.1 Solar energy

Referring to the selected location, the available data allow to reproduce the yearly profile of the global incident solar irradiance on the panels' surface.
For the considered household, a 50°-tilted and south-oriented roof is used to install the panels, resulting in a total incident irradiation on the surface of 0,998 MWh/m^2. The yearly profile is shown in Fig.4.7.
Choosing to adopt high-tilted surfaces it is possible to increase the solar energy production during winter season, characterized by low solar altitude. Therefore, the available irradiation results to be more distributed during the year, rather than concentrated in summer season if low-tilted surfaces were adopted.

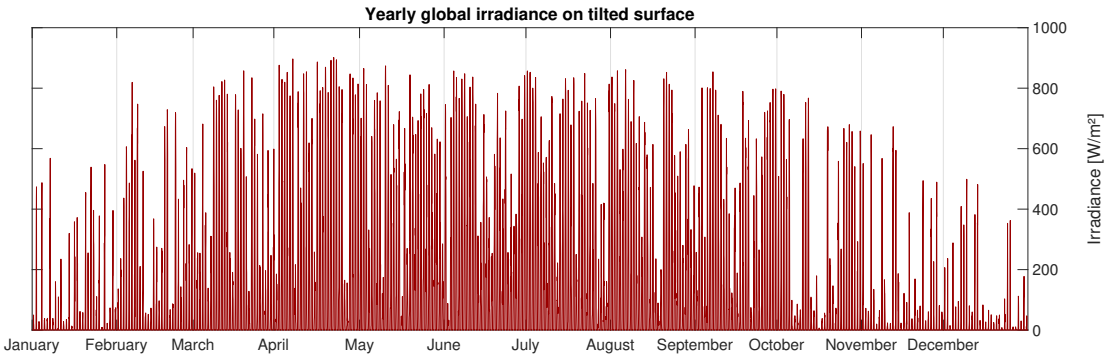

Figure 4.7: Yearly profile of global irradiance on a 50°-tilted surface

Considering to adopt solar panels of the type aleo solar S19 HE, 310 W of nominal power output and dimensions 0,99 x 1,66 m^2, it is possible to install a maximum number of panels equal to 30, having a total useful surface of 58,4 m^2.
The resulting total maximum installed capacity is 9,3 kW.

Finally, correction for the module temperature variation with external ambient conditions is made, and inverter efficiency, set to 90%, is considered.
The resulting yearly solar energy produced by 30 panels, 50°-tilted, is 8,04 MWh/year.

4.2.2 Wind energy

According to the information about windiness of the site, the average wind speed results to be 4,43 m/s at 10 meters from the ground.
It is chosen to adopt a vertical-axes micro turbine of the type SKYLINE SL-10, with a rated output of 1 kW and cut-in speed of 2 m/s. The specific turbine power curve is illustrated in Fig.4.8, while Fig.4.9 shows the yearly power generated according to the actual wind conditions.
The turbine allows to generate 885,5 kWh/year, which increase to 902,2 kWh/year

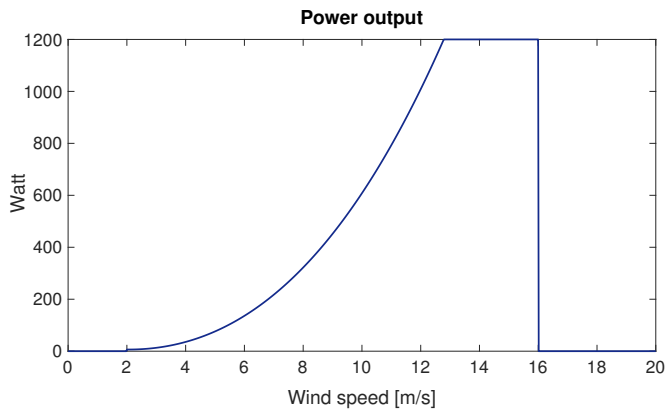

Figure 4.8: Electrical power output curve of the selected wind turbine

considering corrections for external air temperature. Micro wind generation is then able to only satisfy less than half of the appliances demand: an economic analysis should be performed to understand the actual benefit of adopting a micro wind turbine.

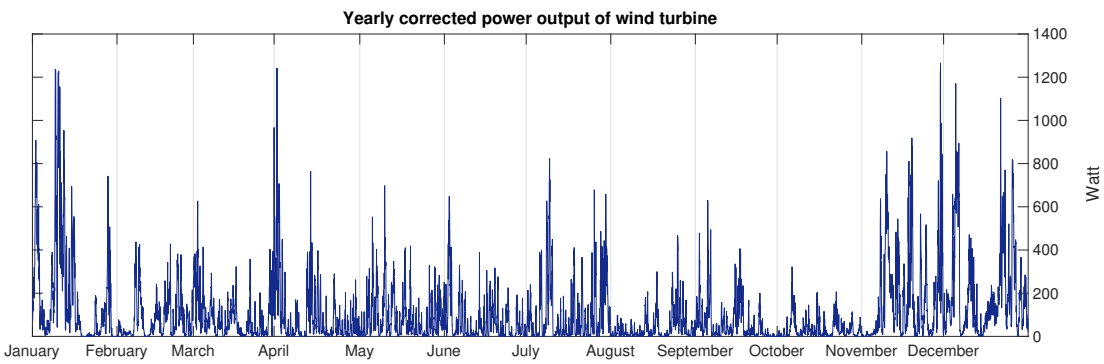

Figure 4.9: Yearly actual power output of the selected wind turbine

4.3 Analysis methodology

The present system matches the demand and the production of energy through the control logic described in Cap.5. The results obtained are described in Cap.6 and are presented in terms of heat pump operation and recharge of the electric vehicles to verify that the household needs are fulfilled. Finally, the system is optimized in terms of minimum grid energy consumption, as described in Cap.7. It is here described the method of Discounted Cash Flow, adopted in the optimization analysis to determine the economic feasibility of the system.

Discounted Cash Flow

It is possible to evaluate the effect of an investment basing on the actualization of cash flows generated by the given system all over the system lifetime; a selected

discount rate takes into account the risk factor and is adopted in the actualization. It is hence calculated the Discounted Cash Flow according to Eq.4.1:

$$DCF = \sum_{k=0}^{n} \frac{CF_k}{(1+r)^k} \tag{4.1}$$

It is here considered n=20 years of lifetime for the whole system and a fixed discount rate equal to r=0,04, assuming to have a low-risk investment. CF_{k} represents the generated cash flow at time k. It includes the investment costs, which are sustained at k=0, and the variable costs associated to energy consumption, which are sustained each year.
It is also possible to write Eq.4.1 making explicit the investment costs term ($C_{\mathrm{investment}}$) as:

$$DCF = C_{\mathrm{investment}} + \sum_{k=1}^{n} \frac{CF_k}{(1+r)^k} \tag{4.2}$$

All the costs items present in the analysis are described below.

Cost items

The investment costs of each technology adopted in the several configurations are here presented:

- Heat Pump (C_{HP}): 8000 €. Referred to the model adopted in the analysis. The price includes a 200-l DHW tank [10];
- Electric Vehicle (C_{EV}): 25800 €. Referred to a Renault Zoe, which is taken as reference in the analysis;
- Buffer storage (C_{buffer}): 386,1 €. Referred to a 2000-Wh-buffer. A scale factor of 0,5599 is considered to adapt the price to bigger-capacity buffer. It is obtained by extrapolation of data provided by the manufacturer [1];
- Battery storage (C_{battery}): 400 €/kWh. Referred to Li-ion batteries LTO (lithium iron phosphate) for stationary applications in Germany in 2016 [17];
- Inverter and Control System (C_{inverter}): 2300 €. Referred to a tripower inverter (SMA Sunny Tripower 10000TL-20) of 10 kW of power [7].
- Gas boiler (C_{boiler}): 1000 €. It is considered an average price of several boilers present in the market, for a heating capacity of 10 kW;
- Internal combustion vehicle (C_{car}): 15000 €. Referred to a Renault Clio.

In addition, the variable costs associated to the consumption of energy are presented hereafter:

- Grid electricity cost (c_{el}): 0,295 €/kWh$_{\mathrm{el}}$. Referred to household end users in Germany in the first half of 2018 [3];

- Natural gas cost (c_{ng}): 0,0608 €/kWh$_{th}$. Referred to household end users in Germany in the first half of 2018 [8];
- Gasoline cost (c_{oil}): 1,45 €/l. Obtained as monthly average of 2018 data. Under the assumption of a fixed specific consumption for a standard car (Renault Clio) of 20 km/l, the final specific consumption results to be 0,0725 €/km [4].

Emission Analysis

An evaluation of the global CO_2 emissions from the adoption of each technology is made to compare the several system configurations. Knowing the energy needs of each sector and knowing the specific emissions, it is easily obtained the yearly amount of CO_2 produced.
The specific CO_2 emissions for each energy source are listed below:

- Grid electricity emission: 0,5 kg/kWh$_{el}$. Referred to the actual emission of power generation sector of Germany in 2017 [6];
- Natural gas emission: 0,2 kg/kWh$_{th}$. Referred to new gas boilers with high efficiency rating [15];
- Gasoline emission: 0,118 kg/km. Referred to average carbon dioxide emissions from new passenger cars in 2017 [2].

Chapter 5

Control Logic

So far the load demand analysis has been done for the three different kinds of load separately, furtherly splitting up the needs of each component. It is possible now to group the demand of each sector and to consider them in a sequential order, as illustrated in Fig.5.1: at first, the generated renewable energy ($P_{TOT,gen}$) is used to satisfy the demand of electric appliances ($P_{load,el}$), then that of the heating system (P_{hp}) and finally the demand of EV's batteries can be fulfilled. The remaining available energy is stored into the battery storage system.
Depending on the amount of energy generated, battery storage is needed when the renewable energy is not sufficient to directly satisfy the demand. Eventually, when also the amount of stored energy is insufficient, the grid supplies the necessary energy needed.

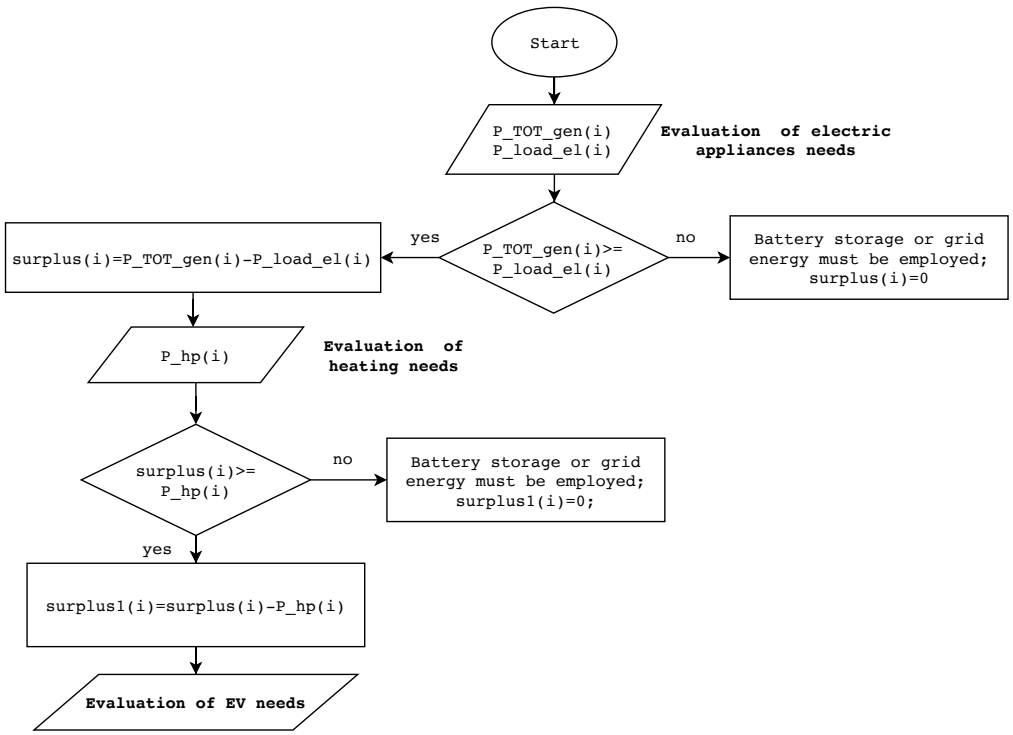

Figure 5.1: General control strategy

5.1 Electric appliances

Electric appliances' need is the first to be fulfilled, according to the defined sequential order. Therefore, in the second step, the net surplus of renewable energy is given by the difference between energy generation and electric appliances demand and is available to fulfill the heating load.

5.2 Heat pump

Control logic for heat pump operation has the task of ensuring the supply of water for sanitary use and for space heating, avoiding any periods of unmet demand. It is reasonable to keep always a minimum level of charge of both tanks. Indeed, for space heating supply, enough energy must be stored to cope with the low heat demand of transition periods (spring and autumn), that may fall below the limit of 25% of heat pump partialization. For domestic hot water, instead, a minimum level of charge is necessary to instantaneously supply water.

Figure 5.2 presents the main variables that have to be considered for the heat pump control strategy: at each interval of time, the program reads at first the inputs: heat demand of DHW and space heating (Q_{DHW} and Q_{heat} respectively), the state of charge of both tanks (SoC_{buffer} for space heating and SoC_{DHW} for DHW), the available renewable surplus and the external temperature.
Afterwards, heat losses are taken into account and DHW tank directly supplies the amount of energy needed.
Finally, the energy necessary to refill completely the storages is computed, as difference of the maximum capacity and state of charge of the considered tank.

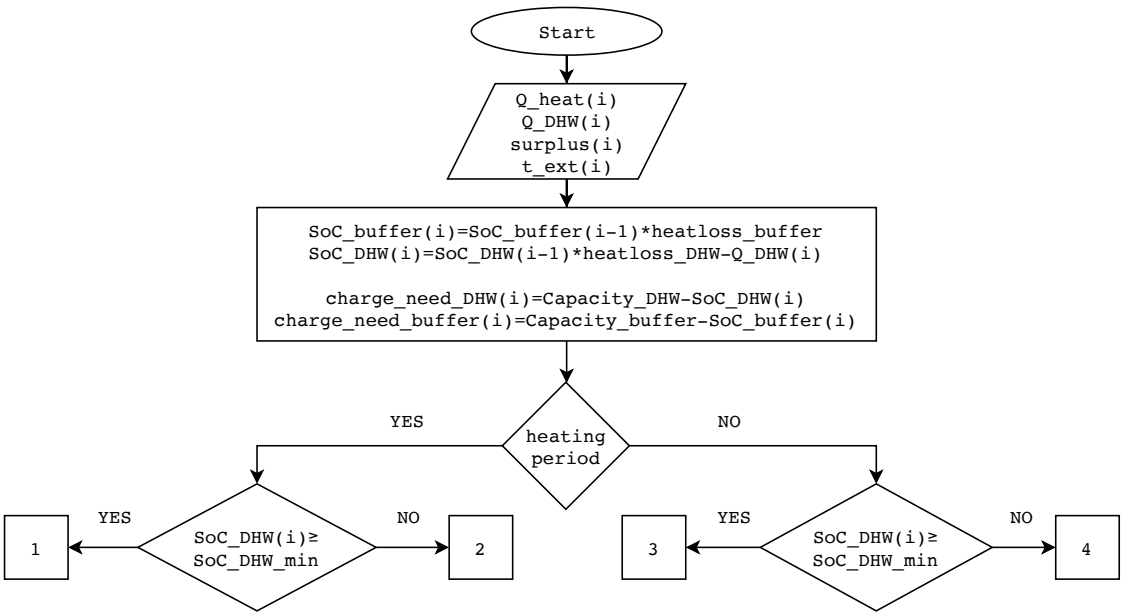

Figure 5.2: Heat pump control strategy

It is reasonable to have differentiation of the control strategy according to the period of the year, because of the huge variation of heating demand: in particular, it is first possible to distinguish between two cases that determine if the heating system is active or not (referred to as heating period) and then it is possible to vary the minimum level of charge of the buffer tank, according to the different season, to better match the demand.
The DHW load is, instead, constant throughout the year, so that no seasonal adjustment is necessary.
The characterization of the heating periods can be distinguished as follows:

- Winter season: it coincides with the period of the year characterized by strong and continuous heat demand, being the external temperature frequently much lower than 16 °C. To establish a convention, winter season is set to start from January, 1st until the first day of the year for which 16 °C are reached (between March and April). Then, it also goes from the first day in October characterized by external temperature lower than 16 °C, until the end of the year.
  In this season a proper level of minimum charge of the buffer tank must be set, in order to ensure to always satisfy the demand in the worst conditions. Moreover, this parameter has to be optimized to obtain reasonable switching on times of the heat pump: the higher the minimum state of charge, the more often heat pump will be switched on to recharge the storage.

- Summer season: it coincides with the period of the year characterized by an average external temperature higher than 16 °C, going from middle of May to middle of August. Consequently, heat demand is always set to zero for the whole duration of the period, and only DHW demand must be satisfied.

- Transition seasons: they are instead characterized by highly variable but less severe heating demand. Both space heating and domestic hot water must be supplied.
  As for the winter case, it is necessary to set a proper minimum level of charge of the buffer tank to minimize the switching on times the heat pump.

Once season-based distinction is made, the state of charge of the DHW tank is analysed to determine which tank has to be recharged and to consequently set the heat pump delivery temperature.
Therefore four main cases are possible, as described below.

Case 1: $\mathbf{SoC_{DHW} \geq SoC_{DHW,min}}$ and heating period ON

The first case is characterized by the DHW tank having a level of charge higher than the minimum value and heating system is switched on.
Figure 5.3 illustrates how to determine the power consumption of the heat pump and the amount of recharge of the buffer tank. At first, the level of partialization f is calculated as ratio between the sum of heat demand and amount of buffer recharge, over the maximum heat pump power. According to the value of f, three sub-cases are possible:

- $f > 1$: the heat pump can only deliver its maximum power. Therefore, if surplus is enough to satisfy the electric power absorbed by the heat pump, the buffer storage is recharged of a quantity equal to $Q_{\text{max,hp}}$ and heating demand is supplied.
  On the contrary, when surplus is not enough three sub-cases are analysed, which modify the heat pump operation in order to minimize the use of non-renewable energy:

  1.1 $\text{SoC}_{\text{buffer}} \geq \text{SoC}_{\text{buffer,min}}$ and $\text{SoC}_{\text{buffer}} \leq \text{Q}_{\text{heat}}$: stored heat is not enough to satisfy the demand but the state of charge is higher than the minimum value. In this case the heat pump delivers only the required space heating demand, independently from the availability of surplus;

  1.2 $\text{SoC}_{\text{buffer}} < \text{SoC}_{\text{buffer,min}}$ and $\text{SoC}_{\text{buffer}} \leq \text{Q}_{\text{heat}}$: the state of charge of buffer tank is lower than the minimum value and is not enough to satisfy directly heating demand. It is therefore necessary to run the heat pump at the maximum power, recharging the storage of an amount equal to ($Q_{\text{max,hp}}$ - Q_{heat}), independently from the availability of surplus;

  1.3 $\text{SoC}_{\text{buffer}} > \text{Q}_{\text{heat}}$: heat demand is directly satisfied from the storage and the heat pump is not switched on.

- $0,25 \leq f \leq 1$: the heat pump can deliver the whole heating demand and the buffer storage can be fully recharged, if surplus is enough. On the contrary, with insufficient surplus, the same previous three sub-cases hold true, with the same recharge strategy. The only difference lies in sub-case 1.2, for which complete recharge of the storage occurs;

- $f < 0,25$: it is not possible to switch on the heat pump, therefore, if heat is required, it must be supplied by the buffer storage.
  It is then checked if DHW tank recharge is possible, in case enough exploitable surplus is available. The same procedure described before for the recharge of the buffer is adopted, which is based on the values of f and the amount of surplus energy. In this case, a new value of f is computed and is determined as the ratio between DHW tank charge need and maximum heat pump power, while the delivery temperature of the heat pump is set to 55 °C.

  - $f > 1$: the heat pump is switched on to supply the maximum power, but only if surplus is greater than the equivalent electrical load; in this case the DHW tank is recharged of a quantity $Q_{\text{max,hp}}$, otherwise it is not recharged;
  - $0,25 \leq f \leq 1$: the heat pump supplies the desired amount of heat, only if surplus is enough to satisfy the equivalent electrical load: in this case the DHW tank is completely recharged;
  - $f < 0,25$: it is not possible to switch on the heat pump and charge the storage.

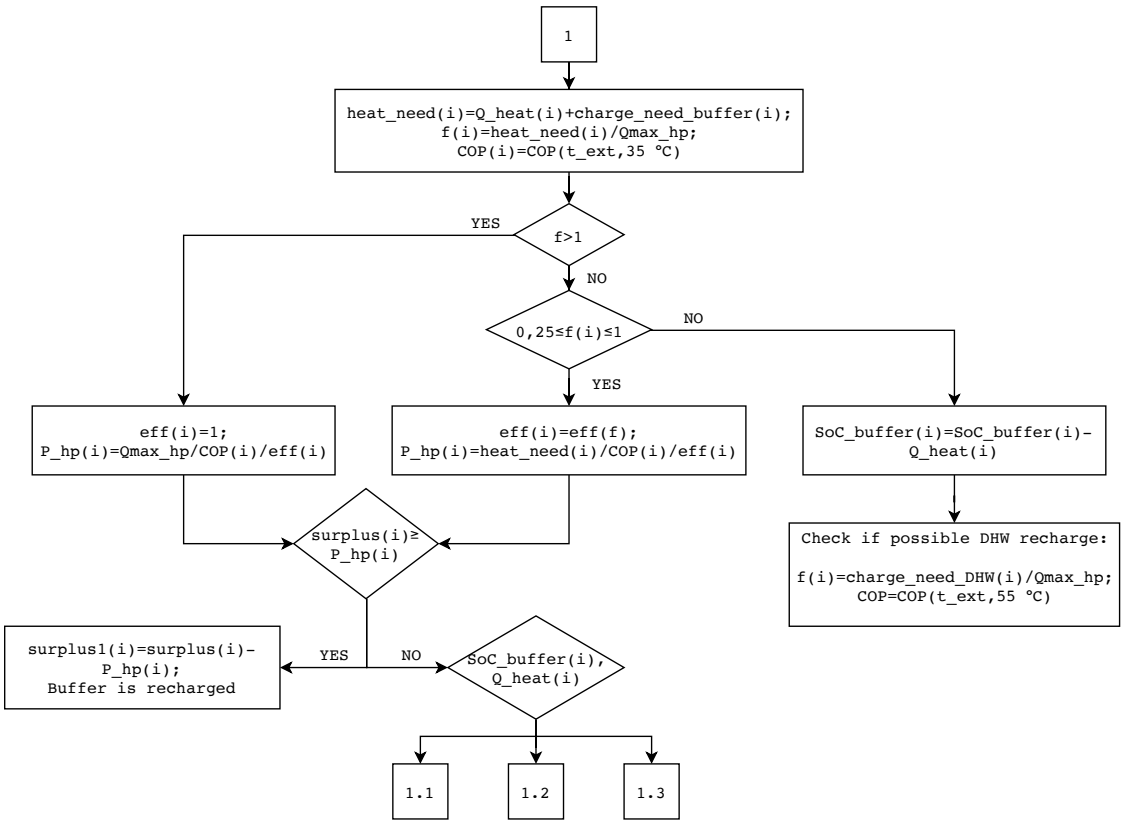

Figure 5.3: Heat pump control strategy: Case 1

Case 2: SoC_{DHW}<$SoC_{DHW,min}$ and heating period ON

The second case, illustrated in Fig.5.4, is characterized by heating system switched on and DHW tank having a level of charge lower than the minimum value: it is therefore necessary to recharge it. In first place, the state of charge of the buffer is analysed:

- SoC_{buffer}>Q_{heat}: the buffer is discharged to supply space heating. It is then necessary to recharge only the DHW storage tank, setting the heat pump deliver temperature to 55 °C; the partialization level f is computed as ratio between DHW tank recharge demand and maximum heat pump power;

- SoC_{buffer}≤Q_{heat}: the buffer is not able to satisfy the heating demand, it is then necessary for the heat pump to supply it, together with the necessary recharging heat for the DHW storage, at 55 °C. The partialization level f is computed as ratio between DHW tank recharge demand plus heating demand, and maximum heat pump power.

According to the value of f obtained, different cases are possible which determine the heat pump output. In Case 2, surplus available is not relevant to the control strategy since using heat at 55 °C for heating demand or recharge of the buffer gives rise to an inefficient process since mixing of cold water is necessary to achieve the right temperature.
Therefore, once the heat pump electrical power is determined, it will be supplied,

according to the availability, by the renewable surplus first, then battery storage and finally grid, in case the previous ones are not sufficient.

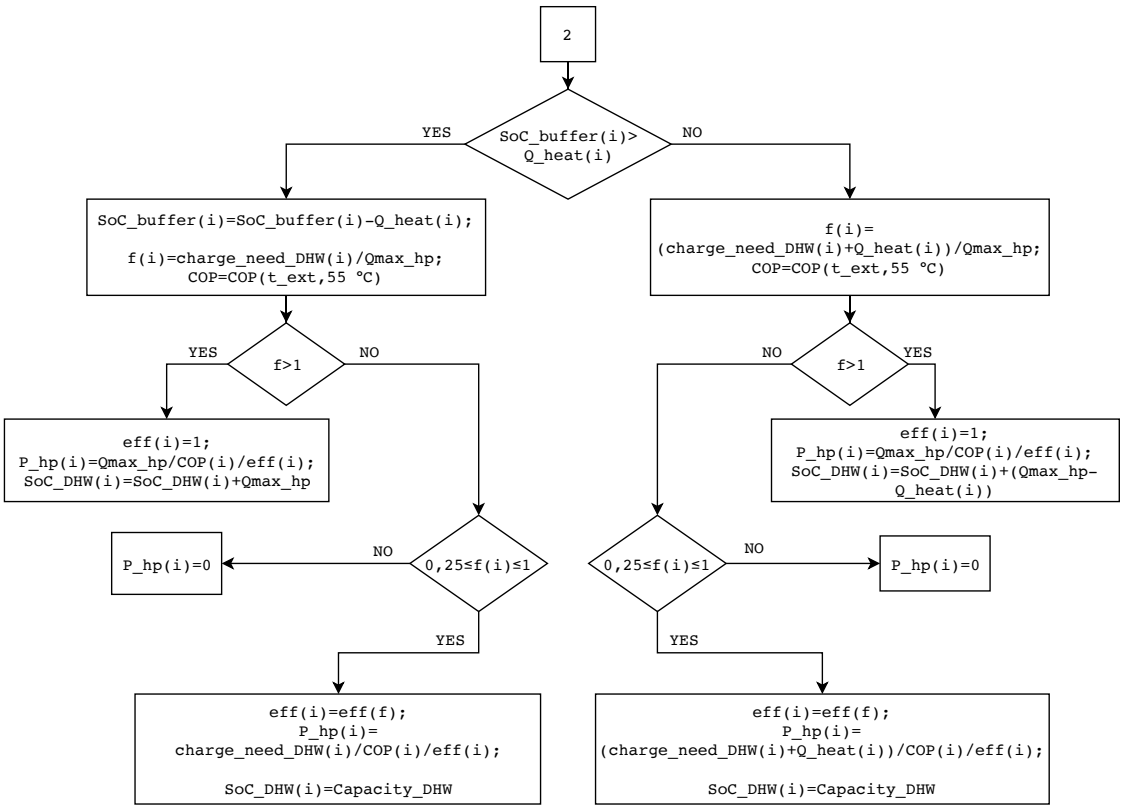

Figure 5.4: Heat pump control strategy: Case 2

Case 3: $SoC_{DHW} \geq SoC_{DHW,min}$ and heating period OFF

The third case is characterized by the DHW tank having a level of charge higher than the minimum value and heating system is switched off.
Fig.5.5 illustrates the control strategy adopted: in this case, recharging the DHW tank is not mandatory and it is accomplished only when enough renewable surplus is available to run the heat pump. The power absorbed by the heat pump depends on the level of partialization required, which is computed as the ratio between DHW tank recharge demand and maximum heat pump power.
This strategy allows to exploit the available renewable energy, but implies that the heat pump has to be switched on more times, increasing the cyclic on/off operation. It is possible to reduce it by imposing a higher minimum partialization level, instead of the standard 25%.

Case 4: $SoC_{DHW} < SoC_{DHW,min}$ and heating period OFF

The fourth scenario, illustrated in Fig.5.6 is characterized by the DHW tank having an insufficient level of charge and heating system is switched off. The recharge of the DHW tank is independent from the level of surplus, being only linked to the level of charge: it takes place every time f is greater than 25%

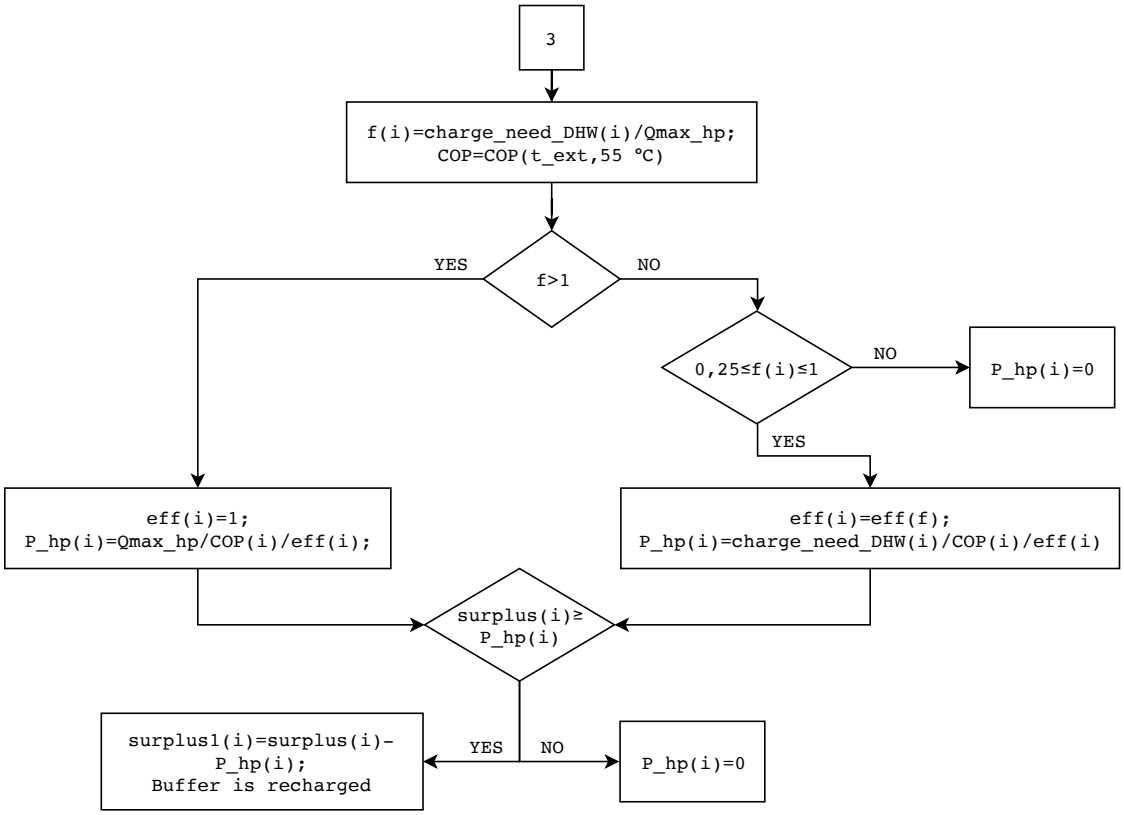

Figure 5.5: Heat pump control strategy: Case 3

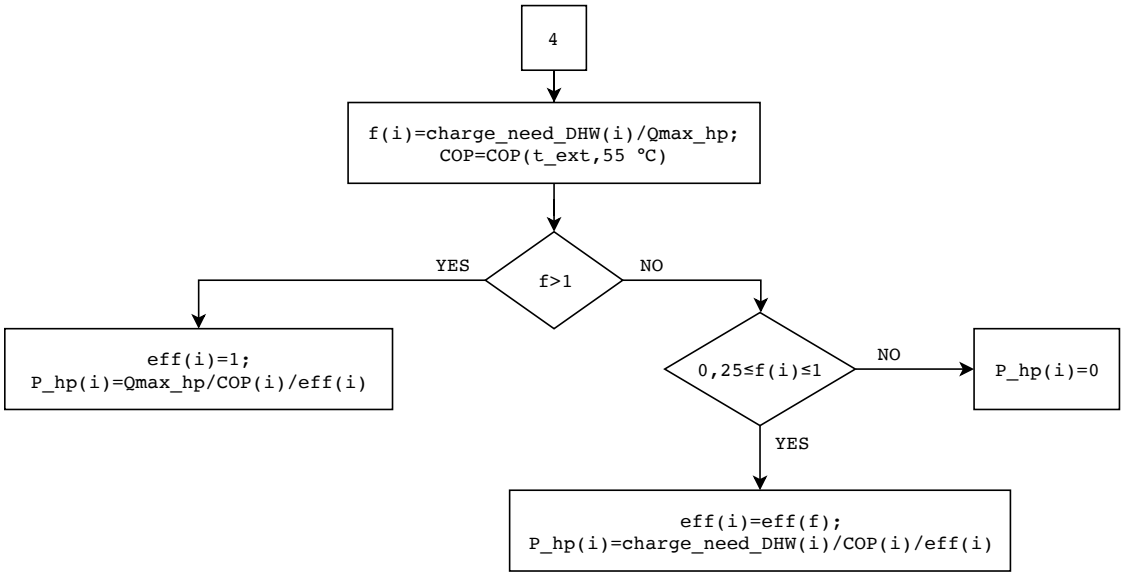

Figure 5.6: Heat pump control strategy: Case 4

5.3 Storage battery and electric vehicles recharge

It is now necessary to define a possible recharging strategy for the storage system to minimize the grid energy consumption.
Electric vehicles' batteries and the battery storage system are treated in this paragraph together, being EV both a source of energy consumption but also means to the storage of energy.
Although different strategies are possible, surplus renewable energy, when available, should always be exploited: small but frequent amount of charge are beneficial to modern batteries, rather than huge charge and discharge cycles.
When dealing with EV, if the surplus renewable energy is not enough to recharge sufficiently the batteries, then a certain amount of energy from storage or grid is required. In order to minimize this quantity, the target state of charge of the battery is set to a minimum level, and is kept fixed in time.
A suitable value must be chosen and at the end of the simulation it is necessary to check that the state of charge of the two vehicles is never below zero, to ensure a complete fulfillment of demand for transport.

Another significant aspect that must be considered, is the constraint on the maximum power charge of electric vehicles: old domestic recharging stations were usually sized to deliver a maximum power of 3,7 kW. However, this value is definitely not suitable when renewable energy is concerned: consistent amounts of energy would be wasted if the system is not able to handle high renewable surplus.
At the present, commercially available high-power recharging stations can reach up to 20 kW, which is the value assumed in this analysis for the constraint on maximum power charge.

The main inputs to consider are shown in Fig.5.7. P_{car1} and P_{car2} are the vectors describing the load curve of the two vehicles; home1 and home2 are the vectors describing the presence of the car at home; then the state of charge of the vehicles' batteries and the available renewable surplus are considered.

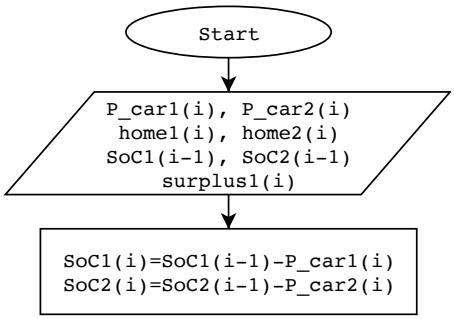

Figure 5.7: Main inputs for EV recharge strategy

According to the values of home1 and home2, SoC1 and SoC2, four main cases are possible:

- Case 1: EV1 is at home and needs charge, while EV2 is either not at home or does not need charge;

- Case 2: EV2 is at home and needs charge, while EV1 is either not at home or does not need charge;
- Case 3: Both vehicles are either not at home or don't need charge, or mixed cases;
- Case 4: Both vehicles are at home and need charge.

A suitable recharging strategy must be identified, to define the priorities among the three batteries, especially when case 4 occurs.
The investigated strategies of recharge are described as follows.

Strategy 1

In first place, it is assumed that the priority of recharge is always given to one of the two vehicles, rather than to the main battery storage and that a complete recharge must be achieved.
In presence of surplus, the strategy is implemented as follows:

- Case 1: surplus1 is first used to achieve a complete recharge of EV1 while the remaining amount goes to the main battery;
- Case 2: surplus1 is first used to achieve a complete recharge of EV2 while the remaining amount goes to the main battery;
- Case 3: the whole available surplus1 goes directly to the main battery;
- Case 4: the first vehicle receives all the available renewable energy to completely satisfy its needs; the other vehicle, receives the surplus energy left from the previous step, recharging the battery as much as possible. Finally, surplus energy recharges the main battery;

When renewable surplus is not present, or is not enough to completely recharge the vehicles' batteries, energy from the main storage or grid will be needed, but only to achieve the minimum state of charge.
This strategy allows to reduce the losses given by flows of current associated to the charge and discharge process of the storage battery. However, the charging process cannot occur when the vehicles are not at home, which usually happens during the central hours of the day, characterized by higher energy production. Moreover, a complete recharge of the vehicles prevents the stored energy from being used for other purposes, other than transport itself.

Strategy 2

A second possibility is to keep the same priority of recharge as Strategy 1, with the only difference that the target state of charge of both vehicles is the minimum value; the surplus energy is sent to the battery storage.
In case of further excess, it is redistributed to the two vehicles, giving the priority to one of the two, which is recharged as much as possible.
In this way, it is possible to minimize the energy stored in the electric vehicles, that cannot be used to supply electricity to the other utilities.

Strategy 3

The third option is to give the priority of recharge to the main battery storage system, that receives all possible renewable energy.
In presence of surplus, the strategy is implemented as follows:

- Case 1: surplus1 is first used to achieve a complete recharge the main battery, while the remaining amount goes to EV1;
- Case 2: surplus1 is first used to achieve a complete recharge the main battery, while the remaining amount goes to EV2;
- Case 3: the whole available surplus1 goes directly to the main battery;
- Case 4: the main battery receives all the available renewable energy to completely recharge; if further surplus is available, it is sent to one of the two vehicles, which is recharged as much as possible. The other vehicle, receives the energy available from the previous step.

Chapter 6

Simulation and Results

In this chapter, after running the implemented Matlab program, the results obtained for the considered case study are presented and discussed.

6.1 Heat pump operation

Summing up the contributions of space heating and DHW demand, it is possible to obtain the thermal power that the heat pump must supply.
Specifically, the maximum heating power required is 5,18 kW, which determines the size of the heat pump. A heat pump with nominal power close to the maximum needed has to be chosen, among the commercially available models.
In this analysis it is chosen to adopt the air/water heat pump NIBE F2120-8, characterized by a nominal power of 6,2 kW.
Since the heating capacity is variable with the external temperature, it is necessary to check that the heat pump is always able to fulfill the demand. Crossing the curves of the building heating demand and that of the heat pump heating capacity at 35 °C [9], as function of the external temperature, it is possible to notice that the heat pump is able to satisfy the design heat load at the design external temperature (Figure 6.1).

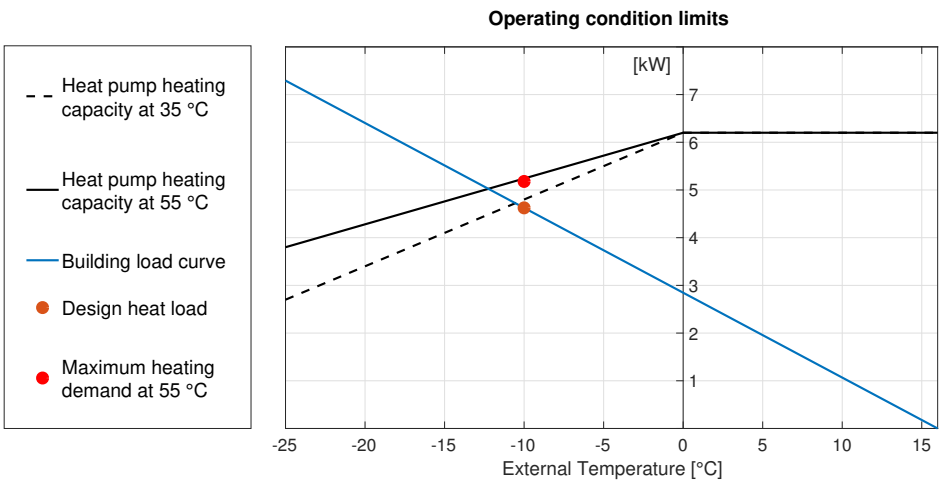

Figure 6.1: Definition of the operating condition of the heat pump

Moreover, the maximum possible load given by the sum of heating and DHW demand, can be satisfied at any moment by the heat pump at the delivery temperature of 55 °C and external temperature equal to −10 °C.
Both limiting cases of demand lie, from the above-mentioned graph, below the respective curves of heat pump operation, so a bigger-capacity heat pump would be unnecessary.
The selected heat pump presents a COP curve as described in Fig.6.2 [9].

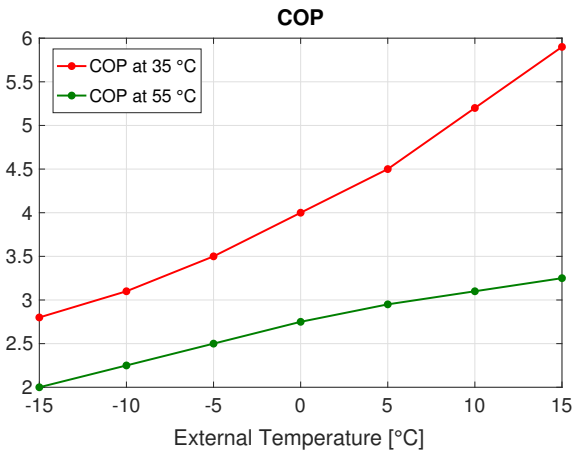

Figure 6.2: Variation of COP with external temperature, for different water delivery temperature

As a standard case it is advisable to adopt a buffer tank of 20-30 liters per kW of heat pump output and a DHW tank size of about 200 litres to satisfy the domestic demand for one day [19].
Therefore, a 180-litres buffer tank (corresponding to about 2100 Wh) and 200-liters DHW tank (corresponding to about 7000 Wh) are adopted. The minimum state of charge of the buffer storage is set to the 40% of the buffer capacity in winter and to the 20% in the transition period. The DHW storage's minimum level of charge is always kept to 1350 Wh, to satisfy the maximum peak load.
In order to analyse the behaviour of the system, it is useful to look at the curves of heat pump operation and state of charge of the storages for three different days having different load demand: one in winter, characterized by the lowest external temperature, one in spring when temperatures fall above 0 °C and one in summer when only DHW load is required.

Winter

In Fig.6.3 it is represented the behaviour of the heating system for one of the coldest days of the year in January, with external temperature always below 0 °C.
It is possible to see that the level of charge of the buffer tank is never enough to directly satisfy the heating demand, therefore the heat pump keeps always working: to face very cold days, it would be necessary to adopt a bigger storage.
Moreover, when the state of charge of DHW tank reaches the minimum value, the

heat pump increases its output to supply heat to recharge the storage and provide heating.

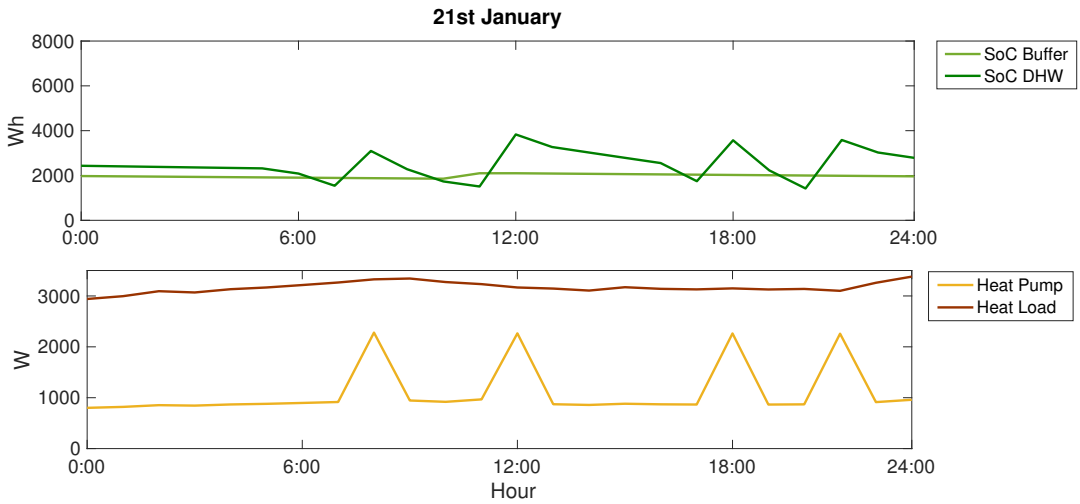

Figure 6.3: Buffer and DHW tank SoC variation and heat pump operation on 21st January

Spring

In Fig.6.4 it is represented the behaviour of the heating system for a typical day in April, being a transition period between winter and summer.
In this case, thanks to the higher temperatures, the heating demand can be directly satisfied from the buffer storage. However, frequent recharge is necessary, when the state of charge falls below the minimum value. The DHW storage, instead, is partially recharged during the day because of the presence of available surplus.
In this case, in order to stabilize the heat pump operation given by the availability of surplus, it would be possible to increase the minimum level of partialization, above the minimum value of 25%.

Summer

In Fig.6.5 it is represented the behaviour of the heating system for a typical day in July, when no heating is required and no recharge of the buffer storage takes place. In this case, only the DHW storage is recharged: in the central hours of the day the recharge occurs because of the presence of surplus, while in the evening it occurs because the minimum state of charge is reached.

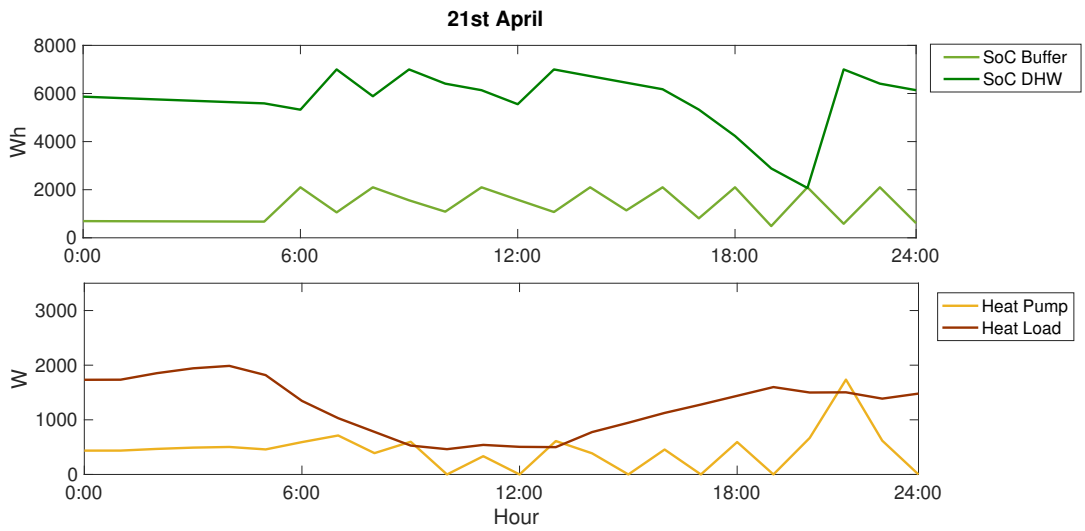

Figure 6.4: Buffer and DHW tank SoC variation and heat pump operation on 21st April

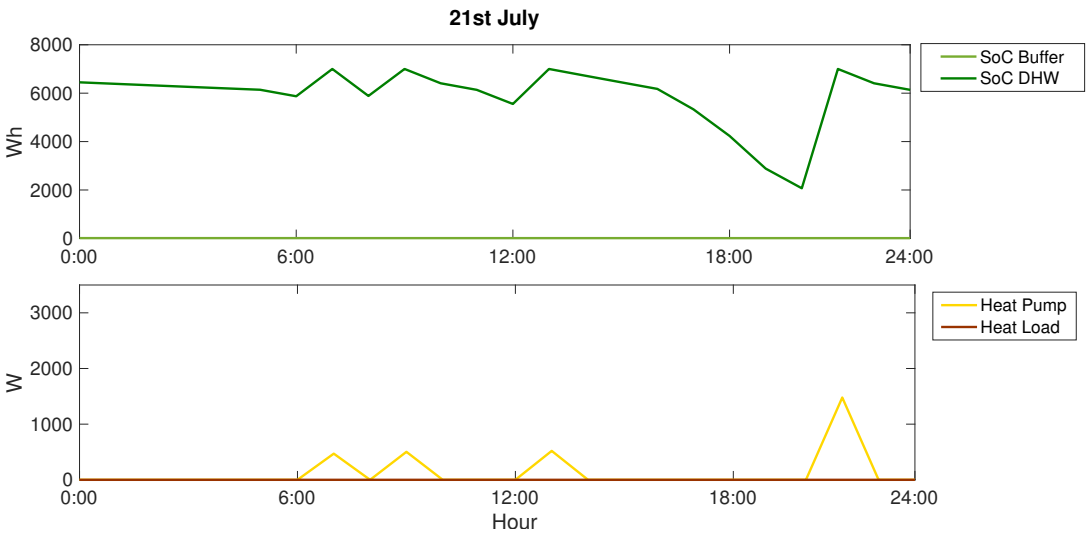

Figure 6.5: Buffer and DHW tank SoC variation and heat pump operation on 21st July

6.2 Electric vehicles and battery charge

As already mentioned in 3.2.3, a battery storage system is always adopted when domestic renewable energy generation takes place. However, a careful evaluation of the size of the storage is necessary to avoid unnecessary expenditures.
Different criteria can be adopted for the sizing of a battery system, which can rely either on the amount of energy generation, or on the energy demand.
Being solar energy production the major contribution to the renewable generation, and being greatly variable in intensity from winter to summer, in this analysis it is preferred to base the sizing of the battery on the household energy consumption.
In first approximation, it is considered that a fully-charged battery system should be able to satisfy the weekly demand for electric appliances only, in case of no renewable generation. Indeed, a standard household, in which no sector coupling takes place, would be provided with non-electric vehicles and gas boiler to meet the heating demand: the battery would only be necessary to satisfy the appliances needs.
In this case, the weekly electrical load corresponds to about 44 kWh: a net capacity of 40 kWh for the battery storage is therefore taken as reference.

Concerning electric vehicles, a minimum level of charge has to be set to always ensure sufficient charge for the following trip: in this analysis it is chosen to adopt a security factor equal to 1,2 with respect to the maximum energy consumption in one trip. It follows that the minimum charge for Electric Vehicle 1 is 9,6 kWh while for Electric Vehicle 2 is equal to 7,2 kWh.
From the information about batteries' dimensions, minimum charge and load curves, the weekly variation of the level of charge for the vehicles and the storage battery is illustrated, together with the available renewable surplus, before and after the recharge.
The following figures present each curve for each recharge strategy, and for two significant seasons of the year, winter (January) and summer (July).

6.2.1 Strategy 1

Figure 6.6 refers to Strategy 1 for the recharge of the batteries. In this case, Surplus' represents the available net surplus from the electric appliances and heating needs, which is directly used to recharge at first EV1 and then EV2. Surplus" represents the energy remaining from the previous step, which is then sent to the battery storage. Surplus"' is the excess energy that cannot be exploited in the recharge process.
In winter period, Surplus' is used to recharge EV1, which in some cases is able to achieve a level of charge higher than the minimum value, while this does not occour for EV2 because of insufficient surplus. No available renewable energy is left from the recharge of the battery.
In summer period, the vehicles are able to reach much higher values of charge, however some renewable surplus is left unused: from one side the size of the battery is unable to collect the whole surplus, from the other, cars cannot be always charged because they are not at home.

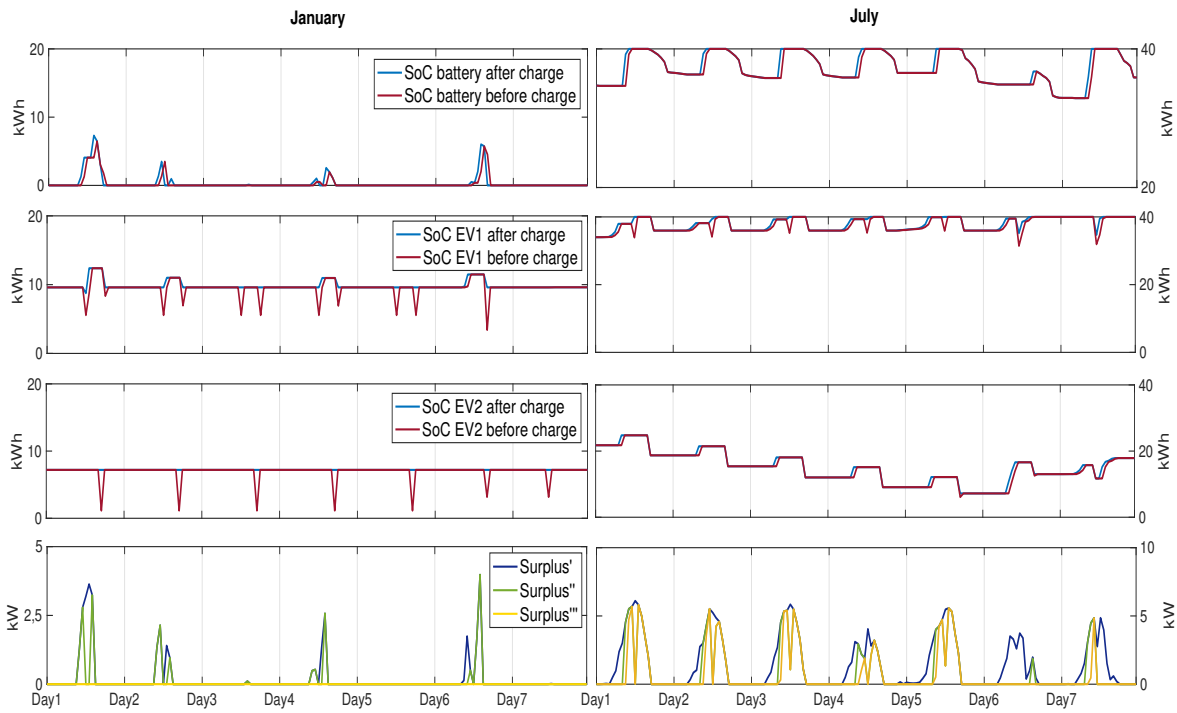

Figure 6.6: Weekly variation of battery charge and surplus for Strategy 1 for a typical day in January and July

6.2.2 Strategy 2

Figure 6.7 refers to Strategy 2 for the recharge of the batteries. In this case, Surplus' represents the available net surplus from the electric appliances and heating needs, which is directly used to recharge at first EV1 and then EV2, but only up to the minimum state of charge. Surplus" represents the energy remaining from the previous step, which is then sent to the battery storage. Surplus"' is the excess energy that cannot be exploited in the recharge process.
In this case, the battery is able to collect a higher amount of energy than the previous case and the two cars are always kept at the minimum charge level in winter. Also in this case, however, summer period is characterized by some renewable energy excess.

6.2.3 Strategy 3

Figure 6.8 refers to Strategy 3 for the recharge of the batteries. In this case, Surplus' represents the available net surplus from the electric appliances and heating needs, which is entirely employed to recharge the main battery storage: indeed, it is characterized by higher level of charge. Surplus" represents the energy remaining from the previous step, which is then sent to EV1 first and EV2 later. Surplus"' is the excess energy that cannot be exploited in the recharge process.
Because of the battery storage recharge priority, in this case the recharge of the vehicles occurs using battery's stored energy when Surplus" is zero: in winter period, both vehicles' charge is kept at the minimum value.

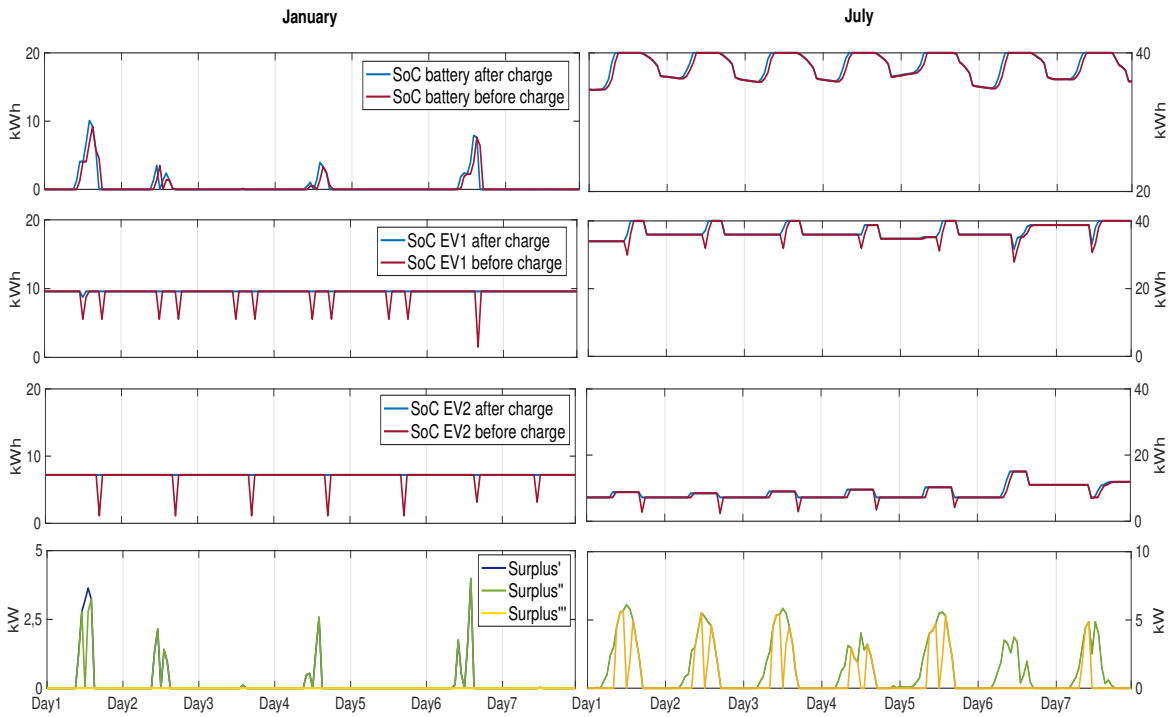

Figure 6.7: Weekly variation of battery charge and surplus for Strategy 2 for a typical day in January and July

Summer period does not differ much from the previous case because of the high excess of renewable generation.

6.2.4 Strategy 4

Figure 6.9 refers to Strategy 4 for the recharge of the batteries. In this case, Surplus' represents the available net surplus from the electric appliances and heating needs, which is entirely employed to recharge the main battery storage. Surplus" represents the energy remaining from the previous step, which is then sent in equal amount to EV1 and EV2. Surplus"' is the excess energy that cannot be exploited in the recharge process.
However, no significant differences are evident in comparison with Strategy 3, except for summer period, for which the difference of charge between the vehicles is less evident.

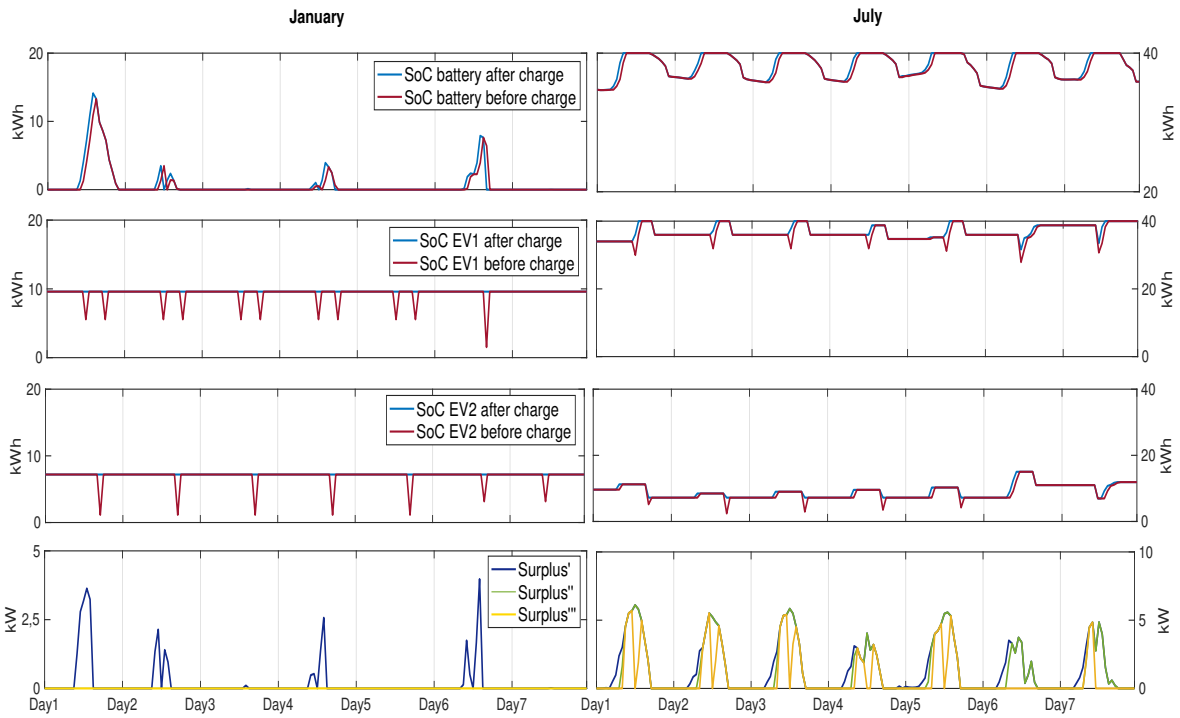

Figure 6.8: Weekly variation of battery charge and surplus for Strategy 3 for a typical day in January and July

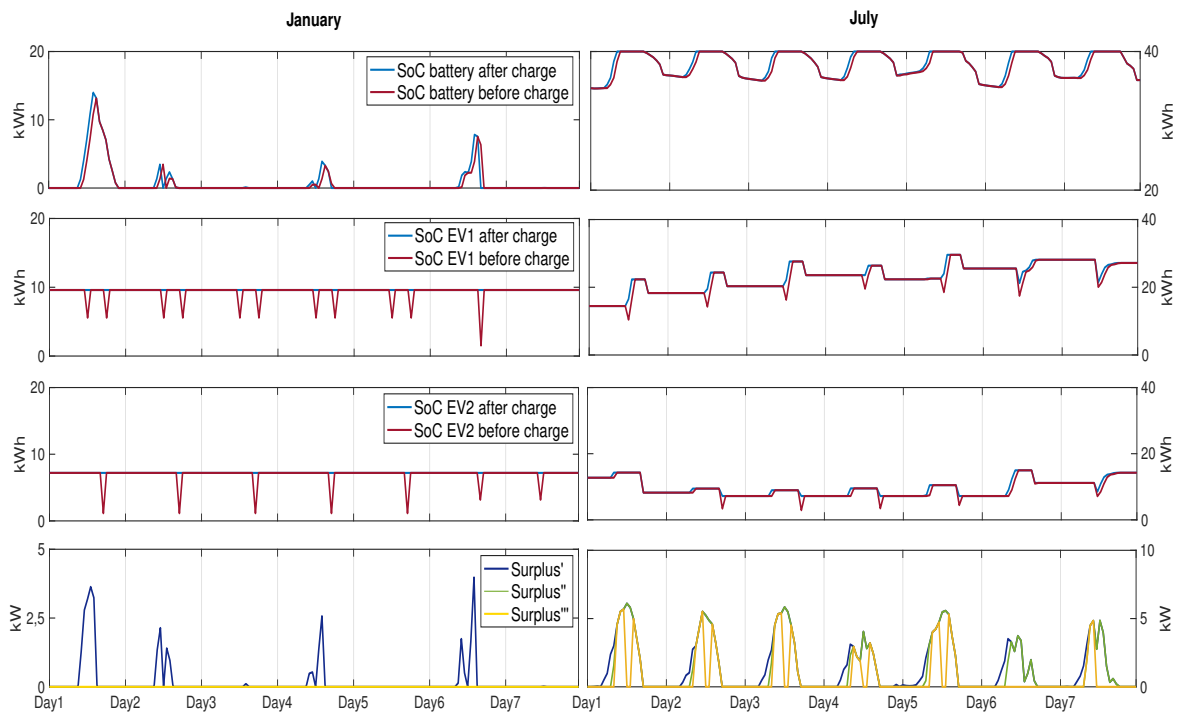

Figure 6.9: Weekly variation of battery charge and surplus for Strategy 4 for a typical day in January and July

6.3 Energy balances

Summing up the different energy flows, it is possible to compare the energy needs for the different sectors and how the system is able to satisfy them. As reference case is taken Strategy 3 for the batteries recharge, which gives priority to the main storage battery.
Figures 6.10 and 6.11 compare the total household demand with the total renewable power generation, giving as output the total grid consumption.

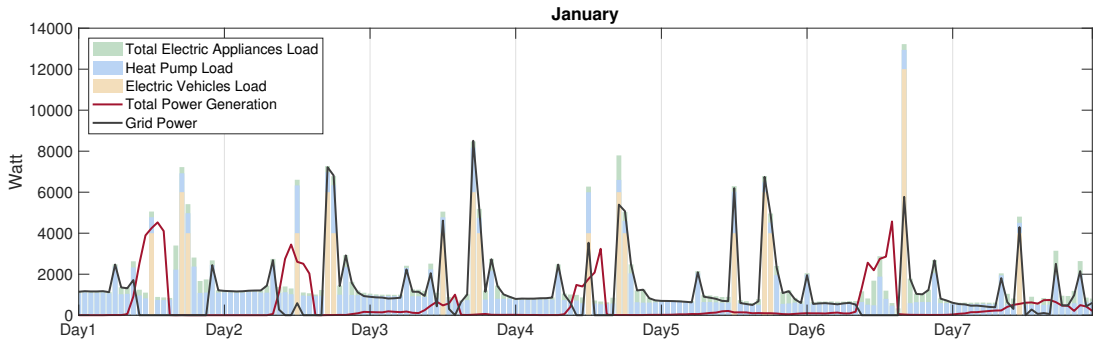

Figure 6.10: Loads and generation profiles for a typical week in Winter period

Figure 6.10 refers to one week in January: it is possible to see that the total power generated is low and not sufficient to satisfy itself the entire demand, especially because of the important contribution of heating.
When grid power results to be zero, either energy is entirely supplied by the battery storage, or electric load is shifted: this occurs for the electric vehicles, for which the energy consumption does not necessarily correspond with the actual moment of battery recharge.
Figure 6.11, instead, refers to a typical week in July: the combined effect of reduced load demand because of the no-heating season and the higher amount of energy generation results in the complete independence from the grid.

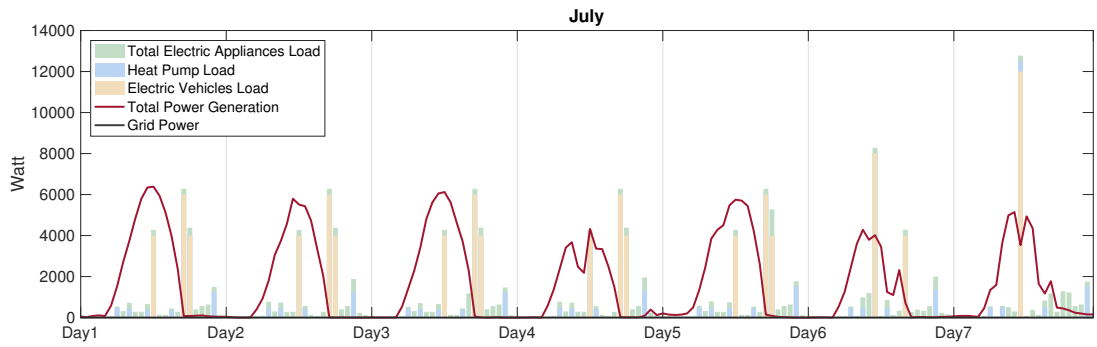

Figure 6.11: Loads and generation profiles for a typical week in Summer period

In conclusion, it is possible to determine the final value of grid energy consumption throughout the year. However, because of the random profile of several loads, each simulation is characterized by a different output value. Considering for

example 200 simulations, the difference between the maximum and minimum value of grid energy can vary in the order of 10^5, over a result in the order of magnitude 10^6. It is therefore necessary to calculate an average value: as shown in Fig.6.12, increasing the number of simulations, the oscillation is strongly reduced.

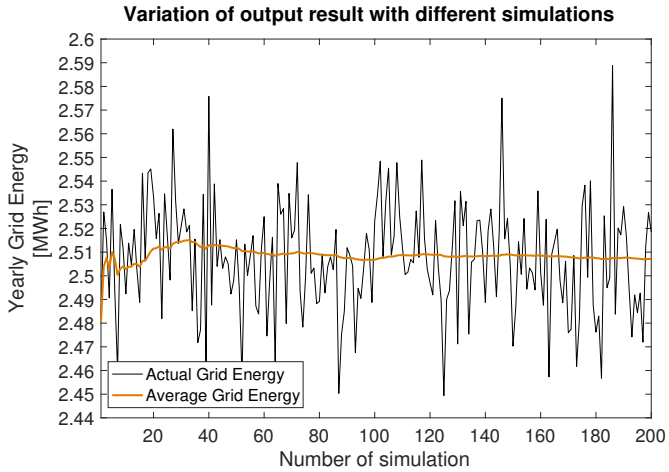

Figure 6.12: Variation of total grid energy value with different simulations

From 100 simulation on, the maximum difference between values of average grid energy is in the order of 10^3, over a result in the order of magnitude 10^6. Therefore, 100 simulations can be considered enough to obtain a sufficiently accurate result.

Finally, the overall average grid energy, over 100 simulations, results to be 2,51 MWh. Splitting up by load component, it is obtained:

- $E_{GRID,appliances}$=0,266 MWh, which is the 12,25% of the total appliances' demand (2,171 MWh);
- $E_{GRID,heating}$=1,19 MWh, which is the 31,53% of the total heat pump electrical demand (3,774 MWh);
- $E_{GRID,EV}$=1,06 MWh, which is the 21,68% of the total transport demand (4,888 MWh);

Analyzing the results, it is clear that although electric vehicles represent the biggest contribution for the total load, their grid consumption results to be lower than that of the heating system.
In conclusion, the optimization of the system should focus in particular on the heating sector's parameters, which is the subject of the next chapter.

Chapter 7

System Optimization

This chapter is devoted to the analysis that the main variables have on the system. An optimization process is performed: its purpose is to determine the value of several variables affecting the system, in order to minimize the non-renewable fraction of energy consumption. Table 7.1 summarizes the involved parameters in the optimization.

Parameter	Optimization range
Battery capacity	40-100 kWh
Buffer capacity	1-16 kWh
DHW capacity	5-11 kWh
Minimum winter SoC_{buffer}	20-80%

Table 7.1: Optimization parameters

The optimization process is performed through a parametric analysis, running several simulations, each at a different value of the parameter involved. The output of each simulation gives the total non-renewable energy need, that has to be supplied by the grid. The optimal configuration is the one for which this amount is minimum. Default input parameters that are used in reference case are summarized in Tab.7.2: these values are employed each time the optimization process does not regard that specific parameter.

Parameter	Default value
Buffer tank capacity	2100 Wh
DHW tank capacity	7000 Wh
Battery storage size	40 kWh
$SoC_{buffer,min,winter}$	40%
$SoC_{buffer,min,summer}$	20%

Table 7.2: Default parameters

7.1 Battery storage and EV recharge strategy

The first optimization parameter that can be easily managed to vary the non-renewable fraction of energy grid is the capacity of the battery storage. Reasonably, the adoption of bigger-size batteries is favourable to the maximization of renewable energy exploitation.
Figure 7.1 shows the total grid energy variation with the increase of the net capacity of the battery, ranging from 40 to 100 kWh. Smaller sizes are excluded, as mentioned in Cap.6.2, therefore no significant convergent effect is visible. The analysis is performed for the four different batteries recharging strategies; the simulation is repeated multiple times to account for the randomly variable load profiles of electric appliances and electric vehicles; the average value is then reported.
Also in this case, 100 simulations are performed and maximum and minimum values are shown in the picture, together with the average one.

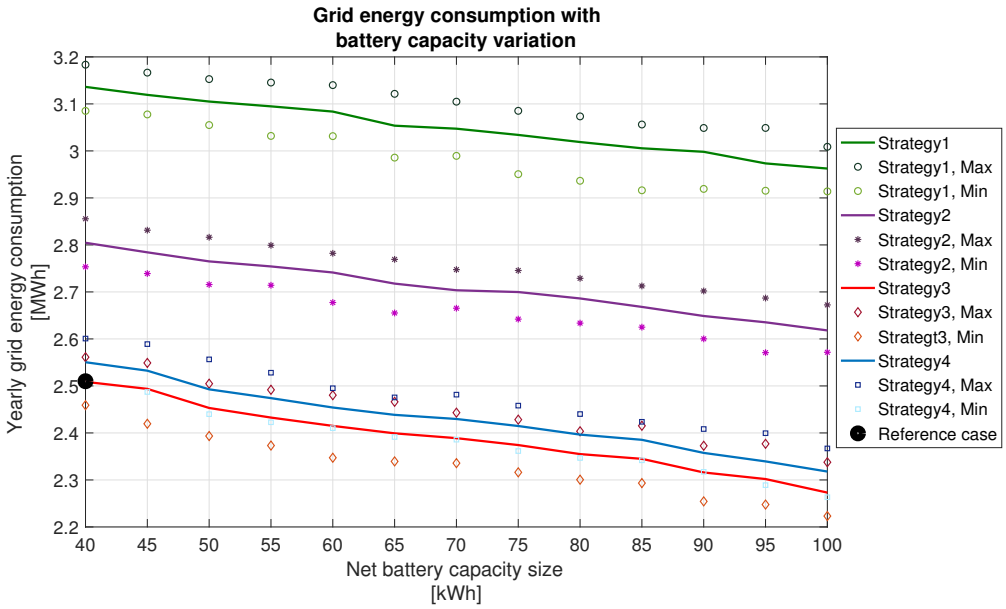

Figure 7.1: Yearly average grid energy consumption with variation of net battery capacity, for the four different recharging strategies

Firstly, for all strategies it is possible to recognize a general decreasing trend of the global grid energy consumption with the increase of the net battery capacity. The four strategies present an almost parallel trend among them.
In particular, Strategy 1, whose priority of recharge is given to the main battery storage, presents the highest values of energy consumption from the grid. The lowest-consuming strategy results to be the third one, whose priority of recharge was given entirely to EV1.
Strategy 3 presents a reduction of grid consumption of 24,4% (-0,81 MWh/year) with respect to Strategy 1, adopting a net capacity of 40 kWh, and a 23,76% reduction (-0,69 MWh/year) at the upper extreme of 100 kWh battery capacity. On average, Strategy 3 allows to reduce grid energy consumption of a total -9,56% (-0.24 MWh/year) with a +150% increase of battery capacity.
Strategy 2 and 4, instead, lie in between the extreme cases.

Moreover, it is important to mention that all the four presented recharge strategies represent a sort of load management of the electric vehicle consumption. Indeed, in a case in which none of the previous strategies are adopted and the recharge of the vehicles occurs as soon as they arrive home, the total non-renewable fraction is quite different. Keeping the same reference values for the different parameters, the average yearly grid energy consumption, over 100 simulations, results to be equal to 3,83 MWh.
An increase of +21,97% is therefore obtained with respect to the value of Strategy 1 and +52,6% with respect to Strategy 3, both evaluated at 40 kWh of battery capacity.

In conclusion, thanks to the load management of the vehicles recharge, it is possible to save up to 1,32 MWh of grid energy consumption. In particular, several strategies are investigated and Strategy 3 results to be clearly the best option among the others, independently from the choice of the battery capacity.
The optimal value of battery capacity is, instead, not possible to determine without performing an economic analysis. Indeed, high batteries' cost could make disadvantageous the adoption of very large storage system.
Finally, basing on these results, Strategy 3 is always adopted hereafter for the following simulations.

7.2 Heat storage

Heating sector presents high potential for optimization of the system, being several parameters such as dimensions of storages and minimum level of charge directly involved.
The first analysis is performed on the variation of buffer capacity and its minimum winter SoC: Fig.7.2 shows the averaged grid energy consumption over 100 simulations, as function of these two parameters.
A general decreasing trend is visible with increasing buffer capacity and a minimum is present at buffer capacity equal to 10 kWh. However, for higher values, no significant variations are visible: it is likely to be caused by the fact that the heating capacity of the heat pump is limited to 6,2 kW, therefore a bigger-capacity storage would not be fully exploited.
The variation of minimum state of charge, instead, is particularly significant at low buffer capacity size: a higher minimum SoC is required to decrease the non-renewable energy demand.
In particular, the minimum occurs at 30% of minimum level of charge, for which it is obtained 2,29 MWh of consumption: a maximum reduction of -8,75% is achieved with respect to the reference case.

Then, the influence of the summer minimum state of charge of the buffer tank is analyzed. In this case it is found out that, for the minimization of grid energy, it has no impact: indeed, the summer heating load is reduced significantly, thus minimizing the effect of this parameter.

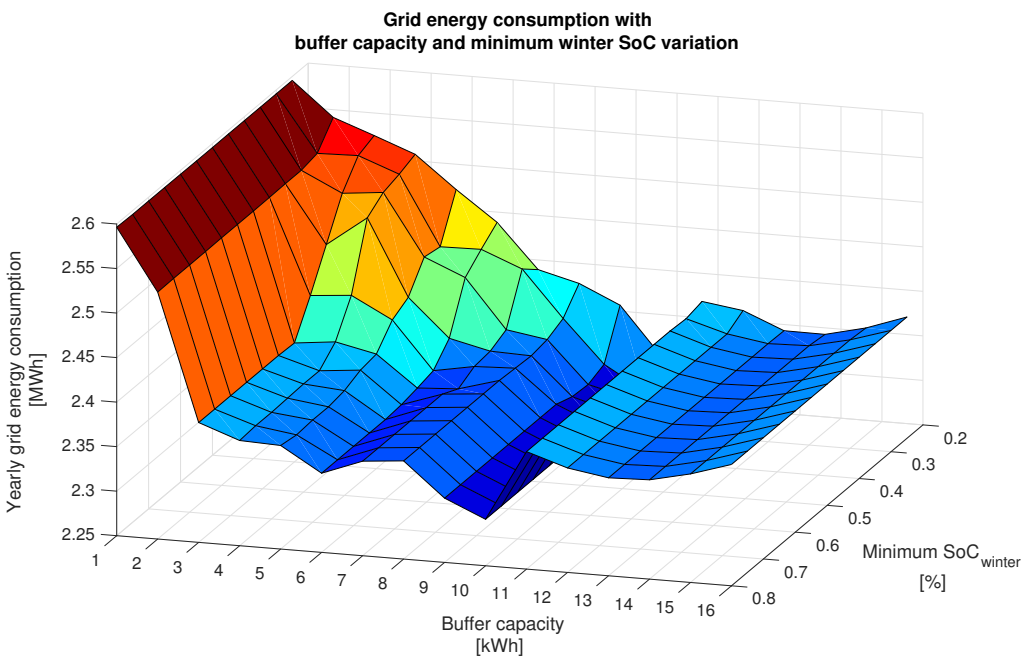

Figure 7.2: Yearly grid energy consumption with variation of buffer capacity and minimum winter buffer's State of Charge

On the other side, however, it is important to chose it wisely in order to reduce the switching-on times of the heat pump, to avoid any damaging effect on the machine.

The second optimization process instead, involves the capacity of the DHW tank and that of the buffer, illustrated in Fig.7.3. While for the buffer a clear decreasing trend is visible with the increase of capacity, the same cannot be said for the DHW storage. Indeed, the recharge of the DHW tank is quite independent from the availability of surplus, since the recharge only occurs when the level of charge falls below the minimum set value, except in summer period when no buffer recharge is required.
The minimum value of energy grid consumption is then found for $\text{Capacity}_{\text{DHW}}$=10 kWh and optimal buffer capacity is confirmed for $\text{Capacity}_{\text{buffer}}$=10 kWh; the minimum value results to be equal to 2,31 MWh (-8,3%).
Setting the minimum buffer SoC equal to the optimal 30% (instead of 40%), it is found a minimum for $\text{Capacity}_{\text{DHW}}$=7 kWh, which gives a total grid energy consumption of 2,29 MWh.

Finally, it is necessary to repeat the same simulations for different values of battery capacity. From the left picture of Fig.7.4, it is observed that the optimum value always falls for the same value of buffer capacity. For DHW capacity, instead, the trend is more irregular, and it might be possible that the optimum value varies with the dimension of battery capacity.
To solve this issue, it is decided to fix the optimal DHW capacity at 7 kWh: indeed, from an economic perspective it is more convenient than the bigger size tank, and, as seen before, the difference in grid energy consumption is around 20 kWh.

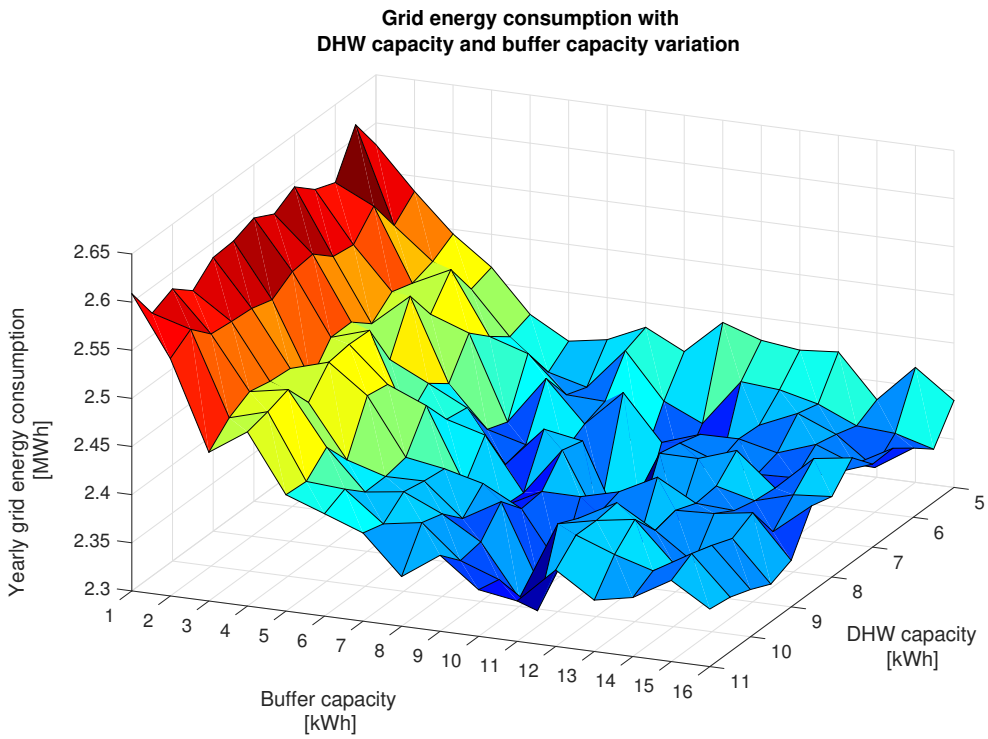

Figure 7.3: Yearly grid energy consumption with variation of buffer capacity and DHW capacity

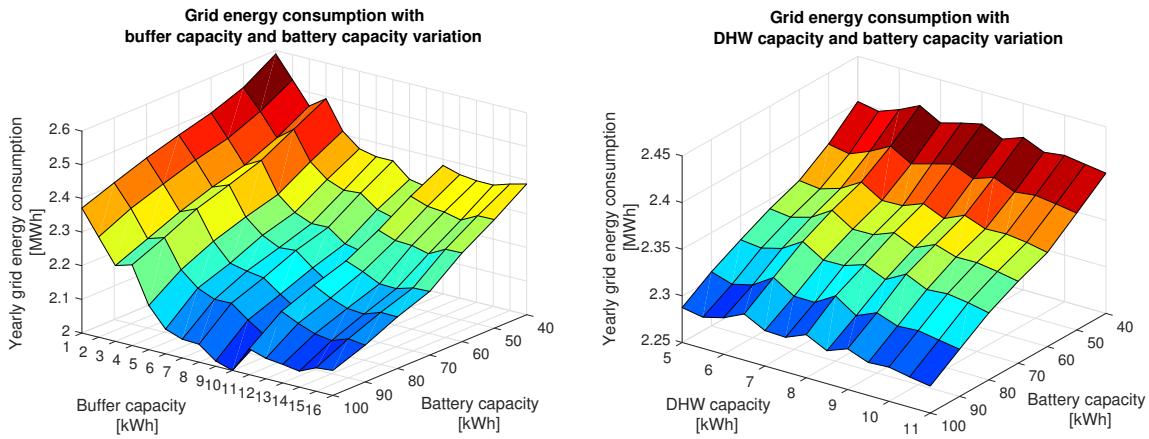

Figure 7.4: Yearly grid energy consumption with variation of battery capacity and buffer capacity (left) and DHW capacity (right)

7.3 Economic and CO_2 emissions evaluation

This section is devoted to the evaluation of the system feasibility under two different aspects: economic feasibility and CO_2 emission abatement.
An economic evaluation is implemented to analyze the feasibility of the system from a practical point of view and, in particular, it is devoted to the determination of the net battery capacity.
As seen in Fig.7.1, grid energy consumption is inversely proportional to the size of the battery. In theory, no limitations are present in the adoption of a very large battery storage system; in practice, the determinant aspect is the cost. Indeed, Li-ion batteries, at the present, are among the most expensive models in the market, but luckily their price is expected to fall below 200 €/kWh by 2030, almost half of the current price [17].

Different systems configurations are analyzed in order to optimize the system, not only in terms of minimization of grid energy consumption but also to determine in which way it is possible to maximize the abatement of CO_2 emission at minimum expense. Two cases in which no sector coupling takes place are briefly analyzed as well to understand the effects of heat pump and electric vehicles on costs and emissions.
The reference case adopted for comparison is a standard system characterized by the use of a natural gas boiler for heating and oil-fuelled cars. Electricity for appliances is provided by the grid and no renewable energy production is taken into account.

The method here adopted for the economic evaluation is the calculation of the Discounted Cash Flow (DCF), presented in Ch.4.3.
Both analysis are performed considering differential values with respect to a reference case which considers the adoption of a standard gas boiler for heating and DHW production and oil-fuelled vehicles for transport. Electricity needs are entirely satisfied from the grid, since no renewable generation is adopted.
It is hence possible to compute the Discounted Cash Flow of each configuration with respect to standard case. The analyzed system configurations with their cost items are presented in Tab.7.3.
Case 1 and 2, which are not characterized by sector coupling and renewable energy generation, are analyzed to compare the specific effect of the adoption of an heat pump (case 1) and of electric vehicles (case 2) with respect to the reference case. Case 3 represents the system implemented in this work, characterized by complete sector coupling. Case 4 and 5, instead, are characterized by partial sector coupling and analyze once again the effects of the adoption of an heat pump or electric vehicles, and are compared to Case 3.
For each case, C_{inv} represents the investment costs at year 0, for each system component.
CF_k represents instead the cash flows due to energy consumption, for each year, where:

- E_i represents the yearly energy consumption in kWh for each sector i (appliances, heating, EV), while it is expressed in kilometers for E_{car};

Case		Electricity	Heating	Transport
0	C_{inv}	-	Gas boiler	Fuel vehicles
	CF_k	$E_{\text{appliances}} \cdot c_{\text{el}}$	$E_{\text{heat}} \cdot c_{\text{ng}}$	$E_{\text{car}} \cdot c_{\text{oil}}$
1	C_{inv}	-	Heat pump+Buffer	Fuel vehicles
	CF_k	$E_{\text{appliances}} \cdot c_{\text{el}}$	$E_{\text{HP}} \cdot c_{\text{el}}$	$E_{\text{car}} \cdot c_{\text{oil}}$
2	C_{inv}	-	Gas boiler	Electric vehicles
	CF_k	$E_{\text{appliances}} \cdot c_{\text{el}}$	$E_{\text{heat}} \cdot c_{\text{ng}}$	$E_{\text{EV}} \cdot c_{\text{el}}$
3	C_{inv}	PV+Inverter+Battery	Heat pump+Buffer	Electric vehicles
	CF_k	$E_{\text{grid,appliances}} \cdot c_{\text{el}}$	$E_{\text{grid,heat}} \cdot c_{\text{el}}$	$E_{\text{grid,EV}} \cdot c_{\text{el}}$
4	C_{inv}	PV+Inverter+Battery	Heat pump+Buffer	Fuel vehicles
	CF_k	$E_{\text{grid,appliances}} \cdot c_{\text{el}}$	$E_{\text{grid,heat}} \cdot c_{\text{el}}$	$E_{\text{car}} \cdot c_{\text{oil}}$
5	C_{inv}	PV+Inverter+Battery	Gas boiler	Electric vehicles
	CF_k	$E_{\text{grid,appliances}} \cdot c_{\text{el}}$	$E_{\text{heat}} \cdot c_{\text{ng}}$	$E_{\text{grid,EV}} \cdot c_{\text{el}}$

Table 7.3: Discounted Cash Flow components for each system configuration

- c_i represents the specific cost in €/kWh for each energy mean (electricity, natural gas, oil), while c_{car} is expressed in €/km.

Emissions instead, are simply computed multiplying the specific CO_2 emission factor times the energy consumed by that kind of configuration, for each component.

Results

It is thus possible to summarize the results analyzing the parameter $Saving = \Delta DCF/\Delta CO_2$ for each case. It determines which is the economic flux (positive or negative) generated by the investment to reduce CO_2 emissions of 1 kg, if that specific system configuration is adopted instead of the base case. Table 7.4 shows the results.

Case	$(\Delta DCF)_1$ [€]	$(\Delta CO_2)_1$ [kg_{CO2}/year]	$Saving_1$ [€/kg_{CO2}]
1	-1,0703e+04	945,4204	-0,5660
2	-6,2580e+03	1,7403e+03	-0,1798
3	-2,5715e+03	6,3884e+03	-0,0201
4	-1,7317e+04	2,0287e+03	-0,4268
5	4,8994e+03	5,0399e+03	0,0486

Table 7.4: Results for Economic and Emission analysis, Case 1

Case 1

Case 1 differs from reference configuration for the adoption of a heat pump and buffer storage, instead of a standard gas boiler and does not include renewable energy generation.
The DCF results to be negative: it means that the investment is not able to be payed back by the avoided costs of the system, with respect to the reference case. However, this system configuration generates a net reduction of emissions.

Case 2

Case 2 differs from reference configuration for the adoption of electric vehicles, instead of a oil-fuelled car and does not include renewable energy generation.
Case 2 results to be economically more convenient than Case 1 because the cost of natural gas is much lower than that of electricity, even though a COP factor higher than 3 links heating load and heat pump electricity load. Besides, the adoption of two electric vehicles allows to obtain a bigger reduction in emission.
Configuration 2, hence requires 0,1798 € of expense to reduce of 1 kg the system emissions.

Case 3

Case 3 is a system characterized by complete sector coupling, in which an heat pump with buffer storage and electric vehicles are adopted. Moreover, 30 photovoltaic panels are installed to produce renewable energy, which can be stored in batteries. A sensitivity analysis is performed on the two variables, the dimension of buffer and battery storage. Table 7.4 shows the results at battery capacity equal to 10 kWh and buffer capacity equal to 2100 kWh.
Is is obtained a negative DCF but less than previous configurations because of the big impact of avoided costs over 20 years of plant lifetime, despite the higher initial investment costs.
Figure 7.5 shows the values of the CO_2 emissions abatement on the right and the values of net saving on the left, with the variation of buffer and battery capacity. For both pictures it is possible to see that the major effect is given by the size of the battery: on the left, a linear increase of battery capacity does not produce a linear reduction of emissions, going instead towards a flat trend. Indeed, it results impossible to get a self-sustained system since the total available energy produced results to be lower than the total household needs. Buffer size increase, instead, influences the reduction of emissions but less relevantly. A maximum CO_2 emission reduction is obtained for 10 kWh of buffer capacity, in agreement with the result in Fig.7.2.
On the right picture, it is possible to observe that the battery has also the biggest impact on the costs of the system, leading to an almost linear trend of DCF per amount of CO2 emission reduction, minimizing the effect of the buffer cost.
Thanks to renewable generation and sector coupling it is possible to achieve a much lower value of expense to get 1-kg reduction of emissions.

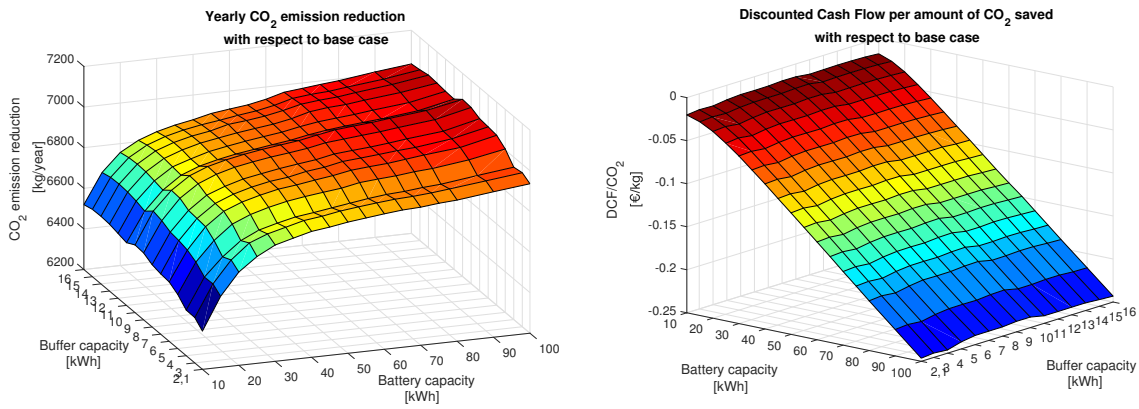

Figure 7.5: Results for Economic and Emission analysis, Case 3

Case 4

Case 4 is a system characterized by partial sector coupling, in which a heat pump with buffer storage is adopted, but oil-fuelled cars are present. Photovoltaic panels are installed and it is assumed to keep the number fixed; batteries are employed as well. A sensitivity analysis is performed on the two variables, the dimension of buffer and battery storage. Table 7.4 shows the results at battery capacity equal to 10 kWh and buffer capacity equal to 2100 kWh.
Results for case 4 show that partial sector coupling is less convenient than Case 3. Despite the lower initial investment costs, the only avoided costs over the system lifetime for the adoption of a heat pump are not sufficient to compete with the previous case. In fact, avoided costs associated to heating with this configuration account for only 61,3146 € per year with respect to conventional heating.
From Fig.7.6 it is possible to see the values of the CO_2 emission reduction on the right and the values of saving on the left with the variation of buffer and battery capacity.

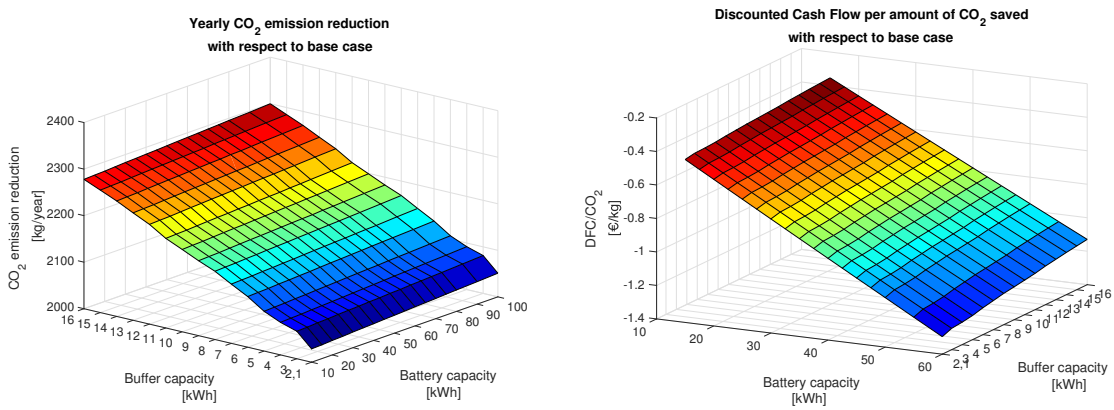

Figure 7.6: Results for Economic and Emission analysis, Case 4

In this case, battery capacity has much lower impact on CO_2 emission reduction than the size of buffer. This is because, without the electric vehicles demand, the generated renewable energy is completely devoted to the fulfillment of heating load, with much smaller impact of the electricity storage system. In the right picture,

instead, the size of the battery still represents the highest contribution in expenses.

Case 5

Case 5 is a system characterized by partial sector coupling, in which only electric vehicles are adopted. Photovoltaic panels are installed and it is assumed to keep the number fixed; batteries are adopted as well. A sensitivity analysis is performed on the capacity of battery storage and Table 7.4 shows the results at battery capacity equal to 10 kWh.
It is here noticed that the net saving results to be positive, in contrast with all previous cases. It means that with the adoption of this configuration, it is possible to obtain the reduction of 1 kg of CO_2 with an income of 0,0486 €.
From Fig.7.7 it is possible to see the values of the CO_2 emission reduction on the right and the values of saving on the left with the variation of buffer and battery capacity.

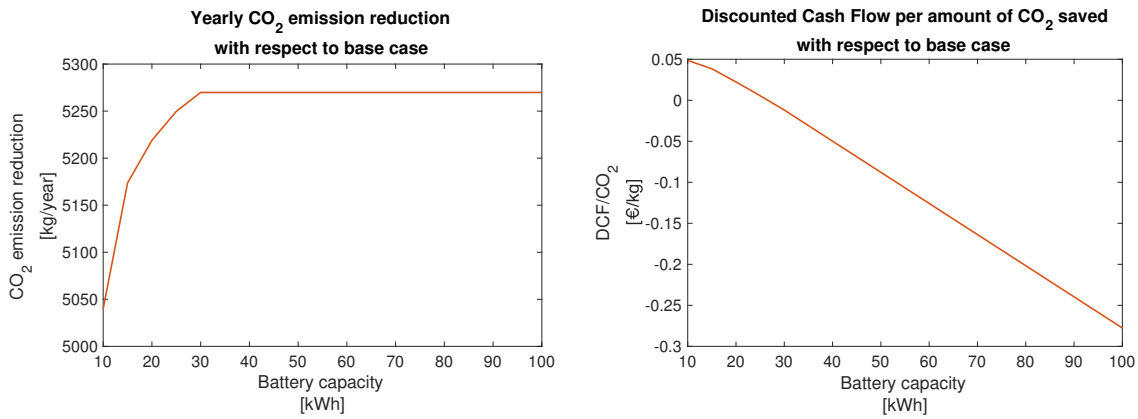

Figure 7.7: Results for Economic and Emission analysis, Case 5

From the left figure, it is noticed that the battery storage allows to reduce the impact of emissions, until reaching a point of maximum reduction, which however does not occur in Case 4, even though both cases are characterized by reduced electric energy demand because of partial sector coupling.
Indeed, with the adoption of a heat pump, the heating load is mainly concentrated in the first months of the year, when the renewable generation is minimum, determining a condition of high load and low energy production.
CO_2 emission reduction results to be higher since the environmental impact of vehicles is more relevant than heating.
Finally, from right picture it is observed that a positive saving is achieved only for low values of battery storage: at 30 kWh, value for which emission reduction reaches the maximum, a negative but low value of saving is obtained.

Chapter 8

Sensitivity Analysis

At last, a sensitivity analysis is carried out, varying the input parameters to the system, such as available irradiation and external temperature, which determine a different heating load and generation profile.
The sensitivity analysis has the objective of understanding the influence that input parameters have on the system.
To do so, it is selected another locality for the implementation of the system: the same reference household of the reference case study is adopted, assuming that all loads keep the same, except for that of heating. Indeed, the new location is chosen in the southern region of the country (latitude: 48,6486°, longitude: 10,5674°), which is characterized by a different profile of external temperature and by different values of solar irradiation. Accordingly, a different generation profile and a different heating load profile are considered.
South locality is characterized by a lower average external temperature which imposes a design external temperature of $-12\,°C$: the resulting design heat load, obtained adopting the procedures described in Appendix B, results to be equal to 5239,56 W, against 4623,15 W of the northern location.
The yearly heating load profile is illustrated in Fig.8.1 , where the no-heating period (for which average external temperature is higher than $16\,°C$ over that period) is the one adopted also in the previous case.

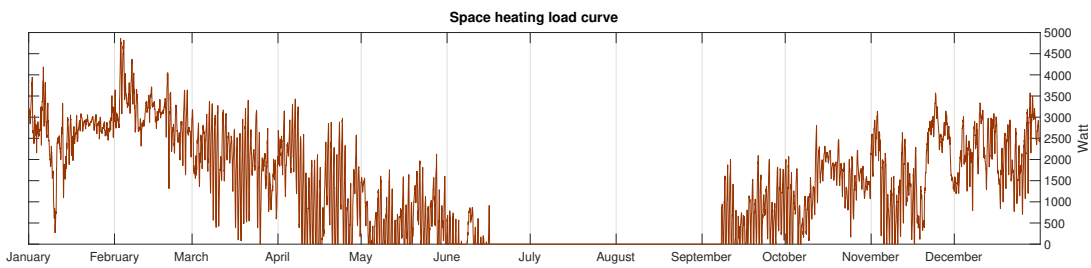

Figure 8.1: Yearly space heating load curve for South locality

Considering to adopt the same heat pump utilized for the reference case, Fig.8.2 shows the operating condition limits of the system. Both limiting cases of design heat load and maximum total heating demand lie above the respective curves of heat pump operation at $-12\,°C$.

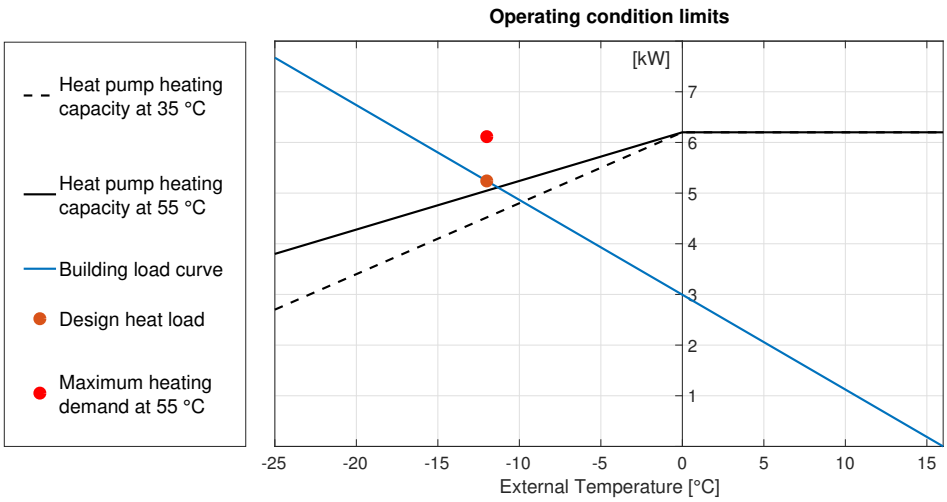

Figure 8.2: Determination of the operating condition of the heat pump

The adoption of a bigger-capacity heat pump could be taken into consideration, however, the condition of very high heat load and such low temperatures occurs for very few times throughout the year. It is then possible to consider the adoption of an electric resistance to supply the necessary heat when the heat pump is not able to operate to fulfill the demand.
The choice of a bigger-capacity heat pump is not straightforward but has to be properly analyzed to avoid oversizing of the system.
In this analysis, it is opted to employ an electrical resistance, being the system also provided with buffer and DHW storages, so that the necessary heating power doesn't have to come entirely from the heat pump.
Therefore, the electric resistance is sized to supply a maximum of 1066 W, which corresponds to the difference between the value of maximum heating demand and heat pump heating capacity at $-12\,°C$ and delivery temperature of $55\,°C$.

From the generation profile point of view, South location is characterized by much higher solar irradiation but lower windiness.
The resulting total irradiance on tilted surface (50°) is 1,09 MWh/m^2 (+9,22% with respect to North location) and its profile can be observed in Fig.8.3.

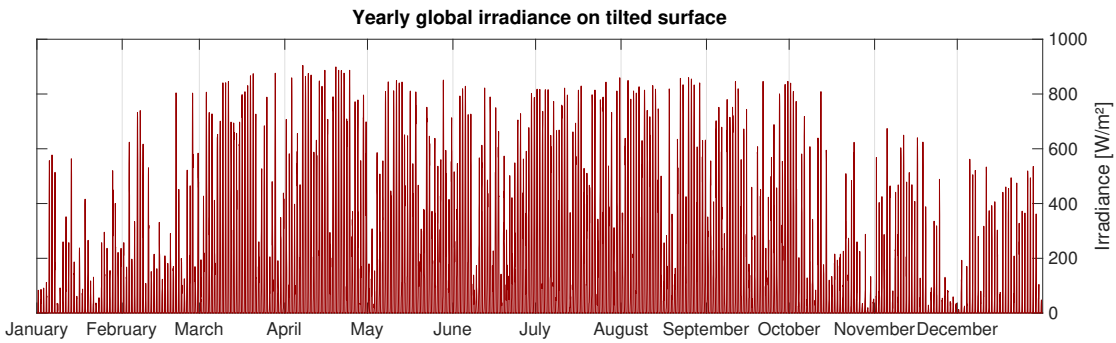

Figure 8.3: Yearly profile of global irradiance on a 50°-tilted surface for South location

Considering to adopt the same number of panels, the same corrections and same value for inverter efficiency, the resulting generated solar energy in one year is 8,699 MWh (+8,2%).

Finally, data about the windiness of the selected location are not favourable, being the average wind speed at 10 m equal to 2,9 m/s. It is then excluded the possibility of installing a micro wind turbine at that height.

8.0.1 Energy balances

Adopting the same method described in Ch.6.3, total grid energy is evaluated over 100 simulations and it results to be equal to 3,27 MWh (+30,28% with respect to North case); splitting up by component, it is obtained:

- $E_{GRID,appliances}$=0,379 MWh (+42,48% with respect to North case);
- $E_{GRID,heating}$=1,77 MWh (+48,74% with respect to North case);
- $E_{GRID,EV}$=1,12 MWh (+5,66% with respect to North case).

From the results, it is possible to assert that the colder climate affects significantly the system, with an increase of the heating demand: it causes, in turn, an increase of the total non-renewable consumption. It may be possible that the system is undersized for the heating needs: from one side, the choice of the heat pump could fall on a bigger-size machine, on the other, the dimension of the storages may not be big enough to cope with the high heating demand.
Therefore, despite the higher energy production (with a peak in the summer period), the system is not able to store enough energy for the house needs. The optimization process is necessary to determine the value that the variables should assume to minimize the non-renewable consumption.

8.1 Optimization for South locality

The optimization process is here focused only on heating sector, having the biggest energy demand increase with respect to North locality. Appliances and transport demand, instead, keep constant.
It is then possible to analyze the variation of grid energy consumption with the variation of buffer capacity and its minimum winter SoC, as illustrated in Fig.8.4.
It is possible to observe that a minimum in energy consumption occurs at buffer capacity equal to 7 kWh, lower than that obtained for North case and at high values of minimum SoC, as for the previous case. However, it might be expected that, at higher heating load, the optimum point would lie at higher values of buffer capacity, which is not occurring in this case: an explanation for that is that the heat pump results to be under-sized for the given needs. Indeed, the heat pump heating capacity is mostly used to feed directly the heating circuit because of the higher demand, thus minimizing the available heat able to be stored.
Therefore, it might be useful to understand the effect that an higher heating capacity

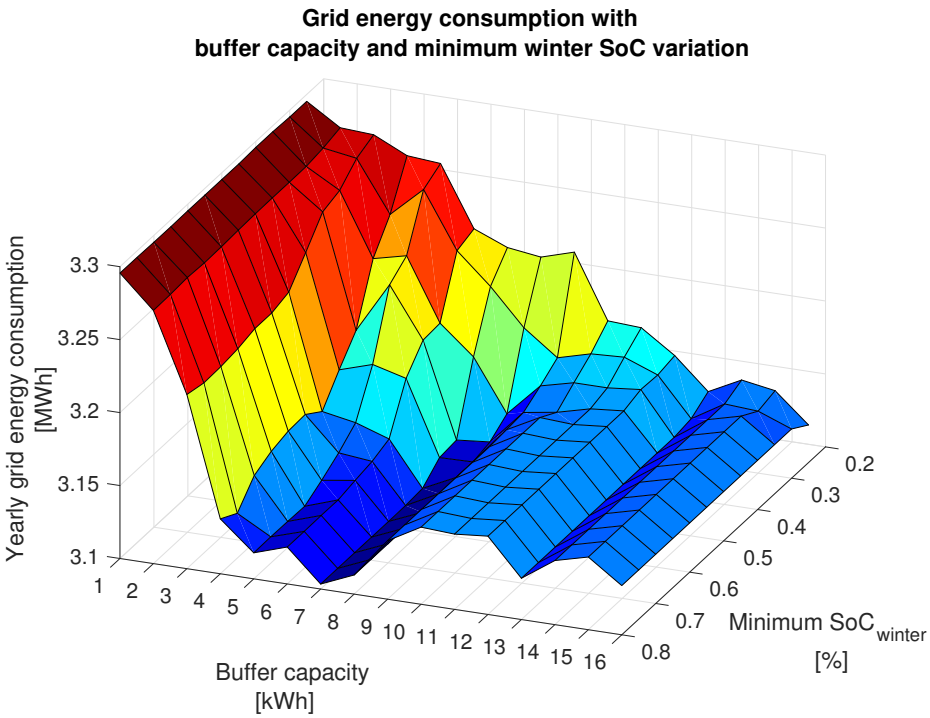

Figure 8.4: Yearly grid energy consumption for South locality with variation of buffer capacity and minimum winter buffer's State of Charge

heat pump would have on the system for the reduction of grid electricity.
Figure 8.5 shows the effect of DHW and buffer capacity on grid energy consumption: as for North case, the size of the DHW capacity is less relevant in the determination of an optimal point, showing no clear trend, for the same reasons presented in Ch.7.2.
With an iterative procedure it is then determined the value of minimum grid energy consumption. Adopting a buffer of 6 kWh capacity, DHW storage of 10,5 kWh capacity and minimum winter state of charge equal to 55% it is obtained a value of 3,099 MWh of total grid energy consumption. A slightly lower value is reached for $SoC_{buffer,min,winter}$=80%, but it is discarded to avoid continuous cycling of the heat pump. In conclusion, a reduction of -5,11% it is achieved if this system configuration is adopted with respect to base case described in Tab.7.2, for which total grid energy consumption is 3,266 MWh.

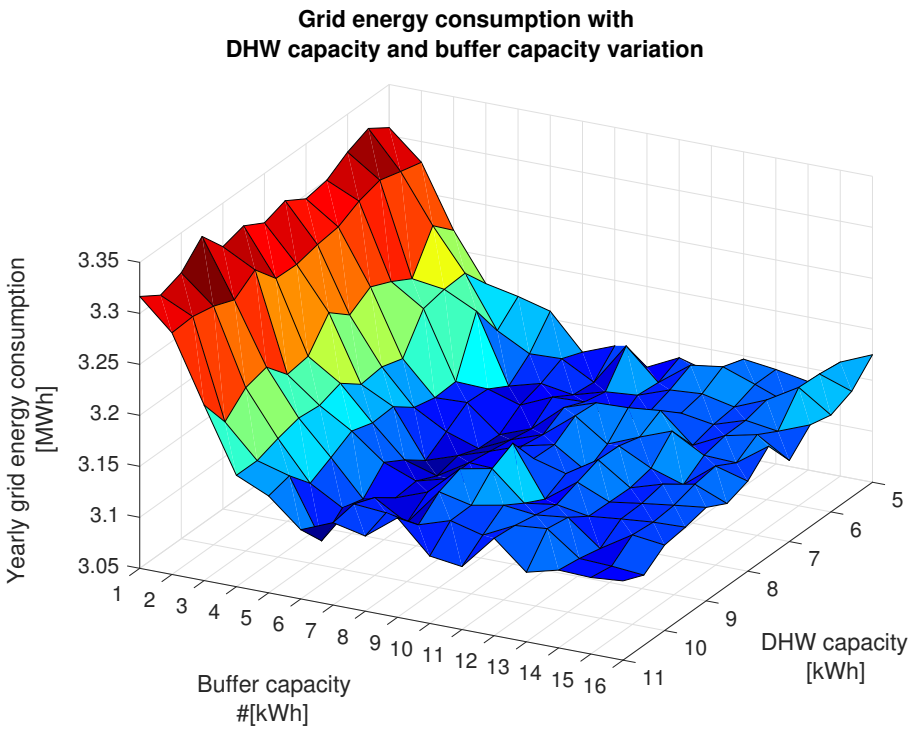

Figure 8.5: Yearly grid energy consumption with variation of buffer capacity and DHW capacity

Conclusions

The present project work was aimed at evaluating the potential of sector coupling in the residential sector in order to minimize greenhouse-gas emissions.
The reason behind this work comes from the rising awareness of the need to take specific actions to reduce environmental impact and limit climate change. In particular, European Union implemented an energy roadmap to 2050, having the final objective of 80-95% greenhouse-gas emissions reduction by that year. In order to achieve this target, among the possible solutions, it has been recognized the need to increase the share of renewable energy consumption.
Sector coupling consists in the use of electricity from renewable sources in the heating sector (Power-to-Heat) and transport (Power-to-Mobility) in order to create a single energy system. In the residential sector this can occur, in particular, thanks to the adoption of electrical heat pumps and electric vehicles, but also through electric boilers and devices for heat storage exploiting excess electricity.

In the specific, this project analyzed the potential of sector coupling for a single family house in Germany, taken as case study and exploiting electricity produced by solar panels and a micro wind turbine mounted on the house roof.
In the analysis, a yearly, one-hour time step simulation of the system was implemented with the Matlab software. The same simulation was performed for two different locations of Germany, one in the North and one in the South, to highlight how resources availability and climate conditions affect the potential of sector coupling.

It was firstly necessary to define the household energy demand. It was identified a standard model of a typical residential household: following a bottom-up approach, the demand of each sector (electrical, heating, transport) was disaggregated in its different components. Electrical appliances load was estimated splitting up the demand of each specific appliance, according to its use. Then the demand for space heating and domestic how water was assessed, considering the adoption of an heat pump coupled with a buffer heat storage for heating and a DHW buffer storage. Finally, electric vehicles consumption was evaluated.
It was then necessary to determine the electricity generation profile for solar and wind energy, starting from yearly values of solar irradiance and windiness of the selected location.

After determining the load curves and generation profiles, a control logic was developed in order to fulfill the household demand at every time step and, in

particular, to define the heat pump operation and the storages recharge. Priority was given to the direct matching of demand with generation; if not possible, excess electricity was set to be used by the heat pump to store heat in the buffer or was set to be directly sent to the battery storage or to electric vehicles, when possible. Four different recharge strategies for electric vehicles recharge were investigated.

The implemented system gave a resulting total electrical grid consumption equal to 2,51 MWh/year, adopting Strategy 3 for vehicles recharge and setting as values for the main parameters involved in the system the following ones: 40 kWh of net battery capacity, 2100 Wh of buffer capacity and 7000 Wh of DHW capacity.

An optimization analysis aimed at minimizing grid energy consumption was performed varying the above-mentioned parameters involved. It can be concluded that:

- Strategy 3 resulted to be the best recharging strategy, allowing to reduce grid consumption of 24,4% with respect to Strategy 1, which represented the worst case;
- Varying battery capacity from 40 kWh to 100 kWh, a net -9,56% of grid energy consumption was obtained;
- Buffer capacity presented an optimum at 10 kWh; setting the minimum $SoC_{buffer,winter}$ equal to 40%, a net reduction of grid consumption of -8,75% with respect to reference case was possible;
- DHW capacity minimizing grid energy consumption resulted to be equal to 7 kWh, obtaining a final value of 2,29 MWh.

Finally, an economic and emission analysis was performed to analyze the system feasibility and to determine the optimal battery capacity able to minimize grid energy consumption (therefore CO_2 emissions) at the minimum expense. It can be concluded that, despite a growing reduction of emissions with the size of the battery, the avoided costs associated with sector coupling implementation are not sufficient to balance the cost of the battery storage: it is therefore economically advisable to adopt the lowest value for battery capacity, which in this case was set to 40 kWh. Economic incentives would be necessary to make the system economically self-sustainable.

Future perspectives for Sector Coupling

At the present situation, the benefits in the implementation of sector coupling include environmental ones but also increased flexibility of the energy system, thanks to the interconnection of sectors through the electricity vector. Current systems which combine different energy sectors are today the Combined Heat and Power generation, rail transport, heat pumps, electric vehicles and many others.
A huge opportunity for sector coupling is possible for countries like Germany, characterized by an energy system still mainly relying on fossil fuels for heating and transport but at the same time producing a considerable fraction of renewable

electricity.

However, in order to foster the development of these systems, several challenges have to be faced. Efforts in the increase of renewable energy production are necessary, together with the achievement of high efficiency in processes in order to keep the energy demand stable and reduce emissions. One important limitation which emerged from the analysis is represented by the economic aspect of the sector coupling implementation, therefore, adequate business models and incentives will be necessary to make these systems economically sustainable. A good opportunity comes from the expected cost reduction of Li-ion batteries, that, nowadays, represent the critical component for the sector coupling progress.
Several possibilities, instead, also come from Power-to-Gas plants implementation, such as the production of fuels like hydrogen from electricity, which could be stocked and used when necessary.
It is then clear that future development of sector coupling relies especially on the implementation of cheap, efficient and flexible energy storage systems.

Appendix A

Complete Electric Appliances' Demand Description

Refrigerator

Assuming to adopt a 357-litres type, A++ class (model: Samsung RB36J8855S4), the energy label reports a consumption of about 262 kWh/year. With 1-hour discretization time, it is possible to assume that the consumption is evenly distributed throughout the 8760 hours of the year, since these appliances are automatically turned on and off according to the temperature measured by the thermostat.
As shown by Fig.A.1 the trend throughout the day is quite flat, but in this case it is chosen to take 30 W (224 kWh/8760 h, rounded to the closest integer) of power consumption since the values presented in the report refer to year 2009.

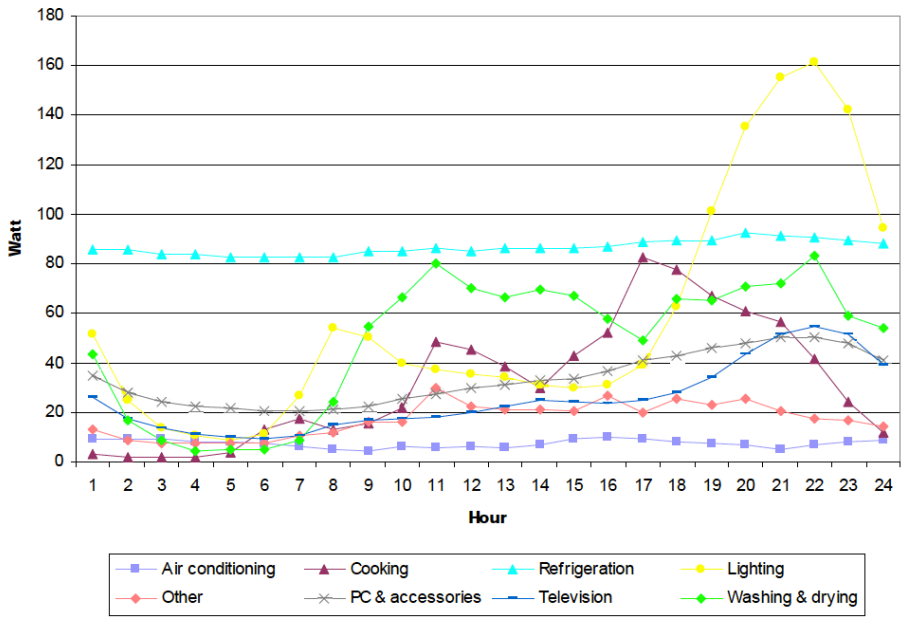

Figure A.1: Electricity consumption of several appliances for a typical household and for a typical day of the week [20].

Lighting

LED Müller-Licht light bulbs are employed, A++ model of 12 W each (equivalent in brightness to the old 100W-incandescent light bulbs). A maximum of 4 lamps can be switched on simultaneously. Starting from the typical day of the households, a pattern for light bulbs consumption is deduced: in particular a peak in the morning and a bigger one in the evening are present, as also shown in Fig.A.2. Moreover, distinction is made between winter and summer days, that are characterized by very different hours of light, especially in northern countries.

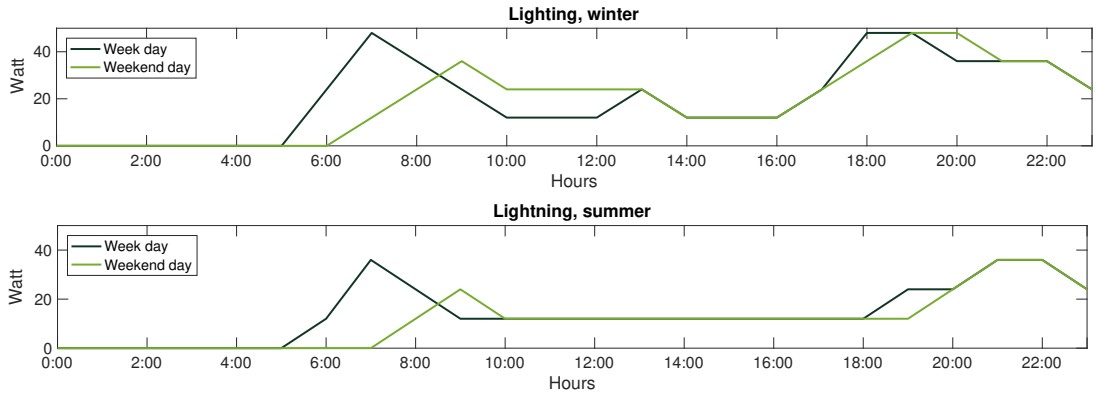

Figure A.2: Daily lighting consumption profile in winter (above) and summer (below)

Television A.3

Two models belonging to A++ class are considered (Philips 43PFS5803 43"), absorbing 37 W each and with stand-by consumption of 0,3 W. For each day of the year, a constant consumption pattern is assumed, distinguishing only between weekdays and week end.

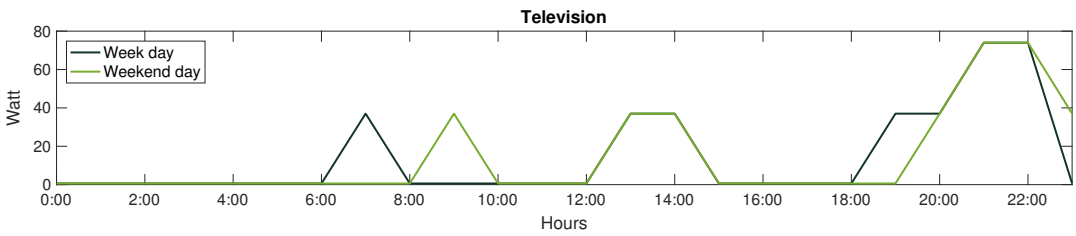

Figure A.3: Daily television consumption profile

Cooking stove A.4

In order to keep energy consumption low, induction cooking stoves are employed, which are not yet subject to energy label regulation. According to the meal and food cooked, energy needs may vary a lot: a sort of unit of measure can be the energy needed to boil one litre of water. To do so, it is necessary to consume 1800 W for 5 minutes, therefore an average of 150 Wh in one hour. Breakfast is the

lowest-consuming meal, while dinner has the highest consumption and takes more time to be prepared. For each day of the year, a constant consumption pattern is assumed, distinguishing only between weekdays and week end.

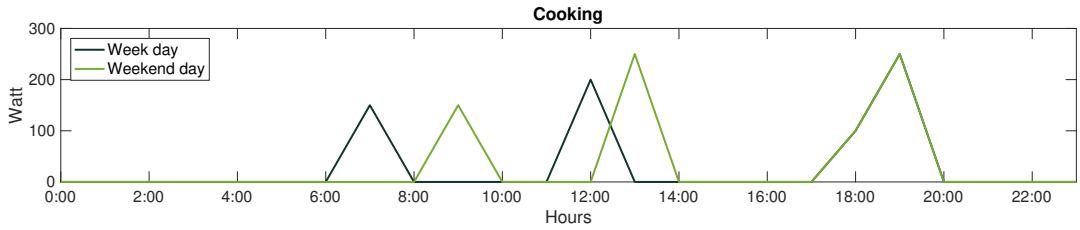

Figure A.4: Daily cooking stove consumption profile

Oven

Considering a 70-liters, A++ model (Aeg BSE892330M) the consumption for a standard cooking at 200 °C is 900 W. It is assumed that it is used once a week for two hours, on Saturday or Sunday when people are more at home.
In order to simulate a random use, it is implemented on Matlab a scrip that allows to choose, every week, a day between Saturday and Sunday, and the switch-on time of appliance within a selected range.
Every week of the year, a day between Saturday (6) and Sunday (7) is chosen thanks to the random function "randi". Possible times of the day for the switch-on are included in the vector "hours2" and again the random function choses one of the six values. Finally, the value of power consumed is assigned to the vector describing the oven use during the day.
Lastly, the consumption of the oven is added to the vector describing the yearly energy need for cooking, in the weekend days.

Dishwasher A.5

An A++ model (Whirlpool WFO 3T123 PF X) consumes 265 kWh/year, and is referred to 280 uses [26]. An average of 946 Wh/cycle are absorbed, therefore assuming 2 hours per cycle, the final power consumption is 473 W. In this case, a daily use is considered and for each day of the year, a constant consumption pattern is assumed, being switched on every day after dinner.

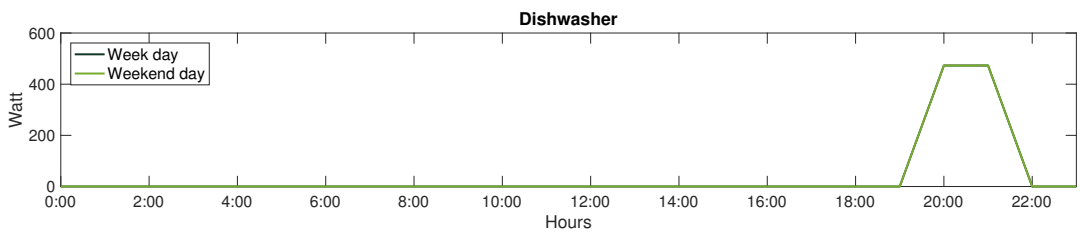

Figure A.5: Daily dishwasher consumption profile

Washing machine

The latest European directives describe the yearly consumption of these appliances assuming 220 washing cycles [26], at mixed conditions of temperature (60 °C and 40 °C) and load (partial or full-load). Therefore, taking as reference an A++ model (Electrolux RWF 1083 EFW), 214 kWh/year are consumed, resulting in 973 Wh/cycle. Each cycle has one-hour duration and an average of 4 cycles per week are considered. A Matlab a script allows to choose randomly, every week, 4 days of functioning of the appliance, and the switch-on time within a selected range.

Mobile phone A.6

Each member of the family owns a mobile phone, that requires 5 W for the recharge, for about two hours. Assuming that the recharge happens as soon as people go to bed, there will be also some consumption when the phone is fully charged and is still plugged in, consuming around 2,5 W. For each day of the year, a constant consumption pattern is assumed.

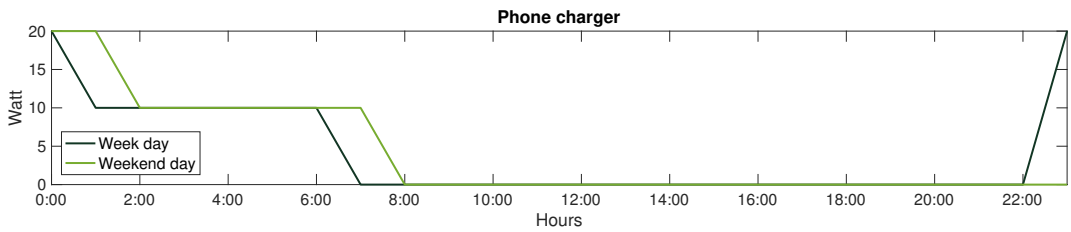

Figure A.6: Daily mobile phone consumption profile

Wi-Fi router

This device has a variable consumption throughout the day, depending on the intensity of internet use. On average, it is possible to assume that it has a constant consumption of 10 W, considering times in which it is simply in stand-by and times in which it's actually working. It represents a constant consumption throughout the year.

Other A.7

This category includes all the devices for which it is not possible to define a constant consumption pattern for every day of the year, but also includes appliances whose use is limited in an interval of time much smaller than the standard one-hour interval. Therefore, energy consumed by these appliances is summed up together and split equally among a selected interval of time that reflects their possible use. The appliances included are listed in Tab.A.1.
Considering that the possible range of time consists in the two intervals of time [8;11] and [16;18], there will be a constant consumption of 215 W during these hours, while in the remaining ones, 10 W account for stand-by consumptions.
There are no significant variations between weekdays and weekend days.

Appliance	Power [W]	Use [min/day]	Energy [Wh]
Iron	1000	10	166,7
Vacuum Cleaner	1000	10	166,7
Hairdryer	200	30	100
Electric Shaver/Toothbrush	5	15	1,25
Toaster	1000	10	166,7
Microwave	800	15	200
PC (3)	180	200	600
Printer	300	2	10
Hi-Fi	70	60	70
Sum			1481,25

Table A.1: Energy demand estimation of a group of appliances without specific consumption pattern

The load curves of the main appliances listed before are illustrated in the following pictures.

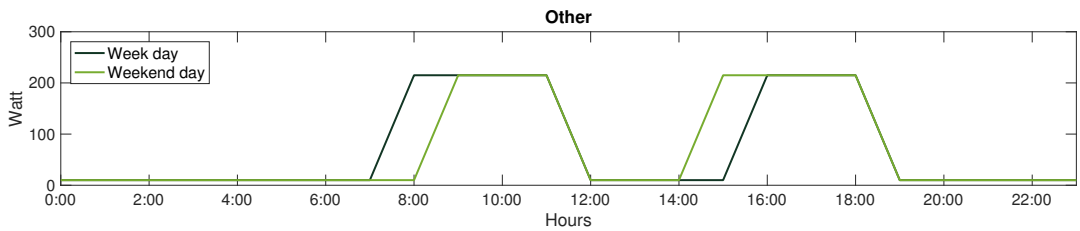

Figure A.7: Daily consumption profile of remaining appliances

Appendix B

Complete Design Heat Load's Description

The European norm EN 12831-1-2017 provides a method for the calculation of the design heat load of a building, where the design heat load is defined as the heat supply (power) needed to maintain the required internal design temperature under design external conditions [16].
Hence, it is necessary at first to set the external design temperature, that corresponds to the minimum air temperature, for which the heat demand is maximum. This value is set to $-10\,°C$ for the locality in northern Germany, and to $-15\,°C$ for the one in southern Germany.

Characterization of the standard house

The standard house is assumed to be a single family household, composed by two floors of 75 m^2 each. The height of the walls is assumed to be 2,8 m and the tilt angle of the roof is 50°. Figure B.1 shows a simplified representation of the building. It is assumed that all the rooms are kept at the same internal temperature, $20\,°C$, and there are no rooms left unheated as basement floors or attics. Therefore, a single-zone model is adopted, in which heat transfer between internal rooms is not specified. Heat losses occurring are those between the whole internal volume and external ambient, through external walls, ground and roof.

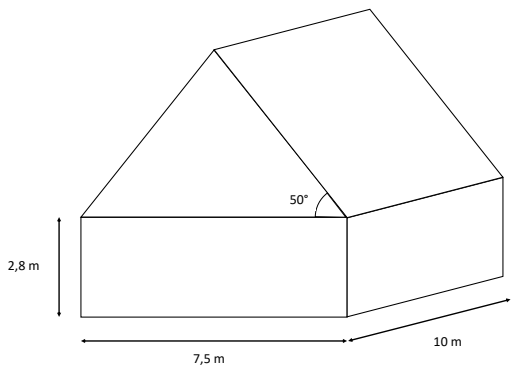

Figure B.1: House model

Reference values for the transmittance set minimum standards that should be achieved by modern buildings to respect the energy saving norms. In the specific, the values used are showed in Tab.B.1.

Element	Reference transmittance value [W/m^{2}K]
Peripheral wall	0,28
Window	1,3
Door	1,8
Ceiling	0,2
Floor	0,35
$\Delta U_{\text{thermal,bridge}}$	0,05

Table B.1: Values of transmittance of several elements for the reference building [13]

B.0.1 Procedure for Design Heat Load determination

The design heat load for a whole building is calculated from Eq.B.1, where all transmission heat losses to the exterior and the ventilation heat loss of the building are taken into account.

$$\Phi_{\text{HL,building}} = \sum_i (\Phi_{\text{T,ie}} + \Phi_{\text{T,ig}}) + \Phi_{\text{V,build}} \qquad [W] \tag{B.1}$$

The terms inside the summation represent the transmission heat losses directly to the exterior for all contained heated spaces, while the last one accounts for ventilation heat losses of the entire building. Heating-up powers and heat gains are optional items that in this analysis are neglected.

The general formulation of transmission heat losses is represented by the product of two terms: the transmission heat transfer coefficient from the heated space to the other space and the temperature difference between the internal heated space and the external design temperature, $(\vartheta_{int,i} - \vartheta_e)$.
The extended formulation of each design heat load's component is described as follows.

$\Phi_{\text{T,ie}}$: Transmission heat losses of a heated space directly to the exterior

$$\begin{aligned}\Phi_{\text{T,ie}} &= H_{\text{T,ie}} \cdot \left(\vartheta_{\text{int,i}} - \vartheta_{\text{e}}\right) \\ &= \sum_k \left(A_k \cdot (U_{\text{k}} + \Delta U_{\text{TB}}) \cdot f_{\text{U,k}} \cdot f_{\text{ie,k}}\right) \cdot \left(\vartheta_{\text{int,i}} - \vartheta_{\text{e}}\right)\end{aligned} \tag{B.2}$$

Where:

- $H_{\text{T,ie}}$: transmission heat transfer coefficient from the heated space to the other space [W/K];

- A_k: surface area of the building element (k) [m^2];
- U_k: thermal transmittance of the building element (k) [W/m^{2}K];
- ΔU_{TB}: blanket additional thermal transmittance for thermal bridges [W/m^{2}K]. The value in Tab.B.1 holds true;
- $f_{U,k}$: correction factor for the influence of building part qualities and meteorological conditions. Set to 1 in absence of specific data;
- $f_{ie,k}$: temperature adjustment factor. Set to 1 in absence of specific data;

It is then possible to compute the total transmission heat losses to the exterior as summarized in Tab.B.2.

	Orient.	External surface [m^2]	Window area [m^2]	Entrance door area [m^2]	Net Wall area [m^2]	$H_{\mathrm{T,ie}}$ [W/K]	$\Phi_{\mathbf{T,ie}}$ [W]
1st fl.	N	28	3	0	25	12,25	364,5
	W	21	1,5	0	19,5	8,385	251,55
	S	28	3	0	25	12,15	364,5
	E	21	1,5	1,89	17,61	11,16	334,90
2nd fl.	N	58,34	2	0	56,34*	16,69	500,55
	W	16,76	1,5	0	15,26	6,99	209,57
	S	58,34	2	0	56,34*	16,69	500,55
	E	16,76	1,5	0	15,26	6,99	209,57
$\sum \Phi_{\mathrm{T,ie}}$							**2735,7**
*Refers to roof surface, instead of peripheral wall							

Table B.2: Values of transmission heat losses from the heated space to the exterior, for each floor

$\Phi_{\mathbf{T,ig}}$: Transmission heat losses of a heated space to the ground

$$\begin{aligned}\Phi_{\mathrm{T,ig}} &= H_{\mathrm{T,ig}} \cdot \left(\vartheta_{\mathrm{int,i}} - \vartheta_{\mathrm{e}}\right) \\ &= f_{\vartheta ann} \cdot \sum_k \left(A_k \cdot U_{eq,k} \cdot f_{ig,k} \cdot f_{GW,k}\right) \cdot \left(\vartheta_{\mathrm{int,i}} - \vartheta_{\mathrm{e}}\right)\end{aligned} \tag{B.3}$$

Where:

- $H_{\mathrm{T,ig}}$: transmission heat transfer coefficient from the heated space to the ground [W/K];
- $f_{\vartheta ann}$: correction factor taking into account the annual variation of the external temperature. Set equal to 1,45 in absence of specific data;
- A_k: area of the building element (k) in contact with the ground [m^2];

- $U_{eq,k}$: equivalent thermal transmittance of the building element (k) in contact with the ground [W/m^{2}K]. Computed from Eq.B.4;

- $f_{ig,k}$: temperature adjustment factor. Set equal to 1 in absence of specific data;

- $f_{GW,k}$: correction factor taking into account the influence of ground water. Set equal to 1 if distance between assumed water table and floor slab is grater than 1 m.

For the computation of $U_{eq,k}$ the following equation holds true:

$$U_{eq,k} = \frac{a}{b + (c_1 + B')^{n_1} + (c_2 + z)^{n_2} + (c_3 + U_k + \Delta U_{TB})^{n_3}} + d \tag{B.4}$$

Where:

- $B' = \frac{A_G}{0{,}5 \cdot P}$ with A_G area of floor slab and P exposed periphery of the floor slab;

- z: depth of the top edge of the floor slab below ground level [m];

- U_k: thermal transmittance of the building element (k) in contact with the ground, from Tab.B.1 [W/m^{2}K];

- ΔU_{TB}: blanket additional thermal transmittance for thermal bridges, from Tab.B.1 [W/m^{2}K];

- a, b, c, d, n: case specific parameters. Assuming to have no basement wall, the values that can be adopted are shown in Tab.B.3.

	a	b	c1	c2	c3	n1	n2	n3	d
Floor	0,9671	-7,455	10,76	9,773	0,0265	0,5532	0,6027	-0,9296	-0,0203

Table B.3: Case specific parameters for the calculation of $U_{eq,k}$

It is hence possible to calculate $U_{eq,k}$ from the values shown in Tab.B.4, while from Eq.B.3, the transmission heat loss to the ground, $\Phi_{T,ig}$, is computed. The respective values obtained are 0,2834 W/m^{2}K and 924,5 W.

A_G [m^2]	P [m]	B' [-]	U_k [W/m^{2}K]	ΔU_{TB} [W/m^{2}K]	z [m]	$U_{eq,k}$ [W/m^{2}K]	$\Phi_{T,ig}$ [W]
75	35	4,2857	0,35	0,05	0	0,2834	**924,5**

Table B.4: Values for the calculation of $U_{eq,k}$ and $\Phi_{T,ig}$

$\Phi_{\mathbf{V,build}}$: Ventilation heat losses of the building

$$\Phi_{\mathrm{V,build}} = \sum_i \left(\rho \cdot c_p \cdot q_{v,min,i}\right) \cdot \left(\vartheta_{int,i} - \vartheta_e\right) \tag{B.5}$$

Where:

- ρ, c_{p}: density of air at the internal design temperature $\vartheta_{int,i}$ [kg/m^3] and specific heat capacity at the internal design temperature [Wh/kgK], respectively. It is possible to assume that $\rho \cdot c_p$=0,34 Wh/m^{3}K.
- $q_{v,min,i}$: minimum air volume flow of the room (i) [m^3/h]. It is computed as the product of the minimum air change rate of the room, $n_{min,i}$, and the internal volume of the room, V_i. For recently-constructed buildings, it may be set $n_{min,i}$=0,25 h^{-1}.

The final value of ventilation heat loss can be computed from values in Tab.B.5.

V_{build} [m^3]	n_{min} [h^{-1}]	$q_{v,min}$ [m^3/h]	$\rho \cdot c_p$ [Wh/m^{3}K]	$\Phi_{\mathbf{V,build}}$ [W]
377,625	0,25	94,4	0,34	**962,94**

Table B.5: Values for the calculation of $\Phi_{V,build}$

Finally, summing up the three contributions, it is found the value of design heat load, which is equal to 4623,15 W for the North locality (at design external temperature $-10\,°$C).
Repeating the same procedure also for the South locality, keeping the same values of reference for the house model, and imposing a design external temperature equal to $-14\,°$C, it is found for this case a design heat load of 5239,56 W.

Appendix C

Determination of total irradiance on solar panel

The general formulation for the calculation of total irradiance on tilted surface is illustrated in Eq.C.1.

$$G_{\mathrm{T}} = G_{\mathrm{d}}\frac{1+cos\beta}{2} + \rho_{\mathrm{g}}G\frac{1-cos\beta}{2} + G_{\mathrm{b}}\frac{cos\vartheta}{cos\vartheta_{\mathrm{z}}} \tag{C.1}$$

Of the three components (diffuse, reflected and beam), reflected radiation from the ground is generally neglected because of its small contribution.
The available database provides the hourly values of G_{d} (diffuse irradiance on horizontal surface) and G_{b} (direct irradiance on horizontal surface).
The angles ϑ_{z} and ϑ are also time-varying, since they describe respectively the Sun incidence angle and Sun Zenith angle: they can be described by Eq.C.2 and Eq.C.3. Only the condition of ϑ lower than 90° is valid, which means that the sun does not fall behind the panels' surface.

$$cos\vartheta_{\mathrm{z}} = sin\Phi \cdot sin\delta + cos\Phi \cdot cos\delta \cdot cos\omega \tag{C.2}$$

$$cos\vartheta = cos\vartheta_{\mathrm{z}} \cdot cos\beta + sin\vartheta_{\mathrm{z}} \cdot sin\beta \cdot cos(\gamma_{\mathrm{s}} - \gamma) \tag{C.3}$$

The tilt angle of the considered panel is represented by β, which is fixed in time, and an optimal value exists such that the energy produced is maximised.
The other quantities present in the previous equations are described below:

- Φ is the Latitude angle of the selected location;
- δ represents the solar declination: it is function of the day of the year, n (n=1...365). Its expression is given in Eq.C.4;
- ω is the hour angle and varies each hour according to Eq.C.5;
- γ_{s} represents the solar Azimuth angle and its hourly variation is described in Eq.C.6;
- γ represents the panel Azimuth angle: it is fixed in time and an optimal value exists such that the energy produced is maximised.

$$\delta = 23{,}45^\circ \cdot sin\left(360\frac{284+n}{365}\right) \tag{C.4}$$

$$\omega = 15^\circ \cdot (ST - 12) \tag{C.5}$$

$$sin\gamma_{\mathrm{s}} = cos\delta\frac{sin\omega}{sin\vartheta_{\mathrm{z}}} \tag{C.6}$$

Finally, it is necessary to describe the variation of ST, which is the solar time, as shown in Eq.C.7. It depends on the actual clock time (CT), on the variation of solar day duration throughout the year, $E(n)$, (Eq.C.8), on the longitude of the location L_{p}, on the reference longitude L_{st} and on the value of daylight saving (DS) that is 1 h in spring and summer when daylight saving is in operation, otherwise zero.

$$ST = CT + \left(\frac{E(n) + 4 \cdot (L_{\mathrm{st}} - L_{\mathrm{p}})}{60}\right) - DS \tag{C.7}$$

$$\begin{aligned} E(n) =& 229.2 \cdot (0.000075 + 0.001868 \cdot cosB - 0.03277 \cdot sinB \\ & - 0.014615 \cdot cos(2B) - 0.04080 \cdot sin(2B)) \end{aligned} \tag{C.8}$$

$$B = (n-1)\frac{360}{365} \tag{C.9}$$

Acronims

IEA	International Energy Agency
COP	Coefficient of Performance
DHW	Domestic Hot Water
IEA	International Energy Agency
EV	Electric Vehicle
SoC	State of Charge
DCF	Discounted Cash Flow

Bibliography

[1] Buffer price. http://www.erregross.com/areariservata/listini/Valmus/20150924-Valmus-Bollitori_2015.pdf.

[2] Car emission. https://www.eea.europa.eu/data-and-maps/daviz/average-emissions-for-new-cars-4#tab-chart_1.

[3] Electricity price for households in germany. https://www.statista.com/statistics/418078/electricity-prices-for-households-in-germany/.

[4] Gasoline price for germany in 2018. https://gasoline-germany.com/statistik.phtml?o=7&display=superbenzin2018.

[5] Germany energy statistics. https://www.iea.org/statistics/.

[6] Grid electricity emission. http://www.energimyndigheten.se/globalassets/om-oss/nog/seminarier-presentationer/philipp-litz.pdf.

[7] Inverter sma sunny tripower price. http://www.europe-solarshop.com/inverters/sma/sma-sunny-tripower/sma-sunny-tripower-10000tl.html.

[8] Natural gas price for households in germany. https://www.statista.com/statistics/418009/natural-gas-prices-for-households-in-germany/.

[9] Nibe f2120 air/water heat pump technical data. https://www.nibe.eu/assets/documents/19854/M11996-2.pdf.

[10] Nibe heat pump price. https://partner.nibe.eu/upload/nibe_co_uk/documents/New%20Air%20to%20Water%20Pack%20Price%20List.pdf.

[11] DIN EN 12831: Heating systems in buildings – Method for calculation of the design heat load – National Annex NA. Standard, DIN Deutsches Institut für Normung e.V., July 2008.

[12] Energy roadmap 2050. European Commission, 2012.

[13] Zweite Verordnung zur Änderung der Energieeinsparverordnung. Bundesgesetzblatt Jahrgang, Part I No. 67, November 2013.

[14] An electricity market for Germany's energy transition: White Paper by the Federal Ministry for Economic Affairs and Energy. Federal Ministry for Economic Affairs and Energy (BMWi), 2015.

[15] Carbon footprint of heat generation. The Parliamentary Office of Science and Technology, May 2016.

[16] BS EN 12831-1:20171: Energy performance of buildings - Method for calculation of the design heat load - Part 1: Space heating load, Module M3-3. Standard, CEN European Committee for Standardization, July 2017.

[17] Electricity Storage and Renewables: Costs and Markets to 2030. International Renewable Energy Agency (IRENA), October 2017.

[18] Energiewende 2030: The Big Picture. Megatrends, Targets, Strategies and a 10-Point Agenda for the Second Phase of Germany's Energy Transition. Agora Energiewende, 2018.

[19] J. Bonin. *Heat Pump Planning Handbook*. Routledge, 2 Park Square, Milton Park, Abingdon, Oxon OX14 4RN, 2015.

[20] A. de Almeida, P. Fonseca, R. Bandeirinha, T. Fernandes, R. Araújo, U. Nunes, et al. Residential Monitoring to Decrease Energy Use and Carbon Emissions in Europe. *European Commission, Joint Research Centre, Institute for Energy and Transport*, 2012.

[21] A. de Almeida, P. Fonseca, B. Schlomann, and N. Feilberg. Characterization of the household electricity consumption in the EU, potential energy savings and specific policy recommendations. *Energy and Buildings*, 43:1884–1894, March 2011.

[22] J. A. Duffie and W. A. Beckman. *Solar Engineering of Thermal Processes*. Wiley, 2013.

[23] E. Energy. Air source heat pumps. https://www.espenergy.co.uk/products/air-source-heat-pumps.

[24] C. Energy Wire. Biogas in Germany: troubled pillar of the Energiewende. https://www.cleanenergywire.org/dossiers/bioenergy-germany.

[25] L. Gasser, I. Wyssen, M. Albert, M. Häusermann, M. Kleingries, and B. Wellig. Effiziente Luft/Wasser-Wärmepumpen durch kontinuierliche Leistungsregelung. *Eidgenössisches Departement für Umwelt, Verkehr, Energie und Kommunikation*, December 2011.

[26] J. Gsellmann and R. Hierzinger. EU-legislation related to energy labels on household appliances. *Come On Lables*, May 2011.

[27] P. J. Hall and E. J. Bain. Energy-storage technologies and electricity generation. *Energy Policy*, 36:4352–4355, October 2008.

[28] A. Luque and S. Hegedus. *Handbook of Photovoltaic Science and Engineering*. Wiley, 2003.

[29] M. J. Moran, H. N. Shapiro, D. D. Boettner, and M. B. Bailey. *Fundamentals of Engineering Thermodynamics*. Wiley, 2014.

[30] G. Pasaoglu, D. Fiorello, A. Martino, G. Scarcella, A. Alemanno, A. Zubaryeva, and C. Thiel. Driving and parking patterns of european car drivers - a mobility survey. *European Commission, Joint Research Centre, Institute for Energy and Transport*, 2012.

[31] Statista. Households' drinking water consumption in Germany in 2015, by usage type. https://www.statista.com/statistics/802254/drinking-water-consumption-in-german-households/.

[32] M. Y. Suberu, M. W. Mustafa, and N. Bashir. Energy storage systems for renewable energy power sector integration and mitigation of intermittency. *Renewable and Sustainable Energy Rreviews*, 35:499–514, May 2014.